NASA CR- 114462
AVAILABLE TO THE
PUBLIC

LIQUID ROCKET PERFORMANCE COMPUTER MODEL WITH DISTRIBUTED ENERGY RELEASE

FINAL REPORT

Contract NAS7-746

Prepared for

NATIONAL AERONAUTICS AND SPACE ADMINISTRATION

Under Technical Management of
Jet Propulsion Laboratory
California Institute of Technology
4800 Oak Grove Drive
Pasadena, California

by

L. P. Combs

ROCKETDYNE
A Division of North American Rockwell Corporation
6633 Canoga Avenue, Canoga Park, California

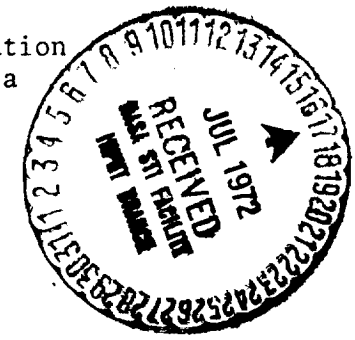

FOREWORD

This document was prepared by Rocketdyne, division of North American Rockwell Corporation, in accordance with Article II, Paragraph D of Contract NAS7-746 with the National Aeronautics and Space Administration. The contract period of performance was 15 August 1969 to 15 January 1972. The contract was administered for NASA by the Jet Propulsion Laboratory, whose Technical Manager was Dr. Raymond Kushida. The Rocketdyne Program Manager was Mr. Spencer Clapp for the first year; he was replaced by Mr. T. A. Coultas for the remainder of the program. Dr. David Campbell served as the Rocketdyne Project Manager.

Several technical people at Rocketdyne performed work on or served as consultants regarding specific aspects of the various program tasks: Mr. W. D. Chadwick in computer programming and checkout, Mssrs. J. C. Hyde, W. H. Moberly, and S. A. Evans with respect to transonic and supersonic flow, Mr. W. S. Hines and Dr. L. J. Zajac with respect to gas/liquid injection spray distributions, and Mssrs. M. D. Schuman and K. W. Fertig in formulating and programming the droplet heating and diffusion model.

This report has been assigned Rocketdyne Report No. R-8888.

ABSTRACT

Development of a computer program for analyzing the effects of bipropellant spray combustion processes on liquid rocket performance is described and discussed. The Distributed Energy Release (DER) computer program was designed to become part of the JANNAF* Liquid Rocket Performance Evaluation Methodology and to account, therein, for performance losses associated with the propellant combustion processes, e.g., incomplete spray gasification, imperfect mixing between sprays and their reacting vapors, residual mixture ratio striations in the flow, and two-phase flow effects. It does not account for losses associated with chemical kinetic deviations from equilibrium nor with the chamber wall boundary layer; those losses are analyzed by other computer programs in the JANNAF methodology.

The DER computer program begins by initializing the combustion field at the injection end of a conventional liquid rocket engine, based on injector and chamber design detail, and on propellant and combustion gas properties. It analyzes bipropellant combustion, proceeding stepwise down the chamber from those initial conditions through the nozzle throat. Analysis of combustion and flow normally assumes axisymmetric stream tube flow. A transonic flow solution is imposed upon the flow in the nozzle. Combustion gas data computed at (or near) the nozzle throat plane are used to initialize the JANNAF reference computer program, TDK, for analyzing the supersonic flow in the nozzle expansion section. Depending upon the version of DER, the TDK analysis may either be included in the DER computations or done subsequently by a separate TDK run. Three different versions of DER have been delivered to the Jet Propulsion Laboratory and are described in this report.

The validity of DER's performance analysis was partially evaluated by comparing predicted performance with a limited amount of experimental data. Accurate predictions are possible, but depend upon proper selection of available adjustments in the input data. Those describing the propellant atomization (mass median drop diameter and distribution of diameters) and the location of the combustion initialization plane are probably the most important adjustments for many engines.

*Joint Army, Navy, NASA, Air Force

CONTENTS

ILLUSTRATIONS

TABLES

NOMENCLATURE

A	area, parameter in droplet diffusion model (Eq. 48)
a	local sound speed
a, b	parameters in Redlich-Kwong state equation (Eq. 44)
$a, b, C_1 \text{---} C_6$	empirical spray coefficients (Eq. 3)
B	parameter in droplet diffusion model (Eq. 47)
C_D	drag coefficient
C_F	thrust coefficient
$C_{k'}$	approximate evaporation coefficient
C_{ND}	nozzle discharge coefficient
C_{pr}	propellant properties coefficient $(\mu\sigma/\rho)^{1/4}$ (Eq. 35)
c	mixture ratio
c^*	characteristic exhaust velocity
c_p	specific heat at constant pressure
$\mathscr{D}$	molecular diffusivity
D	droplet diameter
D_{30}	volume number mean droplet diameter
$\overline{D}$	mass median droplet diameter
d	orifice diameter
E_m	Rupe mixing efficiency factor (Eq. 29)
F	drag force
$F(t)$	function defined in Eq. 51
f	fugacity
g_c	gravitational coefficient
H	enthalpy
I_s	specific impulse
ΔH_v	heat of vaporization
k, k_g	thermal conductivity
k_s'	droplet evaporation coefficient (s denotes stagnant flow condition)
L/D	length to diameter ratio
L^*	combustor characteristic length
M_w	molecular weight
m	droplet mass or spray size group mass
$\dot{m}$	rate of change of mass

N	droplet concentration (no/volume)
$\dot{N}$	number flowrate of droplets
N_{EL}	number of injection elements
Nu	Nusselt number
$\dot{n}_t$	number of stream tubes
P,p	pressure
p*	pressure corresponding to sonic flow
Q	spray or droplet heating rate
Re	Reynolds number
R_u	universal gas constant
R_R	nozzle throat radius ratio (curvature/opening)
R_T,R*	nozzle throat opening radius
r	radial coordinate
Sc	Schmidt number
s	stream tube path length
T	temperature
t	time
u	velocity
$\mathscr{V}$	volume
v	molar or specific volume
$\hat{W}$	propellant weight flux at a spatial mesh point
w	weight
$\hat{w}$	propellant weight flux contribution from an injection element to a mesh point
$\dot{w}$	flowrate
$\hat{w}_{001}$	$\hat{w}(x,y,z)$ for x=y=0, z=1
W_g	stream tube gas flowrate
X	nondimensional distance from nozzle throat
x,y,z	rectangular coordinates (referenced to an injection element origin)
z	axial coordinate
z_0	initial plane for beginning spray combustion analysis

GREEK LETTERS

α	nozzle wall angle (from chamber axis)
γ	ratio of specific heats or adiabatic expansion coefficient
δ_G, δ_L	pseudo-impingement points for gaseous and liquid propellants for a gas/liquid injection element
ε_c	chamber contraction ratio
ε_e	nozzle expansion ratio
ε_{A_t}	decimal tolerance, convergence on throat area
η	efficiency factor
θ	angular coordinate
μ	viscosity
ρ	density
σ	surface tension

SUPERSCRIPTS

$(\bar{})$	average value, or concerned with one-dimensional solution
L	liquid
n	concerned with the n^{th} droplet size group
prime ( )'	value reduced by evaporation
v	vapor
*	sonic flow condition

SUBSCRIPTS

c	chamber
cr	critical point property
d	droplet
E	element
e	expansion section
exper	experimental
f	fuel, spray fan or droplet film

g	combustion gas
h	heat or heating
i	concerned with i^{th} stream tube, summation index
inj	injection
j	concerned with j^{th} propellant or meshpoint, summation index
ℓ	liquid
m,mix	mixing or mixture
o	oxidizer
o,0	initial or stagnation value
s	surface or stream tube path
STC	stream tube combustion model
T	throat
TDK	two-dimensional kinetic model
v,vap	vapor or vaporization
z	in the axial direction

INTRODUCTION

The JANNAF Performance Standardization Working Group has, for several years, directed its efforts toward assembling a methodology for analytically evaluating the performance of liquid rocket engines. The approach taken has been, essentially, to identify performance loss mechanisms and to develop reference computer programs for calculating the degraded performance or the magnitudes of the performance decrements. A long-standing goal has been achievement of performance predictions which are accurate within 1 percent. It was recognized that meeting this goal would require a thorough consideration of all potential loss mechanisms, including interactions between them (Ref. 1).*

The status of the JANNAF performance methodology was summarized in Ref. 2 at about the time that this current program was initiated. Major emphasis had been given to analyzing the gas dynamic loss mechanisms associated with kinetic deviations from equilibrium, striated flow, nozzle divergence, and boundary layers. A series of reference computer programs had been developed and distributed to interested agencies and contractors, viz, ØDE for one-dimensional equilibrium flow, ØDK for one-dimensional kinetic flow, TDK for two-dimensional (axisymmetric) kinetic flow and TBL for turbulent boundary layers. Loss mechanisms associated with propellant spray combustion, such as incomplete spray gasification, imperfect mixing between propellant sprays and their reacting vapors, incomplete reaction within the combustion chamber, and two-phase flow effects were lumped together and termed "energy release losses." These losses were not analyzed, but were accounted for in an approximate, empirical manner: the initial propellant enthalpies supplied to the gas dynamic computer programs were reduced until predicted performance agreed with experimental performance observed in one or more engine firings. The reduced enthalpies were then used in making predictions for similar combustor designs with varied nozzles or operating conditions.

*Reference 1 and others refer to the ICRPG (Interagency Chemical Rocket Propulsion Group) performance analysis methodology. ICRPG has been replaced by JANNAF. The "JANNAF" acronym is used throughout the text of this report, rather than mixing "JANNAF" and "ICRPG."

Analytical studies of bipropellant spray combustion in rockets have also been pursued for many years. Steady-state combustion modeling progressed through the 1950's and early 1960's to a relatively sophisticated state. Nearly all models through that period shared certain common features: they were based on one-dimensional flow equations; their central problem was burning of uniform, completely atomized propellant sprays; spray vaporization was adopted as the combustion-rate-limiting process; and lateral, circulating or striated flows were not considered. Priem and associates at NASA Lewis performed the definitive work of that period, summarized in Ref. 3. Whereas earlier investigators had utilized limiting case assumptions or unrealistic spray droplet dynamics to achieve closed-form solutions, Priem turned to numerical, digital computer solutions and considered realistic spray size distributions and spray dynamics, including transient droplet heating and vaporization.

Later investigators refined Priem's basic model, removing some of its restrictions, e.g., axial pressure and mixture ratio variations and secondary droplet breakup were included (Ref. 4 and 5) and improved numerical integration schemes and two-flame-front models of exothermic droplet burning were developed (Ref. 6 and 7). Some investigators,(e.g., Ref. 4) reverted from the transient droplet heating model for spray burning to the earlier and simpler Godsave (Ref. 8) quasi-steady, evaporation coefficient (k') model.

One-dimensional rocket spray combustion models have been used to analyze propellant spray combustion efficiencies and vaporization-limited c^* efficiency, among other parameters. Usually, a model run is made to obtain specific performance values for specific test conditons, but Priem pursued an extensive parametric variation of propellants, spray drop size distributions, chamber design, and operating conditions, and derived therefrom a correlating equation for vaporization efficiency.

The "energy release losses", however, consist of more than evaporation inefficiencies. Incomplete spray mixing and the resultant mixture-ratio-striated gas flow are quite important contributors to these losses. Additionally, these losses may be coupled, i.e., lower evaporation efficiencies may be experienced in striated flows than in uniform flow, or vice versa.

One approach has been to calculate vaporization and mixing losses separately, as if they were independent, and to combine them as a product of efficiencies. In Ref. 9, for example, the following method was developed: (1) a one-dimensional spray combustion model was used to calculate overall vaporization efficiency, $\bar{\eta}_{vap}$; (2) full-injector cold-flow tests were made to define[1] a mixing c* efficiency, $\eta_{c^*,mix}$; (3) overall c* efficiency was defined as $\eta_{c^*} = \eta_{c^*,mix}\, \bar{\eta}_{vap}$. It was judged to be moderately successful; compared with tests whose c* efficiencies ranged from about 70 to 100 percent, calculated efficiencies were within ±5 percent with a majority of points lying within ±3 percent.

It was shown in Ref. 10 how a related method could be used to calculate equivalent energy release losses for the JANNAF performance methodology. A retinue of engineering experience factors was applied, in an evaluation of the injector, to predict propellant mass and mixture ratio distributions across the injector. From these predictions, the injected propellants were distributed among a large number of combustion stream tubes. Priem's correlating equation for vaporization efficiency was then used to calculate stream tube vaporization efficiencies, combustion gas flowrates, and gas mixture ratios at the nozzle throat plane. Paralleling the foregoing definition of mixing c* efficiency, a mixing specific impulse ratio was defined and used as a multiplier for propellant enthalpies. This gave reduced enthalpy values (for initializing gasdynamic analyses with the ØDK or TDK computer programs) which, together with the calculated combustion gas flowrates (instead of total injected flowrates), completed the energy release loss representation. In the example cases cited in Ref. 10, this method had

---

1. Immiscible propellant simulants were accumulated in a large number, n_t, of liquid sample tubes via a (spatially) continuous rectangular collection matrix. Theoretical c* as a function of mixture ratio, c, and local sample total weights, w_i, and mixture ratios, c_i, were used to calculate

$$\eta_{c^*,mix} = \frac{\sum_{i=1}^{n_t} c^*(c_i)\, w_i}{c^*(\bar{c}_{inj}) \sum_{i=1}^{n_t} w_i}$$

remarkably good prediction accuracy. However, its potential for application as a reference method, to be distributed to many users, is severely limited by the engineering experience factors, which can apparently neither be communicated adequately nor programmed for computer solution.

Meanwhile, as part of a system of computer programs for analyzing injector/chamber compatibility (ICC), a computerized method was being developed for predicting propellant spray distributions produced by liquid rocket injectors (Ref. 11). Its basic premises are that the sprays produced by each individual injection element can be described analytically[1] and that overall injector distributions can be synthesized by linear superposition of the elemental distributions. Formulated in cylindrical coordinates, the LISP (Liquid Injector Spray Pattern) computer program calculates spray mass fluxes, spray droplet velocity vectors, and median drop diameters at a large number of r,θ-mesh points in a "collection plane", some short distance downstream of the injector. Partial spray gasification (burning) upstream of that plane is also estimated.

In the ICC system of computer programs, a liquid rocket combustor is considered to be subdivided into several discrete zones, as shown in Fig. 1 (reproduced from Ref. 12). The LISP computer program analyzes the earliest injection/atomization zone; other computer programs continue the analysis for subsequent zones. The initial rapid combustion zone is analyzed by a 3D-CØMBUST computer program, following its initialization from LISP calculated data. As 3D-CØMBUST analysis proceeds downstream, subsidence of transverse velocities marks the transition to a stream-tube-like flow and is the basis for initializing a simpler analysis, using a stream-tube combustion (STRMTB) computer program. This latter program continues spray combustion analysis through the nozzle throat. Finally, combustion gas product data computed by 3D-CØMBUST and STRMTB at points along the combustion chamber wall are used in boundary layer heat transfer and wall response computer programs to complete the compatibility analysis.

1. Typically, individual element flux distributions are measured in single element, cold-flow simulation experiments and are correlated empirically to a general element flux distribution equation which is used in the computer program.

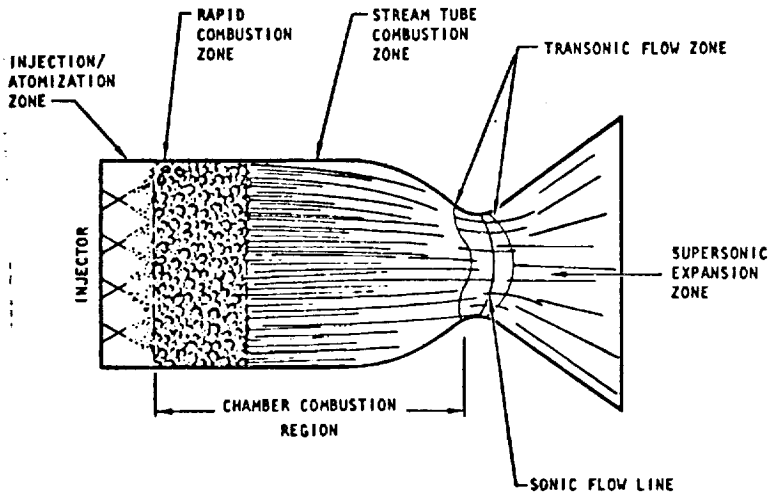

Figure 1. Subdivision of Combustion Chamber Into Zones for Analysis

Both the 3D-CØMBUST and STRMTB computer programs were new combustion models. Each represented distinct advancement of the state of the art beyond the earlier, one-dimensional combustion models and, each in its own way, permitted simultaneous analyses of coupled processes that had previously been analyzed separately, if at all. Because of the complexities involved in the dimensionality aspects of their formulations, the simplest, evaporation-coefficient approach to analyzing spray combustion rates was employed.

Although little emphasis had been placed on calculating performance parameters, the injection and combustion models in the ICC system of computer programs were ideally suited to the development of an "energy release" model for the JANNAF performance analysis methodology. Accordingly, modification of those programs and the JANNAF gas dynamic programs and their assemblage into a single performance analysis model with Distributed Engergy Release (DER) were undertaken and are the subject of this report. Work during the first year of the program was divided into the following tasks:

I. Model Formulation

II. Computer Programming and Checkout

III. Evaluation of Model Validity

IV. Documentation and Delivery (to JPL) of the DER Computer Program

Those tasks were completed and the capabilities and shortcomings of the developed DER computer program were summarized in an "interim final" report (Ref. 13). The program was extended for a second year with the addition of the following tasks:

V(a). Provision of LOX Spray Vaporization Efficiency Charts for High Pressure LOX/GH_2 Combustion

V(b). Replacing the Evaporation Coefficient (k′) Combustion Model with a Droplet Heating and Diffusion Model

VI. Provision of a Gas/Liquid Version of the LISP Computer Subprogram Block

VII. Preparation of a Catalog of Injector Spray Correlations

VIII(a). Interim Delivery of the Revised DER Computer Program Developed Under Task V(b).

VIII(b). Final Documentation and Delivery of the Latest Version of the DER Computer Program

Task VI was structured as a limited-level-of-effort task and was viewed as providing a "first generation" capability for analyzing gas/liquid injection, largely to obtain a clear understanding of how difficult it might be to provide a more realistic, "second generation" capability. During the second contract year, the period of performance was extended by 4 months, particularly so that the Task VII work could best take advantage of work performed under other related contracts. Reports, documents, and presentations resulting from this contract are summarized in Appendix I.

This document is the final report of the Distributed Energy Release Program. Work performed under all of the foregoing tasks is summarized, although it is organized as a computer program description, rather than a task-by-task description. An evaluation of the status of the DER computer program, both with respect to the JANNAF performance methodology and with respect to other programs using related versions of the major subprogram blocks, appears in the last section.

DESCRIPTION OF DER COMPUTER PROGRAM

CONCEPT AND SUMMARIZATION

At its inception, the DER computer program was intended to be a reference program for performing a complete liquid rocket performance analysis, beginning with propellant injection and ending with discharge of combustion products at the nozzle exhaust. Input data regarding propellant properties, injector, chamber, and nozzle design were to be used, with as few user-adjustable parameters as possible. Thus, the program was intended to reflect the influences of hardware-imposed boundary conditions on thrust performance, relating predicted thrust to actual injector design features such as injection hole patterns, hole sizes, impingement angles, and mass flow per element. From a fundamental viewpoint, changes in one or a combination of design parameters may affect performance through altered propellant mass flux distributions and mean spray droplet sizes; evaluating these spray variables is rather nebulous and remote to a design engineer trying to lay out an effective injector design. In developing the DER computer model, a conscious attempt has been made to include those basic combustion processes which are influenced significantly and rather directly by injector design features and to omit calculations which might contribute to a more accurate analysis, but do not interact directly with the injection boundary condition. Thus, models for continued spray dispersion and turbulent mixing in the downstream part of the combustor and for chemical kinetics are not included in DER.

Program formulation and development were imbedded in a few basic concepts. The first was that the fundamental spray combustion mechanisms are well enough known, qualitatively, to support a detailed phenomenological approach to their analysis, rather than a gross integrated approach. The second was that enough is known, quantitatively, about the individual processes' rates, interactions, etc. to support accurate performance predictions. The third lends credence to the first two, that is, there are sufficient existing, developed computer models to perform the entire performance analysis, but they need to be adapted to the performance problem, and to one another, and integrated into one encompassing computer program for solving the performance problem. Finally, it was recognized that the

validity of the solutions would need to be evaluated through critical comparisons with a broad range of experimental engine firing data.

As experience is gained in using the DER program and comparisons are made between predictions and test results, it is expected that specific weaknesses in the combustion model will be revealed. Future program improvements will then be needed to reduce or eliminate the most serious sources of error. An illustrative example of this that has already been undertaken is the extension to a supercritical combustion range, which corrected a weakness revealed by experience with earlier combustion models.

The DER computer program is, essentially, an assemblage of existing computer programs, modified and combined into one large rocket performance analysis model. Distinct computer subprogram blocks are related as shown in Fig. 2. Analysis begins with LISP (Liquid Injector Spray Pattern) computer program calculations of spray mass fluxes, velocity vectors, and droplet diameters at a large number of r,θ-mesh points in an "initial-plane" some short distance downstream of the injector face. These calculations are based on injector design data (number and type of injection elements, element locations and orientation) and empirical parameters which correlate a single injection element's spray mass flux distribution and mean droplet size with its design and operating parameters. Approximations are also made of propellant vaporization (burning) which occurs upstream of the initial plane.

The LISP computer program is the key link between injector design parameters and the combustion model prediction of performance. The approach is strictly empirical and relies upon the availability of valid empirical spray distribution and droplet size data for the individual injection elements being used. Those correlations which now exist have all been derived from cold-flow experiments. While no vis-a-vis comparisons have been obtained relating the cold-flow data to hot-fire distributions, there is some indirect evidence that flowrate distributions are adequately simulated by cold-flow testing and that the major source of error is probably in defining spray droplet sizes.

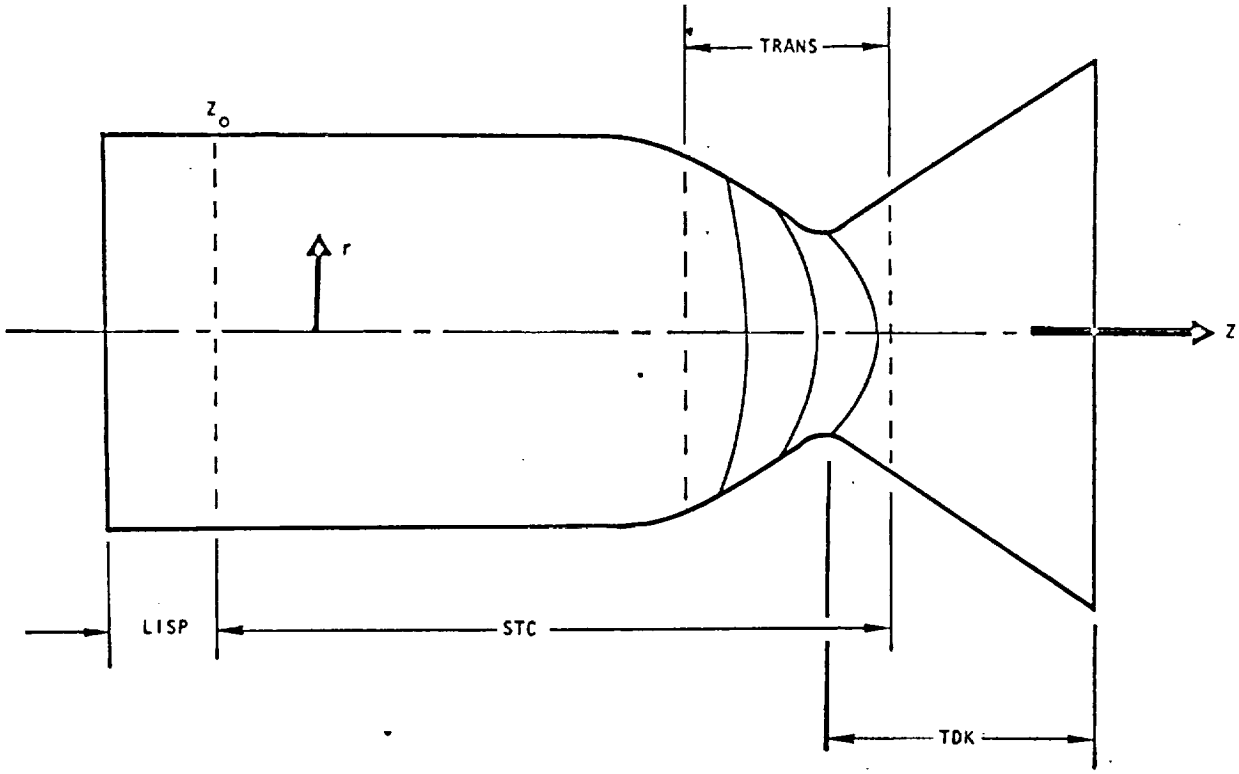

a. Regions of Applicability of Component Computer Programs

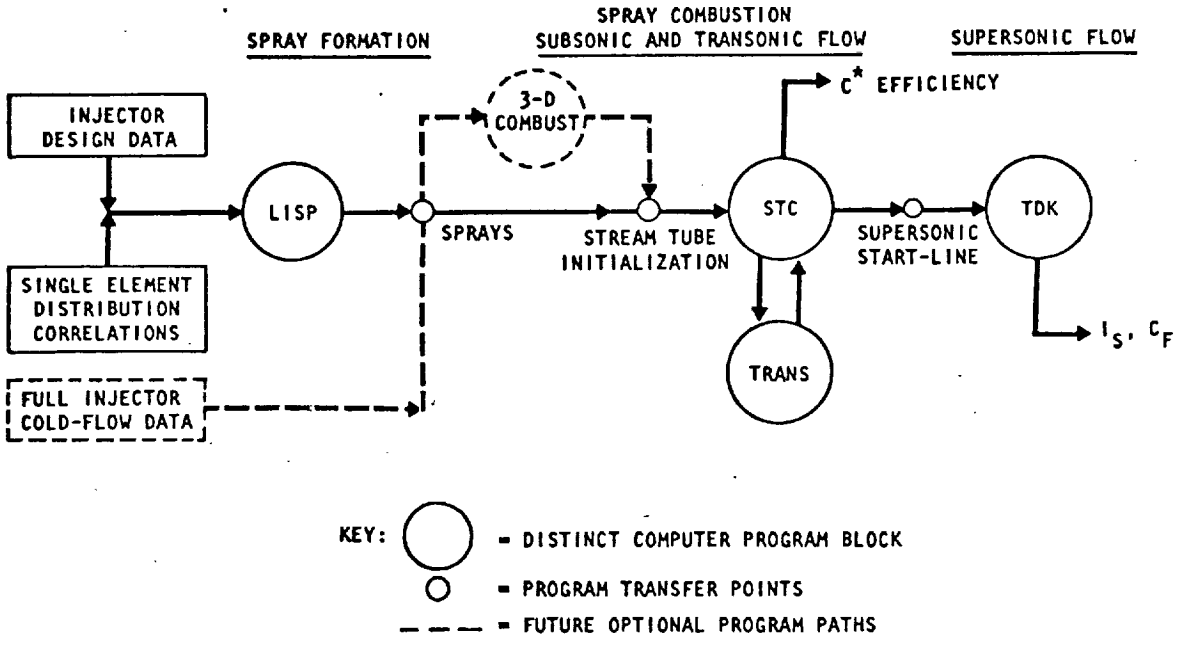

b. Simplified Flow Diagram

Figure 2. Structure of Distributed Energy Release (DER) Computer Program for Performance Analysis

The output from LISP provides the necessary description of the two-phase flow field for initializing the stream tube combustion program. This approach bypasses analysis of the rapid combustion zone. For injectors with large thrust elements, relatively few elements and/or very nonuniform spray mass distributions, this omission may be seriously detrimental. A three-dimensional combustion computer program (3D-CØMBUST), designed for analyzing this zone, has been developed (Ref. 11). Originally projected to be utilized in the DER program, 3D-CØMBUST was omitted from the combined system of computer programs because it had not yet reached a developed, operational status whereby its results could be applied automatically to STC and TDK calculations without prior evaluation of those results by an experienced analyst.

The assemblage of mesh point flow parameters into stream tubes was done recognizing the eventual necessity of mating with existing JANNAF reference nozzle analysis programs. The JANNAF reference programs describe axisymmetric, two-dimensional flow, i.e., parameters do not vary in the θ-direction of an r,θ,z-cylindrical coordinate system. Therefore, the LISP mesh point flows are combined/averaged in the initial plane to initialize the flows into a number of axisymmetric stream tubes. Typically, there are an order of magnitude fewer stream tubes than mesh points. To avoid excessive degradation of transverse mixture ratio differences, the annular stream tube flows are obtained by a complicated breakdown into a selected number of geometric zones, within each of which the mesh point flows are collected into stream tubes of like mixture ratio.

Spray combustion downstream of the initial plane is analyzed by a stream tube combustion (STC) computer program. Propellant flows (both sprays and gases) which enter a given stream tube are thereafter constrained to flow in that tube, without exchanges of mass, momentum or energy among neighboring stream tubes. The flow and combustion in each stream tube are analyzed by a one-dimensional formulation, with local stream path as the independent variable. Stream path variations with r- and z-coordinates are accounted for in the nozzle. Solution is obtained by numerical integration, marching in the z-direction from the initial plane through the nozzle throat. The individual stream tubes' solutions in a plane are coupled with one another through constraints on "area continuity" and

the radial pressure profile. Pressure is assumed to be constant across each z-plane until, at some point in the nozzle convergent section, curvature due to transonic flow effects is considered. Thereafter, rather than continuing to solve for a pressure which satisfies area continuity, absolute pressures are imposed upon the solution. These pressures are calculated by a transonic flow (TRANS) computer program for a nearly-equivalent, constant flowrate, frozen, homogeneous flow.[1]

Three distinct versions of the DER computer program have been developed and delivered to JPL; each is described separately in the subsequent subsections, distinguished from one another by delivery date. The two earliest versions of DER contain a TDK subprogram block, adapted from the JANNAF Two-Dimensional Kinetic reference computer program of Ref. 14. A supersonic, isobaric start line is initialized from STC computed data in the neighborhood of the nozzle throat. STC analysis does not provide gas species concentration data, so the equilibrium section of TDK is used to solve for each stream tube's gas phase composition at the TDK start line. The "long-form option" of TDK is used to continue the multiple axisymmetric stream tube analysis through the supersonic expansion process. The subsequent TDK solution is only slightly modified from that given in Ref. 14. Residual unevaporated spray at the initial line is not analyzed further, but is considered to be flowrate that is lost to the gaseous expansion analysis. It is included as a loss in the calculation of specific impulse.

An improved version of TDK, designed to analyze multiple stream tube kinetic flow through the entire nozzle, has been developed (Ref. 15). Rather than modify the improved TDK for inclusion in DER, and then not be able to take advantage of subsequent TDK improvements, the TDK subprogram block was removed from the third version of DER. In its place, a new subprogram punches out appropriate STC computer data in the NAMELIST format appropriate for subsequent input to the improved TDK computer program.

---

1. The sum of the computed flow areas may then deviate from the true geometric flow area. The fractional deviation of the minimum value of that sum (as calculated at some z-plane in the nozzle) from the nozzle throat area then is used to adjust the chamber pressure level for reiteration through all or a portion of the preceding combustion analysis until the throat boundary condition is satisfied, i.e., the deviation is satisfactorily small.

The two earlier versions of DER conform to the structure illustrated in Fig. 2, differing only in their methods for computing spray combustion rates in subprogram block STC. The September 1970 version uses the evaporation coefficient (k') method and is limited to application at subcritical conditions. The March 1971 version uses a droplet heating and diffusion evaporation/combustion model that permits analyses at supercritical conditions.

The third version of DER, dated December 1971 supercedes the September 1970 version. Its major differences from that earlier version are a LISP capability to analyze gas/liquid injection, simplified LISP input data, deletion of subprogram block TDK, and punch out of STC computed data in a form amenable to direct input to the improved JANNAF reference TDK program.

The three delivered versions of the DER program are described in the following three subsections. The approach taken is to describe the September 1970 version fully and then to describe the modification invoked in deriving the other two versions from it. This approach is used, even though the September 1970 version is obsolete and has been superceded by the December 1971 version, because: (1) it aids in documenting the contact as it was performed, (2) many of the program features have remained unchanged, and (3) nearly all of the model evaluation comparisons between predicted and experimental performance were made with the September 1970 version.

N.B.: This version is no longer in use, but has been superceded by the December 1971 version.

Spray Formation: LISP Subprogram Block

The Liquid Injector Spray Pattern (LISP) computer subprogram block analyzes the propellant spray distributions produced by the injector. Using injection element design, location, and orientation data, and using empirical correlations for elemental mass flux profiles, mean droplet sizes, and spray vaporization, LISP calculates spray and combustion gas mass fluxes, spray velocity vectors, and mean droplet diameters at a large number of mesh points in one or more "collection planes" at specified distance(s) downstream of the propellant injector. Up to a total of 50 individual injection elements can be considered and each may be entirely different from the others in type, design, and/or flow characteristics. As many as 400 combustion zone mesh points can be prescribed.

A simplified flow chart for LISP is shown in Fig. 3.

Mesh System and Injection Elements. LISP is formulated in cylindrical coordinates (r,θ,z) for analyzing hollow, axisymmetric combustors. Propellant spray parameters are calculated at discrete mesh points ($1 \leq j \leq$ NMESH) with coordinates r_j, θ_j, z_0, where z_0 denotes the collection plane. The program is designed to take advantage of radial planes of symmetry and no-flux surfaces to reduce both the amount of input required and the computer run times. Typically, the mesh system is set up to analyze only a pie-slice shaped sector of the injector and chamber flow.

Consider, for example, the injector sketched in Fig. 4, which has 36 unlike doublet elements. The injector pattern consists of the repeating set of elements contained between rays OA and OB. Careful examination shows that line COD represents a plane of symmetry. Rays OA and OC, therefore, define boundaries of symmetry across which there should be no gradients and, thus, they bound an appropriate sector for LISP analysis.

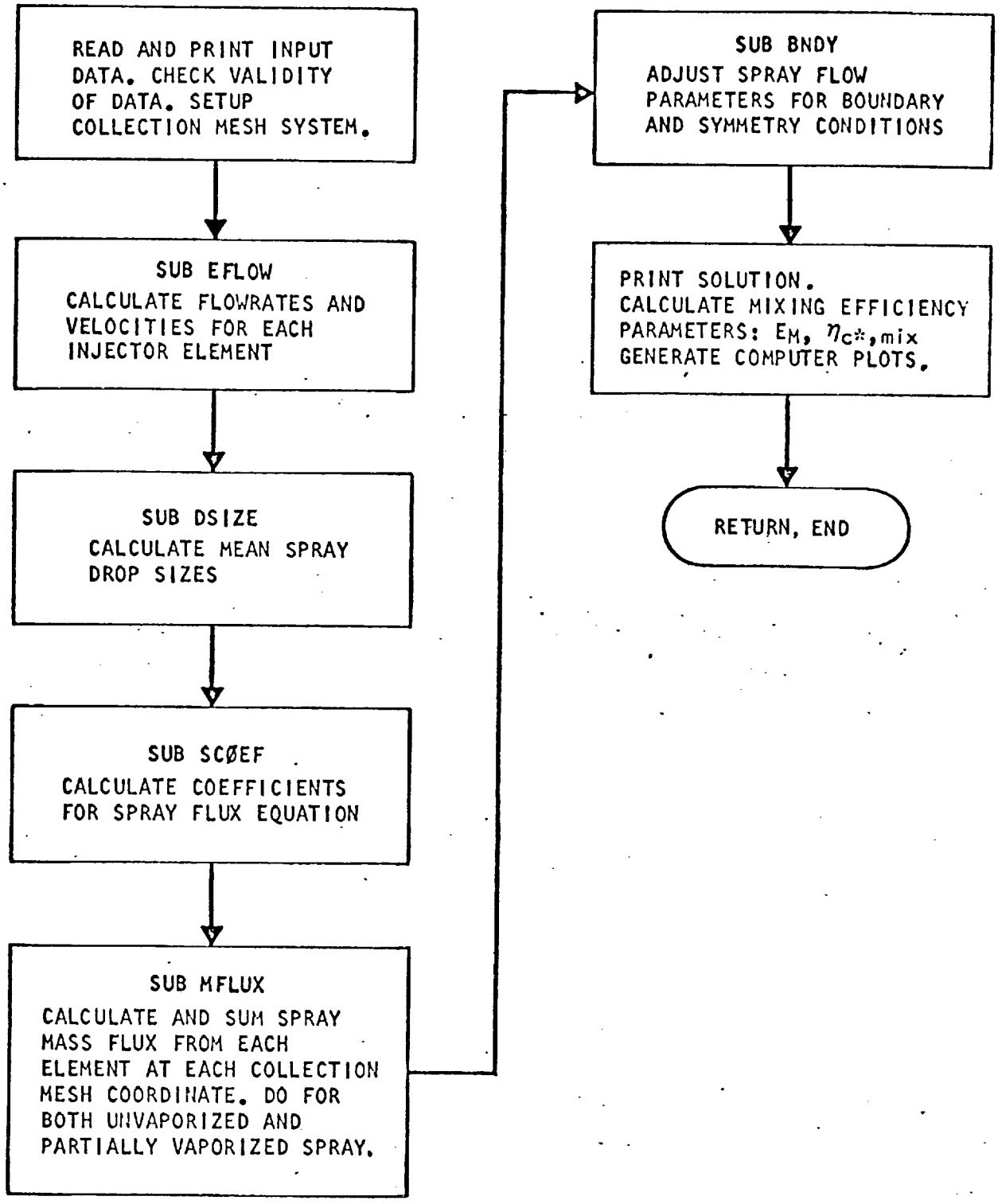

Figure 3. LISP Subprogram Flow Chart

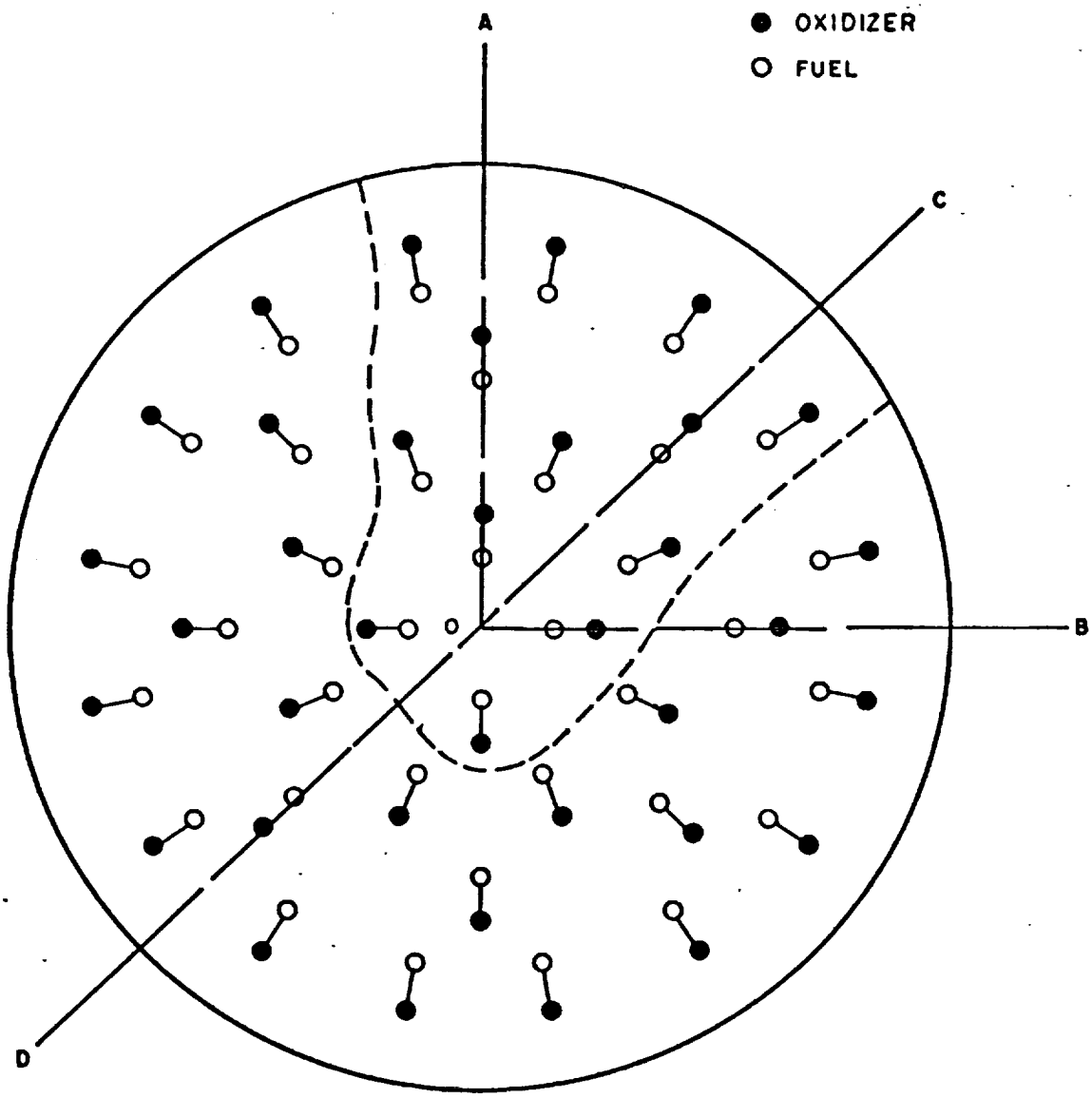

Figure 4. Example of Injector Face Pattern to Show Use of Symmetry Considerations in Defining Thrust Chamber Mesh System

While there is no net flux through planes which are normal to the injector and pass through rays OA and OC, the flow from an individual element is obviously not constrained from flowing through these surfaces. For this reason, LISP must either "reflect" propellant fluxes from planes of symmetry or enough elements must be defined outside of these surfaces to provide inflow equivalent to the outflow. In the example injector of Fig. 4, specification of all elements within the dashed line surrounding AOC would be appropriate, although LISP also contains options for mirror-image or repeating-image "reflection" of fluxes if only elements within the sector under analysis are defined.

The transverse spray velocity components from some elements may result in spray impacting the combustion chamber wall or other solid surface, such as baffles installed on the injector for combustion stabilization. By proper selection of LISP input variables, such impingement upstream of z_0 on the chamber wall and/or radial baffles may be accumulated as abnormally high spray fluxes at surface mesh points. Both this accumulation at solid surfaces and the spray "reflections" at surfaces of symmetry are accomplished by defining mesh points outside of the sector under analysis and folding the calculated flows at those exterior mesh points into the appropriate surface or interior mesh points.

Considerably more details about selecting a sector for analysis, selecting the elements to define, and setting up a mesh system have been given in earlier documents concerning the LISP computer program (Ref. 11 and 16). The version of LISP employed in this version of DER is that of Ref. 11.

Mesh Point Fluxes. It is assumed that the propellant spray fluxes at each mesh point in plane z_0 are the linear sums of the fluxes produced by the individual injection elements. That is:

$$\hat{W}_f\ (r,\theta,z) = \sum_{i=1}^{N_{EL}} \hat{w}_{fi}\ (r,\theta,z) \qquad (1)$$

and

$$\hat{W}_o\ (r,\theta,z) = \sum_{i=1}^{N_{EL}} \hat{w}_{oi}\ (r,\theta,z) \qquad (2)$$

This assumption is justified if: (1) the individual injector elements have reproducible and predictable spray flux patterns which have been (or can be) measured and correlated; and, (2) individual elements' spray patterns are not altered grossly, between their injection sites and the plane z_0, by collisions between sprays from neighboring elements.

Concerning the first of these conditions, Rupe (Ref. 17) has observed experimentally that very reproducible sprays can be produced if quite long (L/D > 50) injection orifices are used. By roughening the orifices to force earlier attainment of fully developed turbulent jet velocity profiles in a shorter length, Rupe also obtained good spray flux reproducibility with L/D ≃ 20. For elements having even shorter orifices, the reproducibility becomes somewhat poorer, but a substantial body of short orifice data has been satisfactorily correlated (Ref. 18). The method of correlation is discussed briefly in the next subsection.

The degree to which sprays from typical impinging-jet rocket injection elements conform to the second condition was discussed in Ref. 11. A propellant droplet from one injection element was estimated to have a mean free path in excess of 1 inch through the dense part of a neighboring element's spray. It was concluded that, while collisions and interactions occur, their effects will usually not be strong enough to invalidate the linear superposition assumption.

Elemental Flux Distributions. The mass flux distributions $\hat{w}_{fi}$ and $\hat{w}_{oi}$, for the individual element have been derived from measured single-element spray flux distributions determined in cold-flow experiments. Single-element flux patterns were fitted to the generalized expression:

$$\hat{w}_i\ (x,y,z) = \frac{\hat{w}_{001}}{z^2} \left\{ \left[1 + C_1 \left(\frac{y}{z}\right) + C_2 \left(\frac{y}{z}\right)^2 \right] + \left[C_3 \left(\frac{x}{z}\right) + C_4 \left(\frac{x}{z}\right)^2 \right] \left[1 + C_5 \left(\frac{y}{z}\right) + C_6 \left(\frac{y}{z}\right)^2 \right] \right\} e^{-a\left(\frac{x}{z}\right)^2 - b\left(\frac{y}{z}\right)^2} \qquad (3)$$

which is applied separately to each propellant from an element. The (x,y,z) coordinate system in Eq. 3 is referenced to the element's impingement point from which its spray is presumed to emanate, while the fluxes required in Eq. 1 and 2 must be referenced to the chamber's cylindrical coordinates. The necessary transformations are performed internally by LISP.

The coefficients a, b, $\hat{w}_{001}$, and C_1 through C_6 are evaluated empirically by means of the cold-flow simulation test data. Briefly, the correlation method consists of:

1. Simplifying Eq. 3 to apply to a specific element type. This usually involves applying symmetry and continuity conditions to identify coefficients which must vanish or are functionally related to other coefficients.

2. Integrating the simplified elemental flux equation, and appropriate x and y moments of it, along the x and y axes or over the entire x, y-plane[1]

3. Performing the equivalant summations (numerical integrations) on the cold-flow distribution data to obtain empirical values of the integrals

4. Equating the appropriate expressions from (2) and (3) to form a system of algegraic equations in the unknown distribution correlation coefficients

5. Solving that set of equations (and, perhaps, starting over with a different set of integrals when a pathological case is encountered)

6. Repeating steps (1) through (5) for several different tests, with element design and operating conditions varied, and correlating the

1. The form of Eq. 3 was selected because it satisfies continuity, predicts the observed inverse square relationship between mass flux and distance downstream of the impingement point, and because it is integrable over intervals like $0 \leq x \leq \infty$, $-\infty \leq y \leq \infty$, etc.

correlation coefficient values to the parameters varied, (typically, varied parameters are orifice diameters, impingement angles, and impinging stream momentum ratios.)

7. Coding a subroutine for the element type so that the foregoing correlation and a method for extracting correlation coefficients from it become part of the LISP subprogram block.

More detailed information on this process, example calculations, and the currently available correlations may be found in Ref. 18 and 19, although the version of LISP being discussed here is limited to the correlations given in Ref. 11. (Those correlations that are provided in the December 1971 version of LISP are detailed in Ref. 19, a catalog of correlation coefficients which was assembled under the contract reported herein. A summarization of the catalog is given on page .)

This version of LISP is strictly for analyzing liquid/liquid propellant injection. It considers an injector to be made up of one or more of the following element types:

Type 1--Unlike Doublets
Type 2--Like Doublet (single)
Type 3--Like Doublet (pairs)
Type 4--Triplets
Type 5--Pentads or 4-on-1 Elements
Type 6--No Logic Provided
Type 7--Showerhead (but, no correlations exist)
Type 8--Special callout by general spray flux equation
Type 9--Special callout by subprogram

LISP Contains subroutines which provide spray flux distribution correlation coefficients for the first five element types. The flux from each element is analyzed by LISP in terms of its own rectangular coordinate system and then transformed to the chamber's cylindrical coordinates for calculating the element's contribution to mesh point fluxes. Basic element coordinate systems, along with certain element design parameters required as LISP input data, are illustrated in Fig. 5. For single impinging stream elements, their origins lie at the geometric impingement point whereas, for a like-doublet pair element, the origin is assigned a central position on the injector face. Element orientations on the injector face which differ from

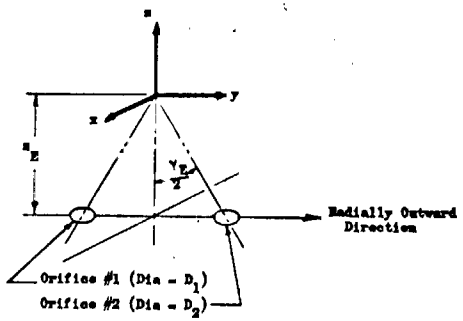

Type 1: Unlike Doublet Element
($D_2 \neq D_1$, in general)

Type 2: Like Doublet Element
($D_2 = D_1$)

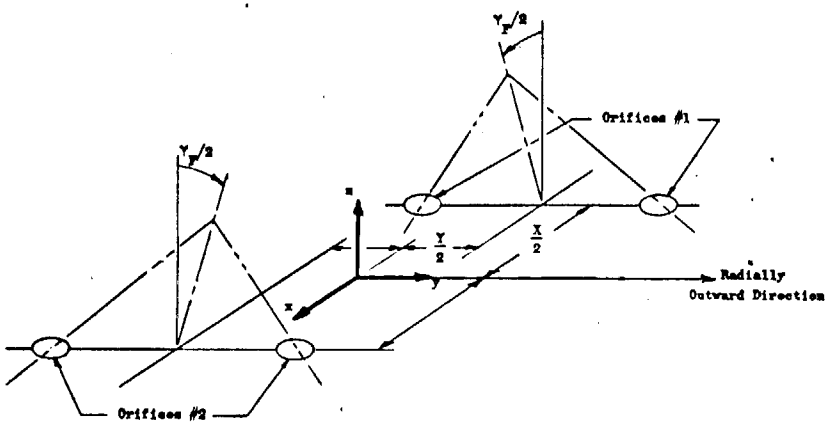

Type 3: Like Double Pair Element
(4 Holes = 1 Element)

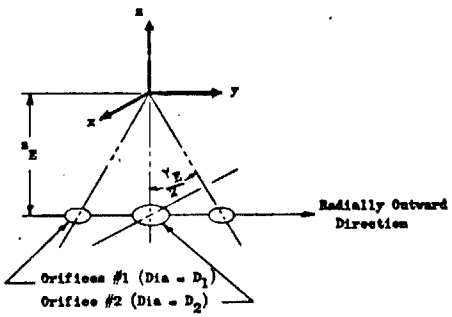

Type 4: Triplet Element

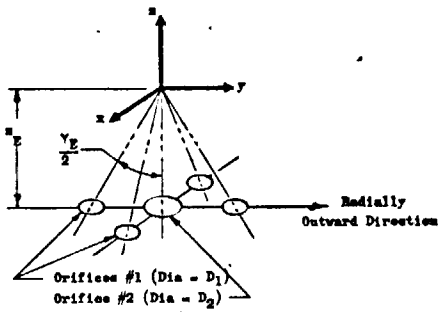

Type 5: Pentad or 4-on-1 Element

Figure 5. Liquid/Liquid Injection Element Types Included in LISP Program Block

these basic coordinate specifications are obtained by making one or more successive angular rotations about specific element coordinate axes.

Elements designated with a Type 8 callout are treated by LISP as if they were unlike doublets, but the user must supply the correlation coefficients for Eq. 3 as input data. This feature permits having cold-flow characterization made of the single element (or elements) to be incorporated into a prospective injector and then employing the correlated spray coefficients from the specific cold-flow experiment in LISP; it is useful for situations where spray coefficients have not been determined previously for the intended elements, and it also permits accounting for factors such as short L/D orifices and manifold cross-flows in LISP calculations by incorporating the effects in single element cold-flow experiments.

The Type 9 callout is intended to be used for element designs whose mass flux profiles cannot be fitted by the general correlation equation. In that event, the user is expected to modify LISP to call a subroutine (which the user will have formulated and programmed) specifying the mass flux distribution for the particular element.

Element Injection Rates. LISP calculates injection rates for both propellants flowing through each element by means of a standard orifice equation:

$$\dot{w}_i = C_{D_i} A_i \sqrt{2 g_c \rho \Delta P} \qquad (4)$$

Injection velocities are then calculated from a simple one-dimensional continuity equation:

$$u_i = \dot{w}_i / (\rho A_i) \qquad (4a)$$

Element Spray Droplet Sizes. A very essential part of the combustion field initialization performed by LISP is the assignment of propellant droplet size distributions. In the DER computer program, LISP computations are concerned

only with a mass median diameter ($\overline{D}$) for each propellant's spray. Later, during STC program block initialization of stream tubes, the sprays are distributed into a discrete number of droplet size groups. The magnitudes of the $\overline{D}$'s frequently have a direct, strong influence on the steady-state propellant combustion efficiency computed by DER. Thus, the correlations used for deriving droplet diameters may be the single most important factor in determining combustor performance and an effort should be made to ensure that the most realistic values of $\overline{D}$ are supplied to LISP.

If an injector element is specified as being any one of Type 1 through Type 5, LISP will calculate a mass median drop diameter for the propellant of each orifice of the element. These calculations for Type 1, 4, and 5 elements are based upon the correlations of Dickerson et al. (Ref. 20) derived from hot wax experiments. Constants in the correlations have been modified to give characteristic diameters which make calculated c* efficiencies compatible with measured results for three injectors tested, analyzed, and reported in Ref. 11. With elements of Type 2 and 3, the mean drop diameters are based on the empirical correlation of Falk, et al. (Ref. 21), modified to make c* efficiencies calculated by the STC computer program correlate with experimental data from that report (Ref. 13). Alternatively, the LISP user may assign his own estimation of drop diameter to the flow from each orifice of a given element. For elements defined as Type 8 or 9, the user always supplies his estimation of a characteristic drop size. The appropriate mean droplet diameter is the mass median diameter.

Mesh Point Droplet Sizes and Velocities. Mass-flux-weighted average values of spray mass median droplet diameters and spray velocity vector components are calculated at each mesh point using the appropriate values for spray arriving from each individual element which contributes to the mesh point. For example:

$$\overline{D}_f\ (r,\theta,z_0) = \frac{\sum_{i=1}^{N_{EL}} \hat{w}_{fi}\ (r,\theta,z_0)\ \overline{D}_{fi}\ (r,\theta,z_0)}{\sum_{i=1}^{N_{EL}} \hat{w}_{fi}\ (r,\theta,z_0)} \qquad (5a)$$

$$u_{zo}\,(r,\theta,z_0) = \frac{\sum_{i=1}^{N_{EL}} \hat{w}_{oi}\,(r,\theta,z_0)\; u_{zoi}\,(r,\theta,z_0)}{\sum_{i=1}^{N_{EL}} \hat{w}_{oi}\,(r,\theta,z_0)} \qquad (5b)$$

Spray Gasification. Partial propellant evaporation upstream of z_0 is calculated by a simplified, integrated evaporation expression

$$\hat{w}'(r,\theta,z_0) = \hat{w}(r,\theta,z_0)\left[1 - \frac{C_{k'}\,\Delta z}{\bar{D}^2 u_d}\right]^{3/2} \qquad (6)$$

where $\hat{w}'$ is the liquid spray flux actually arriving at the point (r,θ,z_0). The coefficient $C_{k'}$ is related to the evaporation coefficient k' used in the subsequent spray combustion analysis. However, because the liquid sprays are not fully atomized over the entire Δz distance, values of $C_{k'}$, including a convective Nusselt number, are usually assumed to be only about 1/5 to 1/4 of the stagnant values of k'. The propellant vapors said to be generated by this calculation are summed over all mesh points to yield a single overall vapor flowrate for each propellant. Use of such a simplified evaporation expression is, to some extent, justified by the relatively small percentage of evaporation in the spray formation zone.

LISP Data Output. Data computed by LISP are output in three forms: (1) tabular computer printout, (2) computer-plotted CRT graphs, and (3) a scratch unit record of data to be transferred to the STC subprogram block.

After listing all of the input data and a table of injection elements, the tabular printout is concerned exclusively with collection plane data. The injection element table lists the coordinates, calculated injection flowrates, and initial propellant median drop diameters for all injection elements included in the analysis. The bulk of the printout consists of two tables of mesh point data. The first of these lists computed mesh point parameters as if there were no spray vaporization, while the second lists the spray mass fluxes and median droplet diameters reduced by vaporization. Finally, if CRT plots of propellant mass flux are generated by LISP, there are rather extensive tables of data detailing the completion of a full circle by repetition of a pie-slice.

One or more of four types of computer-generated data plots may be called for by input option. Two of these are illustrated in Fig. 6. The first shows a cross-sectional graph of the mesh system analyzed and the location of each injection element (Fig. 6a). The second illustrates propellant mass flux distributions by means of contour lines (Fig. 6b). Not illustrated, but related to the contour plots, are shade plots wherein the density of shading is related to local propellant mass flux. Also not illustrated are graphs of fuel and oxidizer mass flux around the chamber slice at specified values of chamber radius.

Spray Combustion: STC Subprogram Block

The Stream Tube Combustion (STC) computer subprogram block analyzes bipropellant liquid spray combustion from the LISP collection plane z_0, where it is initialized, through the nozzle throat. Selected data computed by LISP are transferred (via scratch data unit) to the STC subprogram block. There, by one of two alternate methods, several mesh points' propellant fluxes and flow areas are combined to form one of the stream tube flows to be analyzed by STC. Model solutions for spray gasification and combustion are obtained numerically for several systems (one for each stream tube) of simultaneous ordinary differential and algebraic equations by starting from known conditions at the LISP collection plane and marching downstream in small axial steps.

Input to the STC computer program consists of chamber wall profile, propellant properties, combustion gas properties, and either (1) initial-plane gaseous

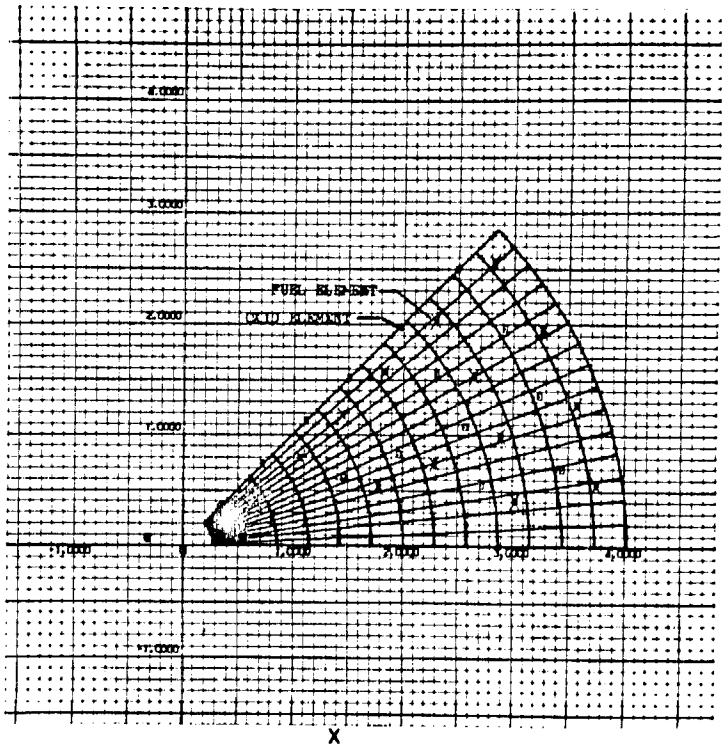

a) Injector Segment, Showing Mesh System and Element Locations

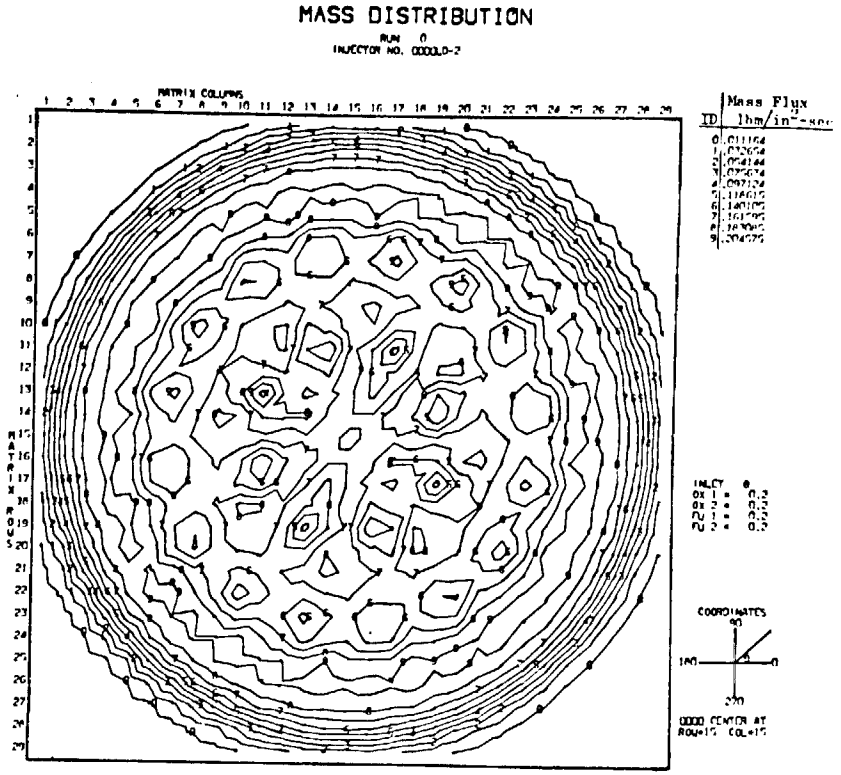

b) Full Injector Contour - Plot of Mass Flux Distribution

Figure 6. Examples of Computer-Plotted Data From LISP Program Block

flowrate and mixture ratio and spray flowrates, velocities, and droplet diameters for all spray size-groups entering each stream tube or (2) data from LISP from which these variables can be calculated. Up to 40 stream tubes can be initialized with as many as 12 spray size-groups (fuel and oxidizer combined) per stream tube. For most cases, using from 10 to 15 stream tubes will probably be nearly as accurate as using the full 40 permissible. On the other hand, it is recommended that not fewer than five spray size groups be specified for describing a liquid spray's size distribution. A special provision has been made, however, for calculating the spray burning rate if only one size group is specified for either propellant (Ref. page 83).

Stream Tube Initialization from LISP Data. Data transferred to STC from LISP are: propellant spray mass fluxes, mean droplet velocities and mass median diameters at each mesh point; mesh point coordinates; and total initial plane flow and how much of it is gasified for each propellant. At this point, the gas mixture ratio is considered to be uniform (constant) across the r,θ,z_0 plane. Axisymmetric stream tube flows may be initialized from these data by means of the following options:

1. All mesh points along each circle (r = constant) of LISP's mesh points are combined into one stream tube. Gasified propellants are retained as transferred from LISP, with uniform mass flux and uniform mixture ratio. This initialization method may be appropriate for injectors that form essentially axisymmetric flows. When applied to injectors which produce angular gradients in local propellant mixture ratio, however, it can effect substantial mixture ratio averaging and result in overcalculation of combustion efficiency.

2. Stream tubes are formed by combining mesh points of similar mixture ratio within specified annular zones. First, however, the gasified propellants are redistributed to provide a nearly uniform gas mass flux profile, but a mixture ratio distribution similar to the spray mixture ratio distribution. The gas mass fluxes are initially approximated as being uniform:

$$\dot{w}_{g_{ij}} = (\dot{W}_{gf} + \dot{W}_{go}) \frac{A_{ij}}{\sum_{i,j} A_{ij}} \qquad (7)$$

Then the gas mixture ratio at each mesh point is said to be equal to the spray mixture ratio there:

$$c_{ij} = \frac{\dot{W}_{o_{i,j}}}{\dot{W}_{f_{ij}}} \tag{8}$$

In general, however, these two assumptions will not be compatible with conservation of propellant species flowrates, e.g.:

$$\dot{W}_{gf} \neq \sum_{ij} \frac{\dot{w}_{g_{ij}}}{1 + c_{ij}} \tag{9}$$

Therefore, the fuel and oxidizer contributions to each mesh point's gas flow are scaled separately to preserve species continuity:

$$\dot{w}_{gf_{ij}} = \frac{\dot{w}_{g_{ij}}}{1 + c_{ij}} \left[\frac{\dot{W}_{gf}}{\sum_{ij} \frac{\dot{w}_{g_{ij}}}{1 + c_{ij}}} \right] \tag{10}$$

$$\dot{w}_{go_{ij}} = \frac{c_{ij}\dot{w}_{g_{ij}}}{1 + c_{ij}} \left[\frac{\dot{W}_{go}}{\sum_{ij} \frac{c_{ij}\dot{w}_{g_{ij}}}{1 + c_{ij}}} \right] \tag{11}$$

These definitions complete the specification of propellant flows at each mesh point.

Following distribution of the gases among the mesh points, a wall boundary layer stream tube is established by combining all the mesh points at the wall.

If that stream tube does not contain more than one-twelfth of the total flow, the next inward circle of mesh points will also be combined into it, etc., until it does. Then the remaining LISP circles of mesh points are divided into a specified few (2 to 4, perhaps) circular or annular zones having roughly equal propellant flowrates.

Within each of these zones, the mesh point flows are accumulated into stream tubes according to their total propellant mixture ratios, rather than positions. the number of stream tubes per zone is specified and they are assigned roughly equal propellant flowrates. The lowest mixture ratio mesh points are combined into the first stream tube until its fraction of the zonal flow rate is reached, the next lowest mixture ratio mesh points are assigned to the second stream tube, etc. Finally, the resultant stream tubes are arbitrarily assigned radial positions within their respective zones, with the fuel-rich stream tubes lying inside of the oxidizer-rich ones.

This method preserves the angular averaging objected to before only at the wall and is accepted for a fraction of the flow to get a wall-bounding stream tube that is characteristic of the mean wall mixture ratio. For the remainder of the flow, the nonphysical combining of mesh points on the basis of mixture ratio has been found to effect only modest changes in calculated mixing efficiencies from those based on the full LISP distributions.

System of Equations. The system of equations for the $i^{\underline{th}}$ stream tube is:

Gas Phase. The gas phase equations are as follows:

Continuity:

$$\frac{d}{ds}\left(\rho_i u_i A_{s_i}\right) = A_{s_i} \sum_{n,j} \left(\dot{m}_j^{\,n}\right)_i \tag{12}$$

Momentum:

$$\frac{d}{ds}\left(\rho_i u_i^2 A_{s_i}\right) = A_{s_i}\left[-g_c\left(\frac{dp}{ds} + \sum_{j,n}\left(F_j^n\right)_i\right) + \sum_{j,n}\left(\dot{m}_j^n\right)_i\left(u_{dj}^n\right)_i\right] \quad (13)$$

Adiabatic Energy Equation:

$$T_i = T_{oi}\left[1 - \frac{\gamma_i - 1}{2}\left(\frac{u_i}{a_{oi}}\right)^2\right] \quad (14)$$

where equilibrium stagnation gas properties

$$T_{oi} = T_o(c_i),\ \gamma_i = \gamma(c_i),\ \text{and}\ M_{wi} = M_w(c_i)$$

are tabulated and

$$a_{oi} = \left[\frac{\gamma_i R_u T_{oi} g_c}{M_{wi}}\right]^{1/2} \quad (15)$$

This corresponds to frozen expansion to local conditions from stagnation equilibrium. These combustion gas properties are obtained from separate calculation of equilibrium chamber stagnation conditions for several mixture ratios and the nominal stagnation chamber pressure for a particular case being analyzed. They are also relatively weak functions of chamber pressure, but this dependence is neglected. Frozen specific heat ratios, γ, are used.

The local stream tube gas mixture ratio is obtained simply by integrating the evaporation rates to get gasified flowrates:

$$\dot{w}_{ji}(z) = \dot{w}_{ji}(z_0) + \int_{z=z_0}^{z} A_i \sum_n \left(\dot{m}_j^n\right)_i dz \quad (16)$$

Mixture Ratio:

$$c_i = \frac{\dot{w}_{oi}^{(z)}}{\dot{w}_{fi}^{(z)}} \tag{17}$$

State:

$$\rho_i = \frac{p\, M_{wi}}{R_u\, T_i} \tag{18}$$

Spray Phase (n^{th} droplet size group of j^{th} propellant). The spray phase equations are as follows:

Mass Continuity:

$$\frac{d}{ds}\left[\left(\rho_{dj}^{n}\right)_i \left(u_{dj}^{n}\right)_i A_{s_i}\right] = -A_{s_i}\left(\dot{m}_j^{n}\right)_i \tag{19}$$

Drop Number Continuity:

$$\frac{d}{ds}\left[\left(N_{dj}^{n}\right)_i \left(u_{dj}^{n}\right)_i A_{s_i}\right] = 0 \tag{20}$$

or, equivalently,

$$\left(\dot{N}_{dj}^{n}\right)_i = \left(N_{dj}^{n}\right)_i \left(u_{dj}^{n}\right)_i A_{s_i} = \text{constant}$$

Momentum:

$$\frac{d}{ds}\left[\left(\rho_{dj}^{n}\right)_i \left(u_{dj}^{n}\right)_i^2 A_{s_i}\right] = A_{s_i}\left[g_c \left(F_j^{n}\right)_i - \left(\dot{m}_j^{n}\right)_i \left(u_{dj}^{n}\right)_i\right] \tag{21}$$

The independent variable in these one-dimensional flow equations is the stream tube path length or flow direction, s_i. This variable is related to the stream tube's cylindrical (r,z) coordinates through the differential expression

$$ds_i = \left(dz_i^2 + d\bar{r}_i^2 \right)^{1/2} \tag{22}$$

where $\bar{r}_i$ is the stream tube's mean radius. For numerical stability in the solution, however, approximations are used that $ds_i = dz$ where the chamber wall is parallel to the axis and that

$$ds_i = dz \left\{ \frac{\left[\bar{r}_i^2 + \left(z_I - z \right)^2 \right]^{1/2}}{|z_I - z|} \right\} \tag{23}$$

in the nozzle. The basis for Eq. 23 may be seen by examining Fig. 7.

In this formulation, A_{s_i} appears as a dependent variable for which a solution is to be found. The gas phase equations are constrained, however, in terms of z-plane area:

$$\sum_i A_{z_i}(z) = A_c(z)$$

Therefore, the foregoing equations were modified for the computer program to permit direct solution for A_{z_i} by substituting:

$$A_{s_i} = A_{z_i} \frac{dz}{ds}$$

and neglecting the stream path curvature, i.e.: $\frac{d^2 z}{ds^2} = 0$.

The sets of gas and liquid phase equations are coupled through mass and momentum exchange between phases. For droplet gasification, the simple evaporation coefficient model is utilized:

$$\dot{m}_j^n = N_j^n \left(\frac{\pi}{8} \right) \rho_{\ell_j}^n D_j^n Nu_j^n k'^n_{s_j} \tag{24}$$

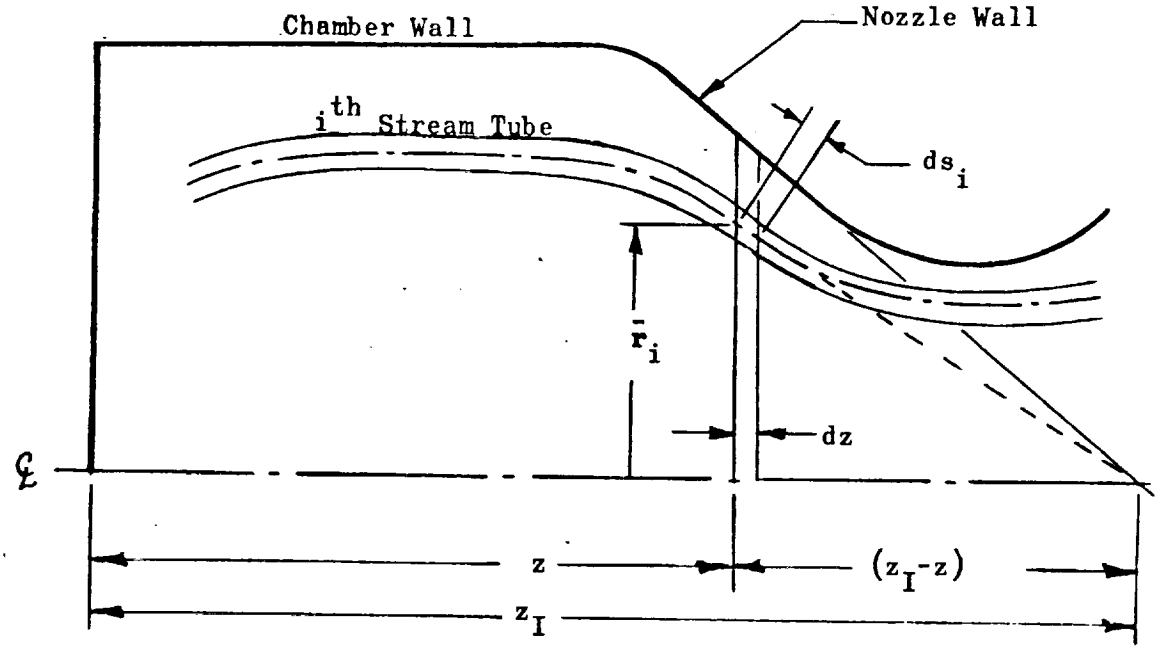

Figure 7. Schematic Illustration of Variables Denoting Local Conical Convergence of Stream Tubes

where the evaporation coefficient is

$$k'_{s_j}{}^{n} = \frac{8}{\rho_{\ell_j}{}^{n}} \int_{T_d}^{T} \frac{k_g}{\Delta H_v + \int_{T_d}^{T} c_{P_v}\, dT}\, dT \tag{25}$$

and

$$Nu_j{}^{n} = 2 + 0.53\, Re_j{}^{n} \tag{26}$$

Drag forces on spray droplets are expressed by

$$F_{j_i}{}^{n} = \frac{\pi}{8 g_c} N_{d_j}{}^{n} \rho_i\, D_j{}^{n}\, C_{D_j}{}^{n} \left(u_i - u_{d_j}{}^{n}\right) \left|u_i - u_{d_j}{}^{n}\right| \tag{27}$$

with the drag coefficient specified as

$$C_{D_j}{}^n = 24 \left(Re_j{}^n\right)^{-0.84} \quad ; \; Re_j{}^n \leq 80 \tag{28}$$

$$= 0.271 \left(Re_j{}^n\right)^{0.217} \quad ; \; Re_j{}^n > 80$$

Performance Parameters. Two separate parameters are calculated which are indicative of the overall degree of propellant mixing. These are calculated once in LISP, based on the flowrates associated with the LISP mesh points, and once in STC, based on the initial flowrates supplied to the stream tubes. One parameter is E_m, a mixing efficiency factor due to Rupe (Ref. 17) which expresses a mass-weighted average approach of local oxidizer mass fractions to the overall injected mass fraction:

$$E_m = 100 \left[1 - \sum_{i=1}^{n} \frac{\dot{w}_i (R - r_i)}{\dot{W} R} - \sum_{i=1}^{\bar{n}} \frac{\dot{w}_i (R - \bar{r}_i)}{\dot{W}(R-1)} \right] \tag{29}$$

where:

n = number of samples with $R > r$
$\bar{n}$ = number of samples with $R < r$
$\dot{w}$ = local propellant flowrate, lb_m/sec
$\dot{W}$ = total propellant flowrate, lb_m/sec
r, $\bar{r}$ = local oxidizer mass fractions, $\dot{w}_o/\dot{w}$
R = injection oxidizer mass fraction, $\dot{W}_o/\dot{W}$

The second parameter is a mixing c* efficiency, $\eta_{c^*,mix}$, which represents the maximum attainable c* efficiency corresponding to complete propellant gasification:

$$\bar{\eta}_{c^*,mix} = \frac{\sum_{i=1}^{n+\bar{n}} c^*(c_i)\dot{w}_i}{c^*(c_{inj})\dot{W}} \tag{30}$$

where c_{inj} is the injection mixture ratio ($\dot{w}_o/\dot{w}_f$), c_i is local mixture ratio ($\dot{w}_{o_i}/\dot{w}_{f_i}$) and $\dot{w}_i$, $\dot{W}$, n and $\bar{n}$ have the same meanings as above. Theoretical characteristic velocity is tabulated as a function of mixture ratio.

During STC's multiple stream tube analysis, a single value of c* efficiency is calculated from the n_t stream tubes' data at the throat plane:

$$\eta_{c^*} = \frac{\sum_{i=1}^{n_t} c^*(c_{g_i})\dot{w}_{g_i}}{c^*(c_{inj})\dot{W}} \tag{31}$$

Note the distinction between Eq. 30 and 31; local gasified propellant mixture ratios and flowrates are used in Eq. 31 rather than local total mixture ratios and flowrates, as in Eq. 30.

Method of Solution. The numerical integration scheme used to solve each stream tube's system of equations is the simplest first-order Runge-Kutta (or Euler) method. Selected for its simplicity, minimal data storage requirements, low execution times, and numerical stability, this method's accuracy is strongly dependent upon using sufficiently small step sizes. This limitation is reduced in importance by using backwards differencing in writing finite-difference equations and by solving the equations twice, using predicted values from the first, or predictor, solution as input data for a second, corrector, solution.

The STC program is first run in a single stream tube mode, i.e., a one-dimensional subsonic combustion analysis is made for the entire chamber using appropriate sums and averages of initial stream tube variables. This is done for two reasons: (1) to verify consistency of input data (initial-plane pressure is adjusted until the one-dimensional throat velocity is within a small tolerance of the calculated throat sound speed), and (2) to provide a mean adiabatic expansion coefficient, $\bar{\gamma}$, for combustion gas flow in the convergent part of the exhaust nozzle.

The latter coefficient is given by:

$$\bar{\gamma} = \left(\frac{\ln \dfrac{\bar{p}^*}{\bar{p}_1}}{\ln \dfrac{\bar{\rho}^*}{\rho_1}} \right) \tag{32}$$

where the subscript 1 refers to the beginning of nozzle convergence, the variables p^* and ρ^* are at sonic conditions and the over-bars refer to the one-dimensional flow analysis. It is used by the TRANS computer program (described in the next subsection) to calculate the coordinates of constant pressure surfaces (isobars) for transonic flow in the nozzle. TRANS isobars are generated and transferred to STC in nondimensional terms, so their use in STC requires knowledge of the nozzle throat radius, R_T (an input parameter), and sonic flow pressure, p^*. An approximate value of p^* is estimated from the nozzle throat plane pressure of the preceding averaged, single stream tube analysis:

$$p^* = \bar{p}^* \; p(z_0)/\bar{p} \; (z_0)$$

Following STC single stream analysis and TRANS analysis, the initial plane is reinitialized with its original input flowrates and is run in a multiple stream tube mode. This analysis is the source of steady-state combustion and performance data, some of which are used in the later TDK analysis.

One of the variables solved for is chamber pressure in each z-plane. Somewhere in the nozzle, the solution method is changed so that, rather than solving for pressure, absolute pressures are imposed upon the flow. These are obtained by multiplying the reduced pressures, p/p^*, of the TRANS isobars by p^*. The furthest upstream TRANS isobar may be planar or curved, depending upon the radius ratio of the nozzle and the shape of its convergent section. If it is curved, it is desirable to introduce a gradual transition from planar isobars to that first curved isobar which the solution encounters. Also, a gradual transition is desirable to smooth out any discontinuity in pressure levels between those solved for upstream and those imposed downstream of the transition. The gradual transition is provided by stopping the solution for pressure level at a position that is upstream of the nozzle throat by 1.3 times the axial distance that the furthest-upstream TRANS isobar intersects the nozzle wall, and using linear interpolation to obtain absolute pressure for the transition interval.

The imposition of absolute pressures overprescribes the problem and the solution then provides absolute values of stream tube areas which may or may not sum to the local nozzle flow area. Area continuity can only be satisfied by finding the appropriate combination of propellant flowrates and pressure level (p^*). This is accomplished only for the minimum flow area (irrespective of whether it is precisely at the throat position) by comparing it with the geometric throat area. The areas must agree within some input tolerance, along with compatibility of engine balance variables, to satisfy the throat boundary conditions. Otherwise, the multiple stream tube analysis is reperformed with adjusted values of initial plane pressure. When the deviations are only slightly too large, computer time is saved by redoing only the nozzle analysis.

STC Data Output. Data computed by STC are also output in the same three forms as are LISP output data, viz., tabular computer printout, a computer-plotted CRT graph, and a scratch unit record of data to be transferred to the TDK subprogram block. Additionally, stream tube initialization data and TDK start-line data may be output in punched-card form.

Unlike LISP's printout, the tabular printout generated by STC is predominantly intermediate data, printed out as the analysis proceeds along the combustor length, rather than end-product data to be used by another program. The printout begins with a listing of input data. This is followed by stream tube initialization data (which may also be punched-out) and other information pertinent to beginning the combustion analysis. The printout progresses, in turn, through the single (averaged) stream tube, transonic flow, and multiple stream tube analyses, including iterations as they occur, and is completed by printing values of variables prepared (and punched-out) for initializing the TDK start line.

Samples of STC printout are shown in Tables 1 and 2. Table 1 illustrates the throat station printout of the single stream tube analysis while Table 2 is a contraction of the throat station printout of the multiple stream tube analysis. The general format, in each case, gives essentially complete local data for the chamber geometry, combustion gas properties, and, finally, individual spray size groups. In the single stream tube case, the printout includes the volume number mean droplet diameter (D_{30}) for each propellant. Note that in the multiple stream tube case, combustion gas velocities and Mach numbers increase with increasing radial distance from the nozzle axis, reflecting the radial pressure distribution imposed upon the nozzle.

One computer-plotted CRT graph is generated from data computed during STC's multiple stream tube analysis (Fig. 8). An axial cross section of the axisymmetric combustion chamber is plotted along with the coordinates of the dividing stream lines between stream tubes, beginning at the STC initial plane and continuing through the nozzle throat.

TABLE 1. EXAMPLE OF DATA PRINTED OUT DURING SINGLE-STREAM TUBE ANALYSIS

BIPROPELLANT LIQUID ROCKET COMBUSTION ANALYSIS USING S T C PROGRAM

SINGLE STREAM TUBE ANALYSIS

Z = 2.650 IN. FROM INJECTOR

GAS VEL.= 3811.00 FT/SEC PRESS.= 77.449 PSIA TEMP.= 5053.97 R

DENSITY = 1.757E-05 LB/IN3 GAS M.W.= 1.7593 GAS FLOWRATE = 0.1420 LB/SEC

FLOW AREA = 0.1765 IN2 CONTR.RATIO = 1.0000 SMACH= 1.0000
PSTAG= 138.585

0.1767 1.0012 **CALCULATED FROM CONTINUITY

OVERALL PERCENT BURNED = 94.450

OXIDIZER PERCENT BURNED = 98.816 MEAN DROP DIAM.= 19.35 MICRONS

FUEL PERCENT BURNED = 87.633 MEAN DROP DIAM = 37.22 MICRONS

PROPELLANT SPRAY DATA

	GROUP NO.	DIAMETER MICRONS	VELOCITY FT/SEC	NO. FLOW DROPS/SEC	NO. CONC. DROPS/IN3	DENSITY LB/IN3	FLOWRATE LB/SEC
FUEL	1	0.97	3811.02	0.0	0.0	0.0	0.0
FUEL	2	6.12	2169.91	1.3465E 03	2.0227E 04	5.8715E-09	2.7003E-05
FUEL	3	16.55	1233.39	6.8849E 07	2.6335E 04	1.0443E-07	2.7298E-04
FUEL	4	26.37	1017.21	3.6492E 07	1.6927E 04	3.3831E-07	7.2936E-04
FUEL	5	41.37	912.04	2.0636E 07	1.7676E 04	6.6167E-07	1.2794E-03
FUEL	6	57.33	826.34	1.1605E 07	6.5110E 03	1.0906E-06	1.9146E-03
FUEL	7	90.96	715.96	4.6103E 06	3.0217E 03	1.9906E-06	3.0375E-03
OXID	8	0.59	3811.02	0.0	0.0	0.0	0.0
OXID	9	0.98	3811.02	0.0	0.0	0.0	0.0
OXID	10	0.35	3811.02	0.0	0.0	0.0	0.0
OXID	11	7.86	1598.52	1.0870E 03	3.2084E 04	2.3341E-08	7.9078E-05
OXID	12	26.01	856.62	3.8154E 07	2.0966E 04	5.5165E-07	1.0039E-03

CALCULATED C*-EFFICIENCY = 54.011 PERCENT

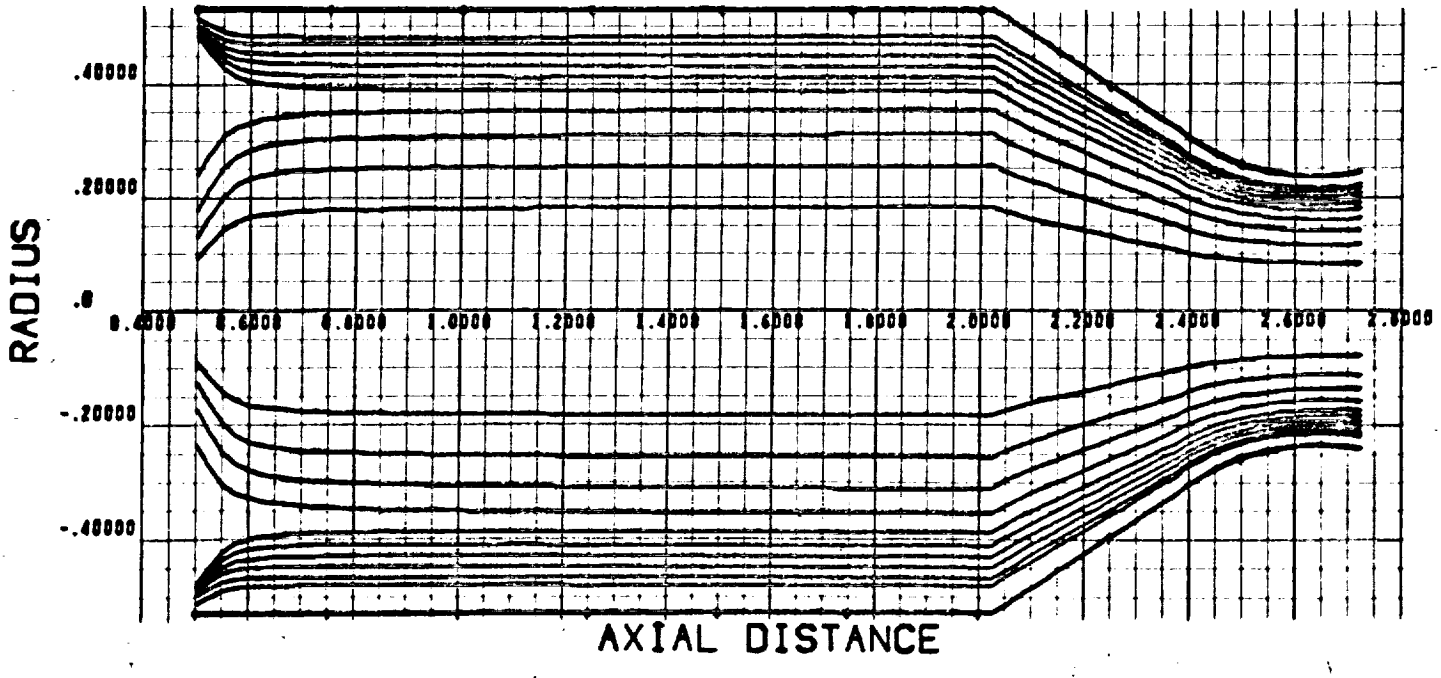

Figure 8. Example of Computer-Plotted Dividing Stream Lines From STC Program Block

TABLE 2. EXAMPLE OF DATA PRINTED OUT DURING MULTIPLE STREAM TUBE ANALYSIS

BIPROPELLANT LIQUID ROCKET COMBUSTION ANALYSIS USING S T C PROGRAM

MULTIPLE STREAM TUBE ANALYSIS

AXIAL POSITION = 2.660 CHAMBER PRESSURE = 82.911

CHAMBER AREA = 0.1765 CONTRACTION RATIO = 1.000

PROPELLANT BURNED (PERCENT)

FUEL = 87.430 OXIDIZER = 98.694 TOTAL = 94.295

STREAM TUBE CONDITIONS - GAS

STRM TUBE	FLOW LB/SEC	MIXTURE RATIO	TEMP R.	DENSITY LB/IN3	STRM VEL FT/SEC	MACH NUMBER	AREA IN2	MEAN RAD., IN	PRESSURE PSIA	PATH INCREMENT	PSTAG
1	0.01587	1.6109	5056.1	1.6632E-05	3554.4	0.9175	0.02583	0.0641	81.948	0.02500	134.391
2	0.01353	1.9163	5156.7	1.4350E-05	3562.7	0.9393	0.01724	0.1047	80.276	0.02500	134.456
3	0.01531	2.2552	5131.9	1.8968E-05	3537.4	0.9277	0.01902	0.1294	78.797	0.02500	134.490
4	0.01646	2.6357	5044.4	1.9479E-05	3514.3	0.9298	0.01984	0.1514	77.123	0.02500	134.768
5	0.01766	4.7740	4369.5	2.4505E-05	3206.0	1.0569	0.01661	0.1695	75.423	0.02500	135.805
6	0.00820	1.1444	4299.4	1.0624E-05	3855.4	1.0031	0.01053	0.1818	74.106	0.02501	134.044
7	0.00804	1.1950	4391.5	1.0517E-05	3912.8	1.0171	0.01037	0.1907	73.048	0.02501	134.089
8	0.00735	1.3370	4606.1	1.0190E-05	3980.6	1.0317	0.00960	0.1989	72.003	0.02501	134.070
9	0.00815	1.5733	4854.0	1.5870E-05	4017.1	1.0492	0.01058	0.2068	70.979	0.02501	134.204
10	0.00660	2.3556	5065.4	1.7439E-05	3868.2	1.0669	0.00827	0.2139	69.820	0.02501	134.529
11	0.02267	0.9394	3855.9	1.4732E-05	4071.4	1.0787	0.02870	0.2273	67.595	0.02501	133.787

STREAM TUBE CONDITIONS - SPRAY

STRM TUBE	GROUP PROP	NO.	DIAMETER MICRONS	VELOCITY FT/SEC	NO. FLOW DROPS/SEC	NO. CONC. DROPS/IN3	DENSITY LB/IN3	FLOWRATE LB/SEC
1	FUEL	1	0.23	3554.10	0.0	0.0	0.0	0.0
1	FUEL	2	6.24	2079.24	2.0753E 07	3.2194E 04	6.8645E-09	4.4251E-06
1	FUEL	3	16.76	1154.16	1.0612E 07	2.8562E 04	1.1808E-07	4.3718E-05
1	FUEL	4	28.64	676.47	5.6243E 06	1.6579E 04	3.8230E-07	1.1574E-04
1	FUEL	5	41.72	875.26	3.1390E 06	1.1721E 04	7.4521E-07	2.0222E-04
1	FUEL	6	57.76	764.96	1.7393E 06	7.2586E 03	1.2244E-06	3.0174E-04
1	FUEL	7	91.15	691.69	7.1066E 05	3.3139E 03	2.1973E-06	4.7121E-04
1	OXID	8	1.23	3554.10	0.0	0.0	0.0	0.0
1	OXID	9	1.04	3554.10	0.0	0.0	0.0	0.0
1	OXID	10	0.34	3554.10	0.0	0.0	0.0	0.0
1	OXID	11	8.12	1525.86	1.0457E 07	3.4798E 04	2.7871E-08	1.3165E-05
1	OXID	12	26.38	823.14	5.7766E 06	2.2635E 04	6.2154E-07	1.5842E-04
2	FUEL	1	1.17	3562.77	0.0	0.0	0.0	0.0
2	FUEL	2	5.99	2131.12	1.2449E 07	2.6229E 04	5.3132E-09	2.3431E-06
2	FUEL	3	16.54	1212.91	6.3659E 06	2.5361E 04	1.0039E-07	2.5197E-05
2	FUEL	4	28.41	985.74	3.3739E 06	1.6540E 04	3.3159E-07	6.7716E-05
2	FUEL	5	41.49	863.32	1.9079E 06	1.0437E 04	6.5195E-07	1.1917E-04
2	FUEL	6	57.50	802.30	1.0731E 06	6.4633E 03	1.0759E-06	1.7862E-04
2	FUEL	7	90.59	697.09	4.4629E 05	2.6514E 03	1.9467E-06	2.9117E-04
2	OXID	8	1.32	3562.77	0.0	0.0	0.0	0.0
2	OXID	9	0.95	3562.77	0.0	0.0	0.0	0.0
2	OXID	10	0.22	3562.77	0.0	0.0	0.0	0.0
2	OXID	11	7.99	1549.92	1.1769E 07	3.6694E 04	2.8031E-08	8.9804E-06
2	OXID	12	26.21	830.94	4.1310E 06	2.4024E 04	6.4712E-07	1.1127E-04
11	FUEL	1	0.98	4069.02	0.0	0.0	0.0	0.0
11	FUEL	2	6.47	2066.77	3.0764E 07	4.3145E 04	1.2237E-08	6.7075E-06
11	FUEL	3	16.93	1253.05	1.5702E 07	3.6330E 04	1.5423E-07	6.7421E-05
11	FUEL	4	28.80	1076.49	8.3215E 06	2.2441E 04	4.8944E-07	1.7407E-04
11	FUEL	5	41.78	968.53	4.7056E 06	1.4111E 04	9.0111E-07	3.0049E-04
11	FUEL	6	57.74	880.83	2.6466E 06	8.7271E 03	1.4707E-06	4.4600E-04
11	FUEL	7	91.65	765.94	1.0514E 06	3.9845E 03	2.6968E-06	7.0855E-04
11	OXID	8	0.47	4069.02	0.0	0.0	0.0	0.0
11	OXID	9	0.94	4069.02	0.0	0.0	0.0	0.0
11	OXID	10	0.39	4069.02	0.0	0.0	0.0	0.0
11	OXID	11	9.40	1433.23	1.4850E 07	3.0194E 04	3.7352E-08	1.8432E-05
11	OXID	12	27.48	897.51	5.2126E 06	1.6886E 04	5.2365E-07	1.6182E-04

CALCULATED C*-EFFICIENCY = 90.295 PERCENT

Transonic Nozzle Flow: TRANS Subprogram Block

A transonic flow analysis section was adapted from the reference TDK computer program (Ref. 14), as modified (Ref. 22) to utilize an elliptic coordinate transformation solution method (Ref. 23). This section was removed from the TDK program and modified so that it would generate a family of isobaric lines throughout the transonic flow regime and provide a computer-plotted graph of that family. The necessary input data are obtained from the averaged, single stream tube solution of STC, so this TRANS subprogram block gives a homogeneous flow solution. For homogeneous flow, TRANS solutions are stable with radius ratios as small as 5/8.

As input data, TRANS needs values only of the nozzle throat radius, R_R, and a mean expansion coefficient, $\overline{\gamma}$. Isobaric coordinates are calculated in terms of axial distance, X, from the throat plane and radial distance, R, from the nozzle axis; both dimensions are normalized to the throat radius. Multiple isobars are generated, one at a time, by starting downstream of the throat and marching upstream with equal intervals, $\Delta\alpha$, in the angle between the nozzle axis and a line tangent to the nozzle wall at the isobar/wall intersection point. The program is structured such that that intersection point for the fifth isobar is at the throat; this isobar later becomes the TDK start line. Four isobar/wall intersection points lie downstream of the throat ($\alpha>0$) and the remainder lie upstream of the throat ($\alpha<0$). The angular interval between isobars is given by:

$$\Delta\alpha = -\left(1 + \frac{2}{R_R}\right) \qquad (33)$$

Generation of isobars continues until either (1) there are 20 of them or (2) an isobar exhibits significant reverse, or upstream curvature. In the latter case, that last upstream-curving isobar is replaced with a planar surface.

The TRANS program also calculates a nozzle discharge coefficient using the third order equation given in Ref. 23:

$$C_{ND} = 1 - \frac{\bar{\gamma}+1}{(1+R_R)^2}\left[\frac{1}{96} - \frac{(8\bar{\gamma}-27)}{2304(1+R_R)} + \frac{(754\,\bar{\gamma}^2 - 757\,\bar{\gamma} + 3633)}{276{,}408(1+R_R)^2}\right] \tag{34}$$

TRANS Data Output. The transonic flow analysis is performed by TRANS between the single and multiple stream tube combustion analyses of STC. Data computed by TRANS are used exclusively by STC, to which they are transformed by label CØMMØN blocks. The isobaric pressures, Mach numbers, coordinates, and local flow directions are also printed out and the isobaric coordinates form the bases of a computer-plotted CRT graph.

Two computer-plotted examples from TRANS analyses are shown in Fig. 9, where: the nozzle axis is at the bottom (R/RT = 0); flow direction is from left to right; a portion of the nozzle wall, defined by $-30° \leq$ wall angle $\leq +8°$, is shown as the upper curve; isobars are generated from right to left at nozzle wall angle intervals of 2.00° (Eq. 33 was not used in these runs). The monotonic downstream curvature of the constant pressure surfaces is apparent, as is its accentuation by lowering the nozzle radius ratio. Included on the figure are tables which list the pressure ratio, p/p*, and Mach number for each isobar.

Supersonic Nozzle Expansion: TDK Subprogram Block

The TDK subprogram block of DER is a shortened and somewhat modified version of the ICRPG reference Two-Dimensional Kinetic computer program of Ref. 14. That program computes the expansion, through a rocket exhaust nozzle, of a kinetically limited, reacting gas flow. The flow may be axisymmetrically striated. However, if the analysis begins from subsonic initial conditions, the flow striations are restricted to two zones. In that case, TDK solves for the equilibrium conditions and compositions at the initial plane and performs one-dimensional kinetic (ØDK)

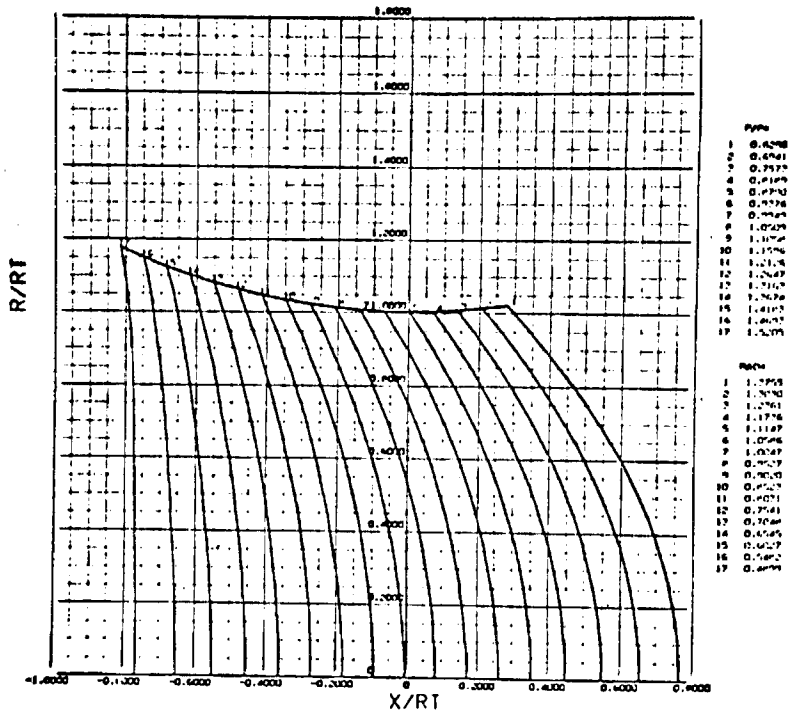

a) Radius Ratio = 2.00

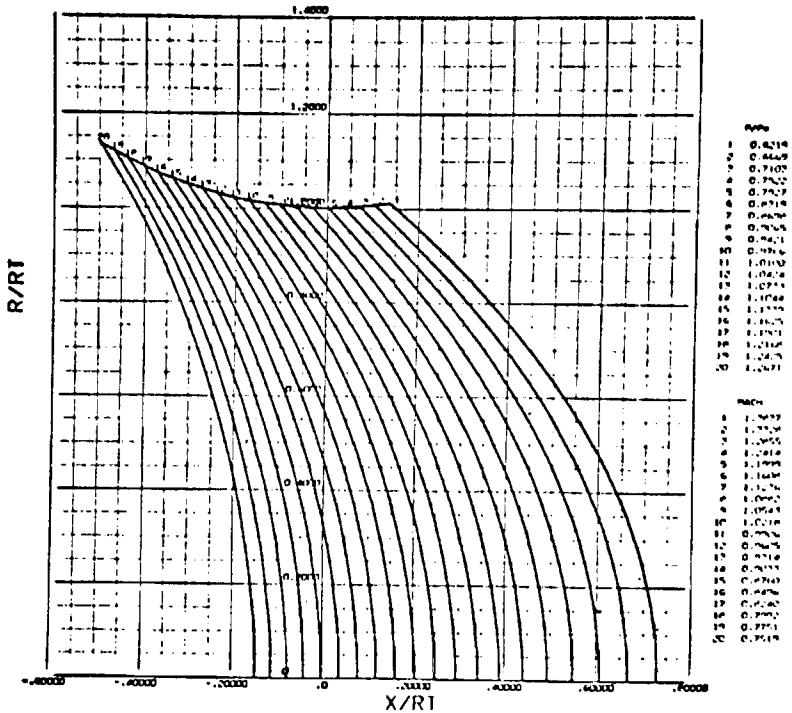

b) Radius Ratio = 1.00

Figure 9. Nozzle Pressure Distributions Calculated by the TRANS Computer Program

expansions through the nozzle throat for each of these zones, independently. The ØDK data are combined, through a two-zone transonic flow solution, to initialize a slightly supersonic "start line" for TDK's principal analysis: a method-of-characteristics solution for the supersonic nozzle expansion.

Flows characterized by more complicated radial mixture ratio distributions than a simple two-zone structure can also be analyzed by TDK. In that case, the analysis is restricted to the supersonic flow and is initialized by the user at the slightly supersonic start line.* In this "long-form-option", the flow is divided into a number ($\leq$24) of discrete zones and complete flow initialization data, including chemical composition, are provided for each zone.

The approach taken in adapting TDK to DER usage was to utilize the long-form option, initializing the supersonic start line from STC-computed data, to the extent possible, supplementing it with other read-in data and TDK computations as required. In essence, the supplemental data describe the nozzle contour and provide program controls, and the equilibrium section of TDK initializes stream tube chemical compositions at the start line.

Initialization from STC Data. Coordinates and flow direction at 40 points along the isobaric TDK initial line, computed by TRANS, are transferred to TDK. In the STC analysis, the intersections of dividing-stream-lines (between neighboring stream tubes) with the TDK initial line are found and their coordinates are transferred to TDK. Also transferred to TDK are the gas mixture ratio and velocity at each stream tube's intersection with the initial line. The initial-line pressure and a mean vaporization efficiency complete the specification of data from STC.

The composition of each stream tube's combustion gases must be specified at the initial line. The simplified tabular specification of stagnation combustion product properties as functions of mixture ratio, which is used in STC, essentially

*This restriction has been removed in an improved version of TDK (Ref. 15).

provides local isentropic frozen expansion from stagnation equilibrium. Species concentrations are not included in that specification because they are not needed for STC computations. Therefore, the equilibrium analysis section of TDK is used to obtain static equilibrium initial line conditions for each stream tube, based on the specified mixture ratio, flow velocity, and pressure. In addition to gas composition, the molecular weight, temperature, and density are derived from the equilibrium solution. Thus, these flow parameters may be discontinuous at the initial line because of the abrupt change from STC's frozen expansion of local stagnation equilibrium to TDK's static equilibrium conditions.

TDK Program Modifications. A large part of the reference TDK program is identical to the reference one-dimensional kinetic (ØDK) computer program. That section of TDK has been modified for DER program usage by:

1. Solving for equilibrium conditions only at the initial-line position in the flow, rather than at chamber stagnation, throat position, and an expansion point (this avoids generation of unneeded data).
2. Performing that initial line equilibrium solution repetitively, once for each stream tube.
3. Bypassing the one-dimensional kinetic nozzle flow analysis.

The transonic flow analysis section of the reference TDK program has been replaced completely. Transonic flow is no longer analyzed here; the functions now performed by this section are distribution of 49 discrete initial-line points among the stream tubes and assignment of appropriate flow properties to those points. Two points, having identical coordinates, but different properties, are required to define each dividing stream line between stream tubes. This limits to 24 the number of stream tubes which can be initialized. If there are n_t stream tubes, there are $49-2n_t$ extra points which are assigned as interior points of the widest stream tubes. The foregoing equilibrium flow properties for each stream tube are then assigned to all initial line points associated with that stream tube.

The section of TDK which calculates the supersonic, kinetic expansion in the nozzle downstream of the initial line has been modified to account for the reduction in specific impulse due to incomplete combustion, i.e., unevaporated propellants passing through the nozzle throat. In the reference program, specific impulse is calculated at any given point in the solution by dividing a local integrated value of thrust by the total gaseous flowrate, obtained by integrating ρu over the initial line. In the modified version, that total gaseous flowrate has been replaced by a total propellant flowrate.

No account is taken of continued evaporation or acceleration that unevaporated propellant sprays might undergo in the supersonic nozzle expansion section. Neither is their momentum added to the initial line impulse; this omission was made consciously, in the belief that it responded to a JANNAF subcommittee discussion concerning the likelihood that the calculated gas-phase momentum would be too high because the residual spray's kinetic energy had not been deducted from the total combustion gas energy. (A subsequent order of magnitude analysis has indicated that the kinetic energy effect is small compared to the neglected momentum effect and, therefore, that this omission is invalid and should be corrected.)

If condensed species are found to exist at any point along the TDK initial line, the reference TDK computer program terminates the analysis and does not perform the supersonic expansion calculations. Because one or more stream tubes may be at mixture ratios which produce some condensed combustion products, the DER version of TDK was modified to bypass this termination control. The mass of the condensed species is neglected and the mass fractions of the attendant gaseous species are normalized so that their sum is unity.

TDK Data Output. Extensive tables of TDK data are printed out. A series of tables, one for each stream tube, details the results of the start-line equilibruim computations. The flow properties at each start-line point are tabulated, as are the coordinates of a series of points along the nozzle wall. The major data printout is a massive table of calculated combustion gas chemical composition and physical properties along selected left-running characteristics in TDK's method of

characteristics solution. To illustrate the physical nature of this TDK output, coordinates of the start line, dividing stream lines and left-running characteristics for an eight stream tube flow are shown in Fig. 10.

Performance data are also printed in this last TDK printout table. When a left-running characteristic intersects the nozzle wall, values of specific impulse and thrust coefficient are printed for that local expansion ratio.

TDK will also punch out a table of data concerning the flow along the nozzle wall, by input option, for subsequent input data to the reference TBL computer program, which calculates wall boundary layer losses. However, the STC subprogram block does not punch out similar data for the flow upstream of the nozzle throat, nor has a logical structure been provided for recomputing nozzle performance with the DER version of TDK with inputs modified to reflect the TBL results. Exercizing this option is not recommended.

Evaluation of Model Validity

This version of DER was developed and evaluated using design and operating conditions corresponding to engine firing tests reported in Ref. 21 using FLOX (80% F_2 - 20% O_2)/LPG(55% CH_4 - 45% C_2H_5) propellants. A large number of variations were made in injector design, chamber design, and operating conditions, and, as a result, a fairly wide range of η_{c^*} was experienced, producing ideal data for evaluating a performance model.

One set of test conditions was selected as a nominal checkout case, and adjustable parameters in the DER computer program input were varied to force predicted η_{c^*} to agree with that measured experimentally. In this particular case, an 8.06-inch-diameter, 30-inch L* combustion chamber has a 12.2-inch-long cylindrical section preceding nozzle convergence, which began abruptly. A short conical convergent section, with 30-degree-half-angle, was tangent to a circular arc throat section with a radius ratio of 2.00; the 5.70-inch diameter throat was 15.7-inch from the injector. Downstream of the throat, the throat circular arc was tangent to a 15-degree-half-angle expansion cone. The chamber contraction ratio and

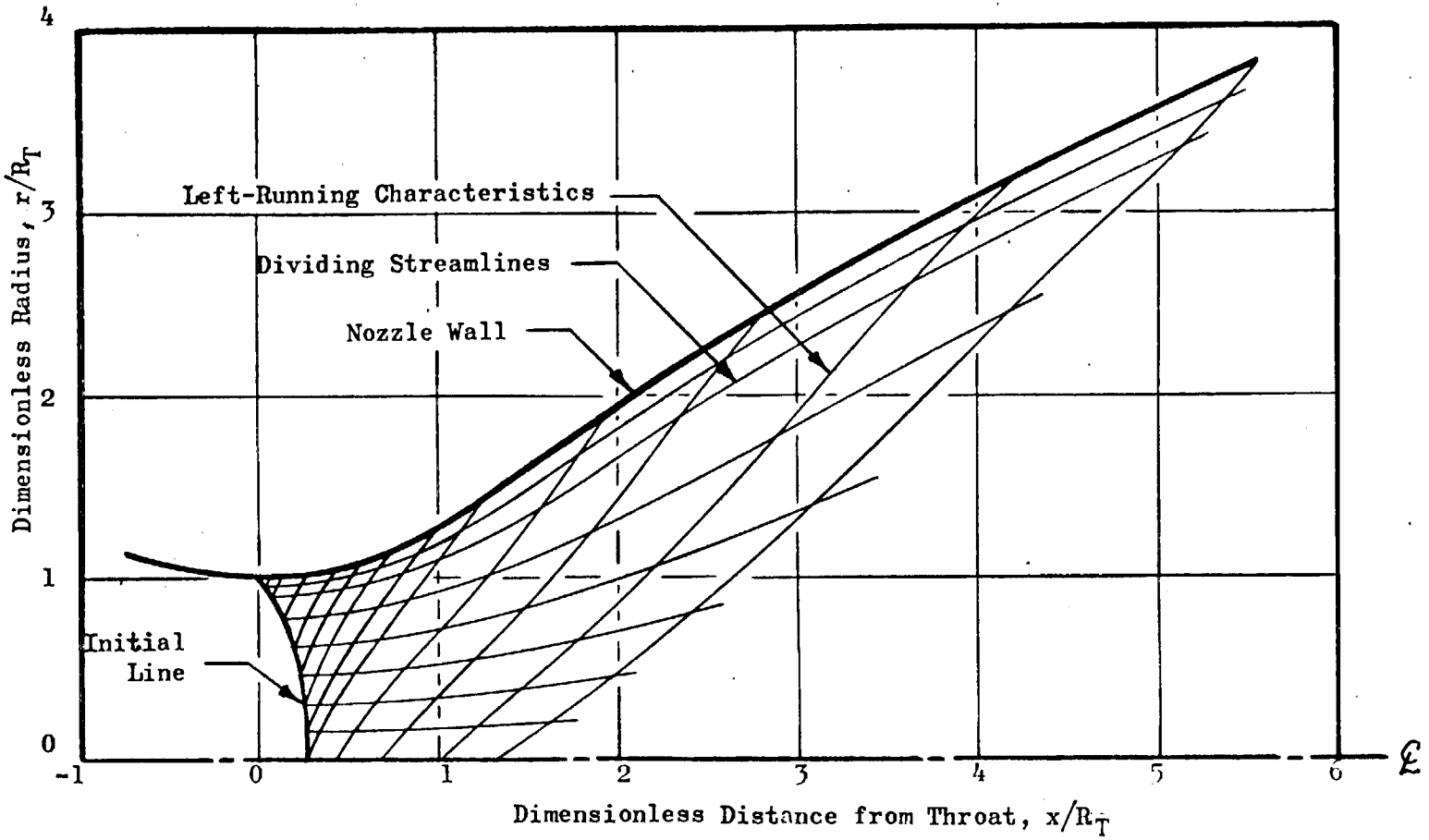

Figure 10. Manually-Plotted Coordinates of Dividing-Stream-Lines and Left-Running-Characteristics From TDK Program Block

nozzle expansion ratio were 2.00 and 1.85, respectively. The nominal injector, designated LD-2, was flat-faced and had 112 like-doublet injection elements for each propellant. The elements were positioned geometrically to link each fuel doublet with an oxidizer doublet to form a like-doublet-pair. Among several like-doublet-pair injectors described in Ref. 21, only the selected LD-2 injector did not produce aligned fuel and oxidizer spray fans. As a result, propellant mixing efficiency - determined by cold-flow experiments - was substantially lower for the LD-2 injector than for the others; this was the reason for its selection as the nominal checkout case. Nominal operating conditions were 100 psia chamber pressure and 5.2 mixture ratio. The experimental value of η_{c^*} was 93.3 percent.

Three empirical adjustments were made to force the DER prediction of η_{c^*} for the nominal checkout case to agree with its experimental value. The first of these was to position the STC initial-plane such that the value of E_m, Rupe's mixing efficiency factor, calculated by LISP matched the cold-flow experimental value of E_m = 88.5 percent. Computed variation of E_m with z_0 is shown in Fig. 11; from which z_0 = 1.70-inch was selected.

The other two adjustments were programmed as changes in the DER computer program. One was concerned with the method for initializing stream tubes from LISP mesh point flow data. Initially, the gaseous propellants produced by LISP were assumed to produce a single homogeneous combustion gas stream. With nonuniform spray fluxes and with approximately 10 percent of the propellants vaporized in LISP, this simplified treatment of the gases resulted in combustion efficiencies as much as 2 percent higher than were predicted by the nonuniform gas method described earlier. The second adjustment, therefore, was provision of nonuniform gases in the STC start plane.

The other empirical program adjustment concerned the influence of combustion chamber contraction ratio on mass droplet diameters calculated by LISP. A modified form of Ingebo's correlation for like doublet atomization (Ref. 24) was developed:

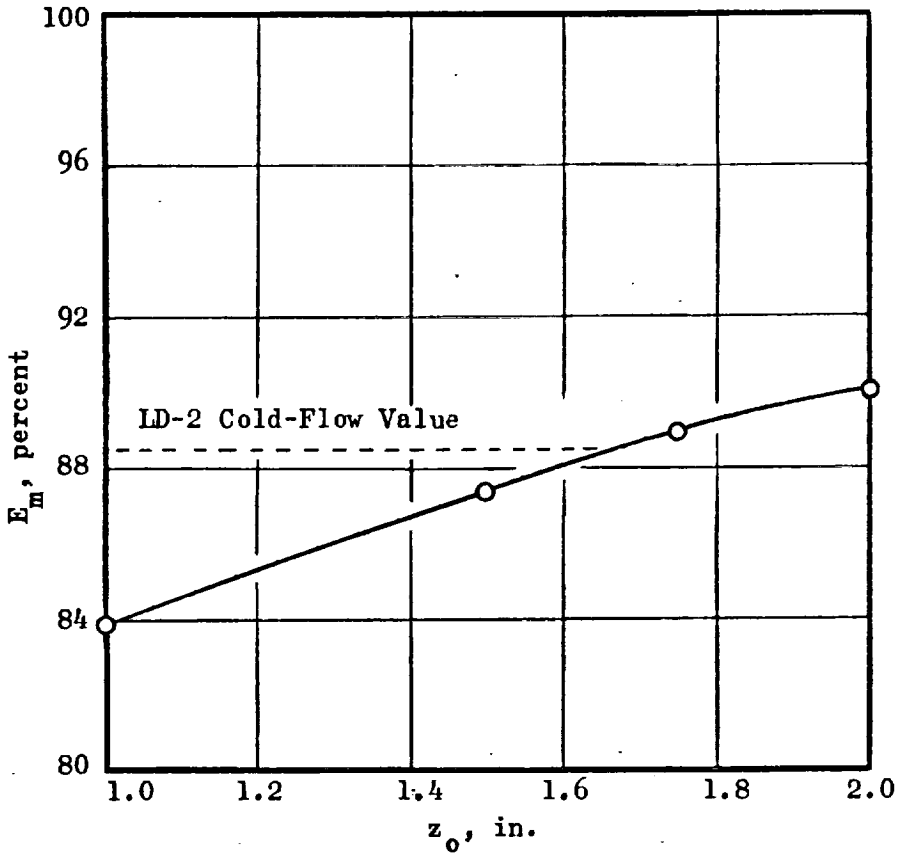

Figure 11. Calculated Variation of Mixing Efficiency vs LISP Collection Plane Position for LD-2 Like Doublet Injector

$$\overline{D} = 1.524 \left\{ 2.64 \left(\frac{u_{inj}}{D_{inj}} \right)^{1/2} + \frac{0.0978}{C_{pr}} f(\varepsilon_c) \left| \frac{480}{\varepsilon_c} - u_{inj} \right| \right\}^{-1} \quad (35)$$

The coefficient 1.524 is the ratio of $\overline{D}$ to D_{30} observed in Ref. 20 for like doublets, the ratio $0.0978/C_{pr}$ is a properties correction from Ingebo's heptane/air system to the propellant being considered, and

$$f(\varepsilon_c) = \frac{5(\varepsilon_c - 1)}{\varepsilon_c + 3} \quad (36)$$

was selected so that η_{c*} calculated by DER agreed with $\eta_{c*,exper}$ for the nominal test case and one $\varepsilon_c = 4$ case.

Comparisons of c* Efficiencies. With no further adjustments, ten computer runs were made to evaluate DER predictions of η_{c*} for varied injector and chamber designs and run conditions. Injector designs considered are summarized in Table 3. The run conditions and a comparison of calculated and experimental results are tabulated in Table 4. Data on the second and third from the last columns of Table 4 are plotted in Fig. 12. Agreement within ± 1 percent is seen to have been achieved. While this degree of success depended upon the empirical adjustments described above, the design and operating perturbations from the nominal test case were substantial.

Specific Impulse Prediction. For several reasons, concerned with program task and interim final report schedule and with the high cost of multiple stream tube TDK runs, complete DER model calculations were made for only one of the cases listed in Table 3. The conditions for this selected case were the LD-3 injector at 100 psia chamber pressure and 5.19 mixture ratio in a 15-inch L*, 2.0 contraction ratio chamber.

TABLE 3. SUMMARY OF LIKE-DOUBLET INJECTOR SPECIFICATIONS (Ref. 21)

Injector Identification Number	Orifice Diameter		Nominal Injector ΔP (psi) at Design Conditions		d_{ox}/d_f	Fan Spacing, inch	Fan Inclination Angle, degrees	Intra-Element Spacing, inch
	Fuel, d_f, inch	Oxidizer, d_{ox}, inch	Oxidizer	Fuel				
LD-2	0.0200	0.0292	290	100	1.46	0.275	0	0.20
LD-3	↓	0.0360	85	↓	1.80	0.00	25	0.25
LD-3-M	0.0260	0.0469	30	30	↓	↓	↓	↓

Notes:

1. Like-doublet element is pair of fuel and oxidizer doublets.

2. All injectors contain six rings of elements. For each injector, elements in the outer ring are canted so that the resultant propellant spray is directed 15 degrees toward the axial centerline of the injector. Resultant propellant spray direction for the remaining elements is parallel to the chamber axis.

TABLE 4. DER EVALUATION TEST CASE RESULTS

FLOX (80% F_2)/LPG (55% CH_4-45% C_2H_6)

Injector	Pc, psia	Mixture Ratio	L* Inch	Contr. Ratio	$\eta_{Evap.}$, Calc.	$\eta_{c^*, Mix}$		η_{c^*}		$\Delta\eta_{c^*}$
						Cold Flow	Calc.	Exptl.	Calc.	
LD-2	100	3.99	30	2.0	97.25	98.3	99.56	96.2	96.88	+0.68
↓	↓	5.19	↓	↓	97.24	95.6	96.26	93.3	93.27	-0.03
↓	↓	6.41	↓	↓	97.01	95.7	95.33	92.9	92.19	-0.71
LD-3	100	5.19	15	2.0	91.02	98.7	98.82	89.8	89.43	-0.37
↓	↓	↓	30	↓	97.84	↓	↓	96.3	96.54	+0.24
↓	↓	↓	60	↓	99.72	↓	↓	98.1	98.51	+0.41
↓	50	↓	30	↓	97.67	98.2	98.59	95.2	96.06	+0.86
↓	200	↓	↓	4.0	- -	98.7	99.18	93.1	92.53	-0.57
LD-3M	100	5.24	15	2.0	91.97	98.4	98.32	88.9	89.23	+0.33
↓	↓	↓	30	↓	97.83	↓	↓	95.4	95.83	+0.43

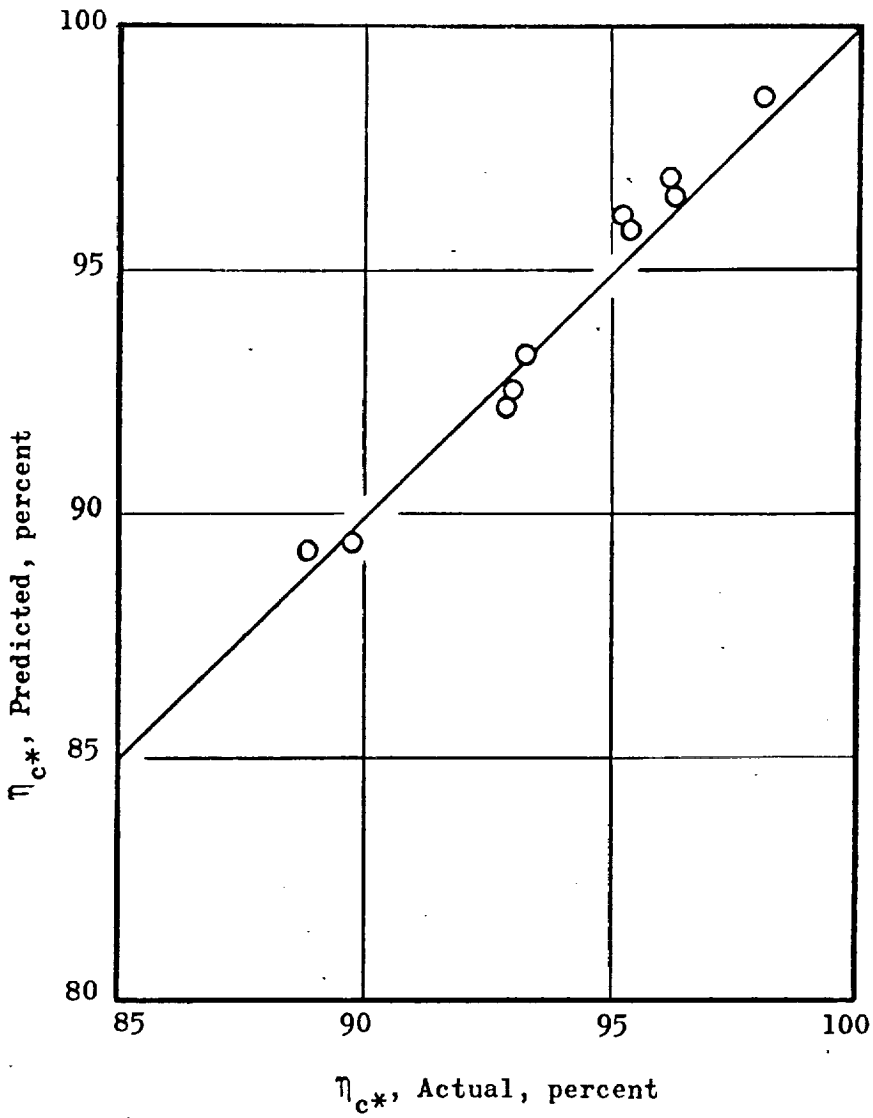

Figure 12. Comparison of Predicted and Actual η_{c*} for Test Cases of Table 4

The TDK program block gives printed-out solutions for c*, I_s, and C_F. The TDK prediction of c* efficiency was 2.2 percent higher than the experimental value. The TDK prediction of vacuum specific impulse was I_s = 276.04 lb_f-sec/lb_m compared with an experimental value, corrected to vacuum conditions of 269.5 lb_f-sec/lb_m; the difference is +2.4 percent of the experimental value.

These deviations were substantially larger than the $\Delta\eta_{c*}$ values in Table 4. The performance evaluation methods of Ref. 21 and the computed data from STC and TDK were examined to determine possible explanations for this discrepancy.

The vacuum thrust values in Ref. 21 had been corrected by 1.0 percent for combustor and nozzle heat transfer losses. By examination of calculated boundary layer losses for other combustors and conditions, it was inferred that the loss for this case should be about one percent. The implication is that both the predicted and experimental specific impulses should be lowered by about the same amount in accounting for boundary layer losses, i.e., essentially none of the 2.4 percent deviation can be attributed to boundary layer losses.

It was concluded that a strong contributor to the deviations in both c* and I_s is a discontinuity at the TDK initial line. Changing there from STC's frozen isentropic local expansion, from equilibrium stagnation conditions, to TDK's true equilibrium solution produced a jump shift in gas properties. For the case analyzed, the magnitude of the discontinuity was quite significant: the equilibrium static temperatures and molecular weights at the initial line were about 11 percent and 3 percent higher, respectively, than the corresponding STC computed values. With the prescribed values of pressure and stream tube areas and gas velocities assumed to be invariant across the initial line, these combine to produce discontinuous drops of about 8 percent in stream tube gas densities and gas flowrates. This is substantially larger than the modest discontinuities that were anticipated and were expected to have only slight effects on prediction accuracy. Considering the equilibrium values to be correct, the implication is that the pressure level for the entire STC analysis, including the TDK initial line, is too high. This would not only affect the values of the initial line integrals upon which TDK's computation of c* and thrust are based, but might

change the spray vaporization efficiency as well. Interestingly, these effects should cause the c* and I_s predictions to deviate by comparable magnitudes, as was observed.

This erroneous discontinuity has not been corrected either in the September 1970 or in the March 1971 versions of DER. It was left unresolved primarily because the version of TDK which had been adopted and incorporated into DER was being made obsolete by development of an improved version (Ref. 15). It was anticipated that a corrected STC/TDK interface solution method might take advantage of a new TDK capability to analyze kinetically limited multiple stream tube flows in the subsonic and transonic regimes. The problem was corrected in another project, however, when the September 1970 version of DER was adopted to analysis of pulse mode engine performance (Ref. 25). The method used was conversion of the read-in combustion gas properties tables from stagnation equilibrium to static equilibrium at several Mach numbers followed by internal calculation of corresponding pseudo-stagnation values so that STC's existing formulation need not be restructured. The TDK start-line flow properties computed by STC and by TDK then agreed within about 0.1 percent.

(Rather than adopting that solution, however, the TDK program was removed from the December 1971 version of DER, and logic was added for punching out STC data appropriate for initializing the improved version of the reference TDK program, as discussed further on pages 74 through 77.)

LIQUID/LIQUID DROPLET HEATING (SUPERCRITICAL) VERSION (MARCH 1971)

This version of the DER computer program differs from the preceding (September 1970) version only in its method of analyzing propellant spray combustion rates: the evaporation coefficient (k') model was replaced by a droplet heating and diffusion model. No other changes were made in the basic STC solution method nor were the LISP, TRANS, and TDK subprogram blocks altered. Whereas the (September 1970) version was restricted in application to chamber pressures substantially below the propellants' critical pressures, this version is intended for use at both subcritical and supercritical chamber pressures.

Spray Combustion Model: STC Modifications

Background. The quasi-steady evaporation coefficient approach to droplet heating and burning, while empirically based on the observation that a burning droplet's diameter squared varies linearly with time, has been expressed analytically in increasingly comprehensive formulations by Godsave (Ref. 8), Penner (Ref. 26), and Williams (Ref. 27). These models are based on the concept that a spherical flame surface surrounds a spherical droplet, with simultaneous heat transfer to and evaporation from the droplet being enhanced by the presence of the flame. These models have all been formulated as quasi-steady problems (i.e., time variation has been neglected in writing the conservation equations), although there are no other assumptions in either Penner's or Williams' model that preclude droplet heating. Dickerson (Ref. 28), in fact, has added the diffusion equation to Penner's formulation and developed a thin-flame model that includes uniform droplet heating. A problem that arises in applying such a model, however, is that the initial heating and burning rates may be over-predicted by assuming a flame exists when the vapor concentrations are too low to support it. Another problem is that the derived formulae for the burning rate (or the evaporation coefficient), in all of these models have singularities (blow-up logarithmically) if droplet temperatures approach propellant critical temperatures. One final problem is that exposing the droplet to even mild forced convection is likely to blow the flame into the droplet wake or extinguish it, so that flame-enhancement of vaporization does not occur.

As a consequence of these limitations and problems, propellant droplet gasification and burning has also been analyzed from a vaporization standpoint, with vapors diffusing into and mixing with a high-temperature gas stream. So far as the droplet is concerned, combustion reactions within that gas stream serve to keep the gas temperature high and the vapor concentration low. (In practice, reaction to local thermodynamic equilibrium is usually assumed.) To the extent that the free-stream gas temperature is lower than the stoichiometric flame temperature (the thin-flame model's driving temperature), a vaporization model will predict lower droplet burning rates than will a thin-flame model.

An evaporation model that is commonly used for analyzing spray gasification in rockets is that of El Wakil (Ref. 29) and others at the University of Wisconsin. By solving spherically symmetric, quasi-steady conservation equations for simultaneous heat and mass transfer, the droplet mass evaporation rate and (uniform) heating rate are given by

$$\dot{m}_j^n = 2\pi D_j^n \left(\frac{pM_{v_j}}{RT}\right)_f \mathcal{D}_{v_j f} \left(\frac{Nu_m}{2}\right) \ln\left[\frac{1 - x_{v_{cg}}}{1 - x_{v_j}^n}\right] \tag{37}$$

$$Q_j^n = \left(\frac{\pi k_f z Nu_h D_j^n}{c_{pv_{jf}}}\right) \left[\frac{c_{pv_{jf}}\left(T_{cg} - T_j^n\right)}{(e^z - 1)} - \Delta H_{v_j}^n\right] \tag{38}$$

where

$$z = \left(\frac{c_{pv_{jf}}}{k_f}\right)\left(\frac{Nu_m}{Nu_h}\right)\left(\frac{pM_{v_{jf}}}{RT_f}\right) \mathcal{D}_{v_{jf}} \ln\left[\frac{1 - x_{v_{cg}}}{1 - x_{v_j}^n}\right] \tag{39}$$

It is possible to calculate nonuniform temperature distributions within a droplet undergoing heating (e.g., Ref. 30), but it is usually assumed that internal temperature gradients are prevented from building up by strong internal circulation. Under convective flow conditions, surface shear does promote circulation and this simplification is probably quite valid. Then the uniform droplet temperature is obtained from:

$$\left[\frac{d(T_j^n)}{dt}\right]\left[\frac{\pi}{6}\ \rho_{\ell_j}^n\ c_{p\ell}\ \left(D_j^n\right)^3\right] = Q_j^n \tag{40}$$

Forced convection and resultant nonspherical transfer processes are accounted for through empirical Nusselt number correlations for both heat and mass transfer. The Nusselt number correlations used in the mass transport equation were obtained by Ranz and Marshall (Ref. 31):

$$Nu_m = 2\left(1 + 0.3\ Sc_f^{1/3} Re_f^{1/2}\right) \tag{41a}$$

$$Nu_h = 2\left(1 + 0.3\ Pr_f^{1/3} Re_f^{1/2}\right) \tag{41b}$$

They verified this correlation with data from vaporization of water droplets in heated air. The equations derived thus account for both droplet heating and evaporation.

The foregoing droplet heating and evaporation model has been used in a number of rocket spray combustion models since its first application by Priem and Heidmann (Ref. 3). It is capable of computing droplet behavior to complete combustion at subcritical chamber pressures, although the vaporization rate blows up logarithmically as droplet temperatures approach the boiling temperature ($X_{V_j}^n \rightarrow 1$). For most conditions, the "wet-bulb" effect suppresses the equilibrium droplet temperature enough below the boiling point to avoid the singularity. There, however, the evaporation rate is strongly dependent upon droplet temperature and, because an implicit solution of the system of equations is required, many iterations may

be needed to obtain convergence. Recent work by Savery (Ref. 32) gives good correlation with experimental data under such conditions, even up to high pressures, if the effects of the presence of other gases on the vapor pressure and "heat of vaporization" are taken into account.

Real Gas Effects. For vapor-liquid equilibrium, the free energy is the same on either side of a phase interface. This fundamental relationship for vapor-liquid equilibrium is conveniently written in terms of fugacities; for each component i, the fugacity of the vapor f_i^V is equal to that of the liquid f_i^L (Ref. 33). Since the liquid senses the total pressure while the vapor senses only its partial pressure, the equilibrium relationship can be written as

$$f_i^V\left(P_v\right) = f_i^L\left(P_{Total}\right) \tag{42}$$

Hence, at constant temperature, as the total pressure increases the partial pressure of the vapor has to increase to maintain the required relationship for equilibrium. For a non-ideal gas, the enthalpy is a function of the partial pressure of the gas (Ref. 34). Hence, the heat of vaporization, ΔH_{vap}, will be a function of total pressure since

$$\Delta H_v = H_v - H_\ell \tag{43}$$

In the calculation of vapor-liquid equilibrium, the vapor has to be considered a non-ideal gas. Of the four two-constant equations of state which have been widely used, the Redlich and Kwong equation is more accurate and the best at high pressures. The Redlich-Kwong equation is:

$$P = \frac{RT}{(v-b)} - \frac{a}{T^{0.5}\, v(v+b)} \tag{44}$$

where a and b are determined from mixing rules (Ref. 33). To match data over wide ranges, a and b have been programmed as functions of temperature.

These "real gas" corrections have been neglected in most prior applications of the El Wakil droplet vaporization model. Under supercritical pressures, some conditions led to calculated equilibrium temperatures below the critical temperature, but usually no equilibrium temperature was reached and the droplets were heated through the critical temperature. The model could be used beyond this point, but it usually was not because a physical model is lacking for X_v at the "surface" of the pure supercritical vapor pocket. Instead, most users either assumed instantaneous mixing of such supercritical vapors with the surrounding gases, which is obviously unsatisfactory, or switched to a supercritical burning model due to Spalding (Ref. 35). This latter model, however, treats only the mass transfer and assumes that the vapor pocket remains at its critical temperature. As a result, no prior combustion model employing the El Wakil vaporization formulation can be adopted carte blanche for supercritical spray heating and combustion.

Interestingly, introduction of the real gas corrections for vapor pressure and heat of vaporization causes the El Wakil solution for droplet temperature to reach a subcritical equilibrium temperature for all conditions. This is known from photographic evidence (Ref. 36) to be unreal, so the need for an improved formulation is apparent.

New Droplet Heating and Diffusion Model. The El Wakil model has been extended and improved to overcome this physically unrealistic result (Ref. 37). The new model is referred to as the droplet diffusion model. The main difference between it and the old model is this: In the El Wakil formulation only the propellant vapor is considered to have a non-zero net flux in the film surrounding the droplet, while in the new model the radial mass flux of combustion gas in the film surrounding the droplet is no longer assumed to be equal to zero. Instead, the molar flux of combustion gas is defined at the droplet surface through a moving control volume formulation such that changes in the droplet radius, due

to droplet density changes and mass diffusion, cause it to be greater than or less than zero. That is

$$M_{cg}\ N_{cg} = \left(\rho_{md}\right)_j^n \quad \frac{d\left(r_d\right)_j^n}{dt} \tag{45}$$

Thus, as the droplet "burns" the external diffusing combustion gas is allowed to enter the control volume and occupy that fraction of the volume vacated by the receding droplet surface.

The diffusion rate, or burning rate, is defined by the diffusion equation and is

$$\dot{m}_j^n = \left(\frac{2\pi D_j^n}{B}\right)\left(\frac{pM_{v_{jf}}}{RT_f}\right)\mathcal{D}_{v_{jf}}\left(\frac{Nu_m}{2}\right)\ \ln\left[\frac{1 - Bx_{v_{cg}}}{1 - Bx_{v_j}^n}\right] \tag{46}$$

where

$$B \equiv 1 - A\left(\frac{M_{v_{jf}}}{M_{cgf}}\right) \tag{47}$$

(NOTE: Here f refers to "film" conditions.)

$$A = \left(\frac{\rho_{m_d}}{\rho_d}\right)_j^n \left[1 + \frac{\sqrt{d}}{\dot{m}_j^n} \quad \frac{\partial}{\partial t}\ (\rho_d)_j^n\right] \tag{48}$$

The droplet heatup rate is defined to be

$$Q_j^n = \frac{\pi k_f z Nu_h D_j^n}{\left(c_{p_{v_{jf}}} - Ac_{p_{cgf}}\right)} \left\{\left[\frac{\left(c_{p_{v_{jf}}} - Ac_{p_{cgf}}\right)}{(e^z - 1)}\right]\left(T_{cg} - T_j^n\right) - \Delta H_{v_j}{}^n\right\} \tag{49}$$

where

$$z \equiv \frac{\left(c_{p_{v_{jf}}} - Ac_{p_{cgf}}\right)}{Bk_f} \left(\frac{Nu_m}{Nu_h}\right) \left(\frac{pM_{v_{jf}}}{T_f}\right) \mathcal{D}_{v_{jf}} \ln\left[\frac{1 - Bx_{v_{cg}}}{1 - Bx_{v_j}^{n}}\right] \quad (50)$$

The droplet diffusion model no longer has the logarithmic singularity at either the droplet boiling or propellant critical temperatures because, as droplets are heated through these temperatures, the value of B is such that $(1 - Bx_v)$ does not vanish. It thus becomes possible to continue analyzing spray droplets' behavior after they have become fully gasified, but have not yet been diffused and mixed into the surrounding combustion gas stream.

It should be noted that the model does not include the solubility of the combustion gas in the propellant, either as a liquid droplet or as a gas pocket. Upon being heated through the critical temperature, a liquid droplet may be thought of as a "virtual droplet" with a discrete semipermeable surface which permits outflow of propellant vapor but blocks inflow of combustion gases.

Comparison of the foregoing droplet diffusion model equations with the old model equations, e.g., as given by El Wakil, shows them to be very similar. The major differences are the appearance of the parameters A and B in Eq. 46, 49, and 50. Examination of Eq. 45, 47, and 48 shows, however, that A and B depend upon the heating and vaporization rates so that the droplet diffusion model must be solved implicitly by iterative methods. If the heating and vaporization rates are low enough that dr_d/dt vanishes, $A \to 0$, $B \to 1$ and the droplet diffusion model reduces rigorously to the El Wakil model. This is consistent with all the assumptions in their derivations being identical except for that expressed by Eq. 45. Chemical reactions are not taken into account directly in the droplet heating and diffusion model, but combustion is simulated by specifying a bulk gas equilibrium flame temperature and zero droplet vapor mass fraction in the local free stream.

Programming. The foregoing droplet diffusion model had been included in a Rocketdyne H_2/O_2 combustion computer program (CSS) for analyzing LOX jet atomization, spray and gas mixing, spray vaporization, and combustion with coaxial jet injection (Ref. 37). In that application, the droplet diffusion model was programmed as a set of subroutines that is specific to the gaseous hydrogen/liquid oxygen propellant combination and to the solution method used in that computer program. In this current program, that set of subroutines was generalized for use with other propellants, including liquid/liquid combinations, and incorporated into the DER computer program's STC (stream tube combustion) program block.

Extension to other propellants was rather straightforward; for most subroutines, it involved generalizing molecular weights, critical properties, etc., and having STC call the subroutines twice if two liquid propellants are being analyzed. In some subroutines, O_2/H_2 properties data were given in data statements; these were modified so that the data are read-in as general propellant punched card data with the rest of the STC portion of the data deck.

The numerical solution scheme in the STC program uses predictor-corrector cycles with backwards differencing of first-order difference equations. The droplet diffusion model had been programmed for one-step forward differencing; thus, some modifications were required to make the subroutines compatible with the revised solution scheme.

A bisection method is used for the implicit, iterative solution of the droplet diffusion model equations. In solving for a droplet's temperature, for example, known and estimated values of droplet temperatures and their derivatives at planes 1 and 2 bounding a given chamber length interval are used to evaluate:

$$F(T) = T_2 - T_1 - \left(\frac{dT_1}{dz} + \frac{dT_2}{dz}\right)\frac{\Delta z}{2} \qquad (51)$$

A solution of the system of equations corresponds to $F(T) = 0$. If it is initially assumed that $T_2 = T_1$, it is found that $F(T) < 0$. A second estimate, that

$T_2 = T_1 + \frac{dT_1}{dz}\Delta z$ (or $T_2 = T_{cgl}$, whichever is smaller) obviously gives $F(T) > 0$. In bisection, the average of these two values of T_2 is taken as the next estimate and is used to replace the previous estimate which gave the same sign for $F(T)$. This process is continued until a root is found which satisfies the equation, i.e., gives $0 \leq |F(T)| \leq \varepsilon$. Bi-section is used three ways in stepping across a chamber-length increment: one to find initial values of A, B and z; one to solve for downstream droplet temperature (and corresponding vaporization rate) and one to solve for A, B and z within the bisection loop on temperature. Convergence upon a solution takes several (5 to 10) iterations and, with multiple iterations within iterations, execution times are substantially increased over those for the evaporation coefficient model.

Required Propellant Properties Data. Extensive tables of propellant properties are required by the droplet diffusion model. The first of these tables gives the vapor mass fraction, X_v, at the droplet surface (equivalent to a reduced partial pressure), the heat of vaporization, ΔH_v, and parameters a and b for the Redlich-Kwong equation of state. Variability of X_v and ΔH_v with both total pressure and temperature are provided for, while a and b are taken to be functions only of temperature. Values in these tables should account for temperatures ranging from injection temperature to the critical temperature only. Pressures must cover the range of variation experienced in the subsonic flow portion of a combustor under analysis. (It is probably preferable to input data for much wider variation so that the same tables can be used for other engines using the same propellants.) Values of X_v and ΔH_v should include dependence upon total pressure level, i.e., real gas effects.

Liquid specific heats are needed for both propellants as functions of pressure and liquid temperature. Although these are denoted as "liquid" c_p's, the tables should provide data to temperatures as high as the combustion gas temperature; for temperatures higher than the saturation temperature corresponding to the tabulated pressure, the pure vapor specific heats are used.

Vapor specific heats at constant pressure and vapor viscosities are also required. These may be derived from tabulations of experimental data or from standard correlation methods, e.g., such as those given in Ref. 34.

Binary molecular diffusion coefficients are assumed to be functions of temperature. An equation for binary diffusion coefficients, based on use of the Lennard-Jones potential in a kinetic theory model, is given in Ref. 34 as:

$$\mathscr{D}_{12} = \frac{0.001858\ T^{3/2}\ \left[(M_1 + M_2)/M_1M_2\right]^{1/2}}{P\ \mathring{\sigma}_{12}^{2}\ \Omega_D} \tag{52}$$

Dividing this equation for general temperature and pressure by the same equation for some reference temperature and pressure gives:

$$\mathscr{D}_{12} = (\mathscr{D}_{12})_{ref} = \left(\frac{(\sigma_{12})^2_{ref}\ (\Omega_D)_{ref}}{P\sigma_{12}^2\ \Omega_D}\right)\left(\frac{T}{T_{ref}}\right)^{3/2}\left(\frac{P_{ref}}{P}\right) \tag{53}$$

DER accepts input tables of the parametric product

$$(\mathscr{D}_{12})_{ref.}\ \frac{(\sigma_{12})^2_{ref}\ (\Omega_D)_{ref}}{\sigma_{12}^2\ \Omega_D} \tag{54}$$

which is assumed to vary with temperature, but not to vary appreciably with pressure. If it can reasonably be assumed to be constant, then only one temperature level needs to be given in the table. For each propellant species, coefficients are needed for diffusion into its own vapors, the other propellant's vapors, and into stoichiometric combustion products. For lower (higher) mixture ratio combustion gases, multicomponent diffusion coefficients are approximated by the

program for each specie diffusing into a mixture of stoichiometric products and excess fuel (oxidizer) vapor.

Revised STC Data Output. The printout of data from STC was revised to reflect the substantially increased quantity of input data, concerning propellant properties and initial spray droplet size-group temperatures, and to report the calculated droplet size-group temperatures as the analysis proceeds. Examples of the calculated size group diameters and temperatures for LOX spray burning in H_2/O_2 combustion products are shown in Fig. 13.

Computer Program Checkout.

The development of this March 1971 version of DER was the first task of the second contract year so that it might be available, if required by NASA, for use in evaluating a major engine development contract. For that reason, even though it can analyze bipropellant liquids, the computer program was checked out with the liquid oxygen/gaseous hydrogen combination, exclusively. LISP did not have a gas/liquid capability, so the checkout runs involved only the STC subprogram block with direct input of stream tube initialization data.

It was intended that the computer program be at least partially evaluated by comparing computed performance with some available supercritical LOX/GH_2 engine data. The J-2S engine, developed for NASA by Rocketdyne, and operating at 1250 psia chamber pressure, was considered to be a good candidate evaluation engine. However, checkout of the computer program took longer than anticipated and its run times (execution costs) were so high that there was neither time nor funds for analyzing any evaluation cases. This version has, therefore, been only partially checked out (a liquid fuel was not analyzed) and its validity has not been established.

Most checkout runs were made with a rather simple case designed to evaluate computational features, but also to minimize run times. Thus, only one or three stream tubes, five or nine spray size groups, and 2 to 5 inches of chamber length were analyzed. Liquid oxygen injection temperature was fixed at 180 R. Chamber pressure was 1200 psia.

One of these checkout cases was supplied as an example case when this version of the DER computer program was delivered to JPL.

Evaluation of Model

No comparisons have been made between performance predictions and engine data for this version of DER. That is, the model's validity has not been checked directly. Because the spray burning analysis is the same as that used in the CSS model of Ref. 37, however, it may be inferred that the model's evaluation is also applicable to this version of DER. Data are given in Ref. 37 showing favorable comparisons of CSS predicted c* efficiencies with J-2, J-2S and H_2/O_2 aerospike engine efficiencies in the range 96 to 100 percent. It thus appears that the spray combustion analysis is good enough that DER's prediction accuracy will depend primarily upon valid input data concerning stream tube flowrates, mixture ratios, and initial spray atomization.

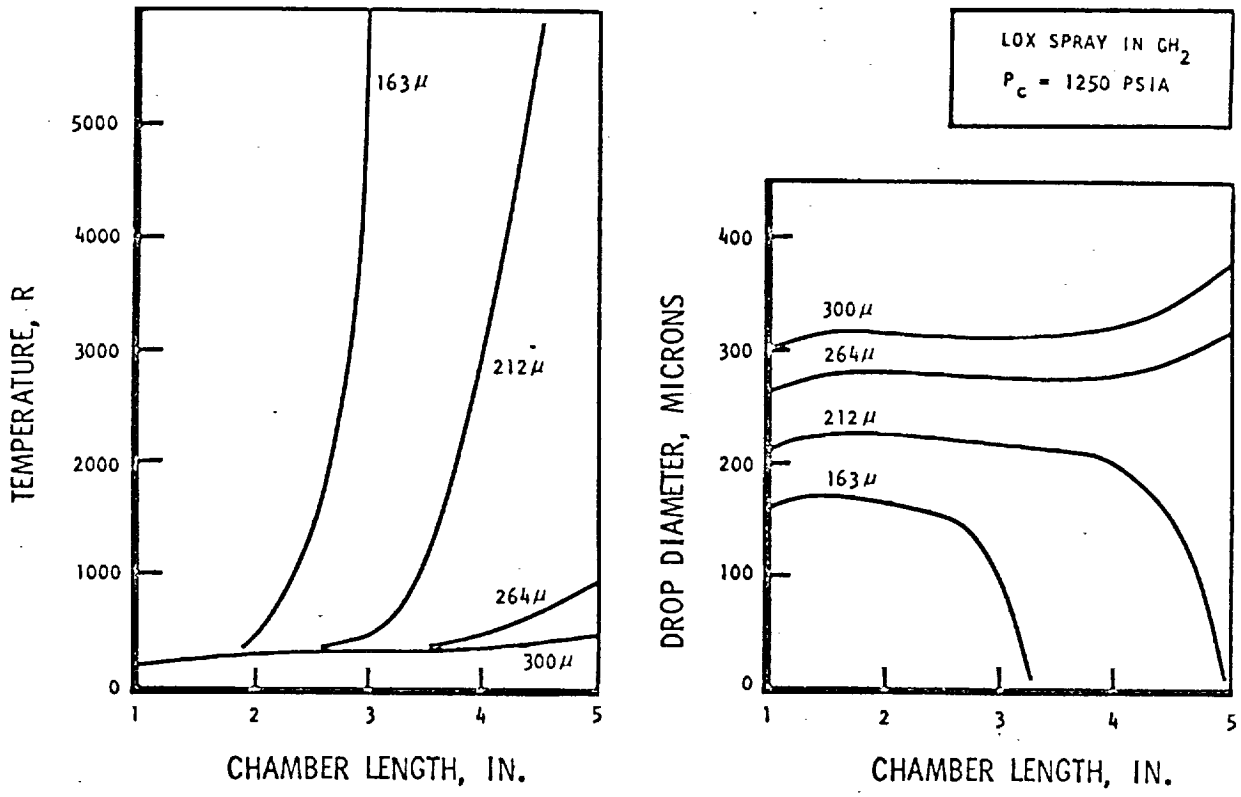

Figure 13. Typical Supercritical Burning Results

GAS/LIQUID k' (SUBCRITICAL) VERSION (December 1971)

This latest version of the DER computer program represents a substantial revision of the first (September 1970) version. The LISP subprogram block has been modified to provide a capability for analyzing injection of gaseous fuel/liquid oxidizer propellants, with coaxial jet and triplet elements, to simplify the data input and to improve the data plotting subroutines. The STC subprogram was modified to better initialize stream tubes when there is no spray of one propellant, and to generate, print, and punch a portion of the data needed for subsequent initialization of the improved TDK computer program. At the same time, the DER version of TDK was removed from the December 1971 version of DER.

The changes concerning TDK were made to simultaneously bypass the earlier STC/TDK interface problem and make it possible to use the latest version of TDK for performing the nozzle expansion analysis.

Gas/Liquid Distributions: LISP Modifications

Modifications of the LISP subprogram block employed in the December 1971 version of DER were partially provided under three separate programs: the Thrust Chamber Compatibility Model program (contract F04611-70-C-0056 and Ref. 18), the Pulse Mode Performance Model program, (contract F04611-70-C-0074 and Ref. 25), and the current Distributed Energy Release program.

The input data required for defining the injection element were simplified by means of "element specifications". These define the general design features of each group of elements that are identical except for each element's location and orientation on the injector. The only individual element data required, then, are its specification number, its angular and radial position on the injector, and a rotational orientation angle. The total number of elements which may be considered was expanded to 60, and there may be as many as 10 different specifications.

Additionally, input data concerning element canting or tilting, in any direction, were made more systematic and easier to use. An earlier error in element orientation was corrected simultaneously.

LISP's subroutines for generating contour and shade plots of spray weight flux and mixture ratio were replaced. The earlier system was based on transforming LISP's data calculated in polar coordinates to rectangular plotting coordinates. The new method plots directly in polar coordinates. It effects substantial reductions in complexity and core storage requirements, and corrects some errors in circle-completion logic, as well. Shade plots were eliminated entirely. Contour plots of fuel flux, oxidizer flux, total propellant flux, and a mixture ratio function (which varies between zero and unity) are optionally available.

Distribution of Gaseous Propellants. The most significant modifications in this version of LISP deal with prediction of propellant flux distributions produced by gas/liquid injectors. This task was undertaken as an exploratory effort to produce a "first generation" gas/liquid analysis capability whose results and behavior might reveal what is needed in formulating a more adequate model. This approach was necessitated by a number of obvious complications:

1. LISP had heretofore been concerned only with distributing noncontinuum sprays; gases produced were treated as a uniform bulk flow. Gaseous propellants are continuous, and flow from neighboring elements cannot be as independent as are liquid sprays.

2. More gasification in the injection/atomization region is likely to occur with gas/liquid injection than with liquid/liquid combinations. Thus, errors in approximating the quantity of that spray vaporization are probably larger and will probably have a significant effect on performance prediction accuracy. An important part of this problem is determining how to distribute the vapors produced among the gaseous injectants, i.e., defining the gas mixture ratio distribution.

3. The quantity of available single element gas/liquid cold-flow data is quite limited. Also, few demonstrations of correspondence between cold-flow data and engine performance have been achieved.

4. Applications of gas/liquid injection tend to have chamber pressures that are supercritical for the liquid, so the use of a k' evaporation model in LISP becomes questionable.

The approach taken in this "first generation" gas/liquid LISP was to recognize, but ignore these complications, saying, in effect, "Let's see how bad they make things." The basic premises of the liquid/liquid LISP were retained: full injector propellant fluxes are linear summations of individual elements' fluxes, and individual element fluxes can be mathematically described by correlation of cold-flow distribution data. The distribution of the gaseous injectant is calculated as if it were a low-density, noncontinuum spray. Minor LISP modifications treating it as a gas were made to satisfy continuity.

With this approach, the primary analytical efforts required were correlating gas/liquid cold-flow flux distributions to obtain LISP input correlation coefficients (described in Ref. 19) and determining adequate and workable disposition of vapors produced by partial gasification of the liquid propellant.

Elemental Flux Distributions. LISP's treatment for coaxial jet injection of gaseous fuel/liquid oxidizer propellants was adopted from its development discussed in Ref. 18. Only a summarization is given here.

Single element, cold-flow data for gas/liquid coaxial jet elements, obtained under Contract NAS3-1119 (Ref. 38), were correlated. Liquid (water) was injected through a central cylindrical tube as an oxidizer simulant, while gaseous nitrogen flowed through a narrow annular passage outside of the post to simulate gaseous fuel. Data were used from nine tests, including some in which the discharge end of the liquid tube was recessed below the injector face.

Because the elements and propellant flows are both axisymmetric, the usual Cartesiam coordinate correlating equation (Eq. 3) was transformed to cylindrical coordinates for correlating the data. Both liquid and gas flows were assumed to be emitted from point sources ("pseudo-impingement points") located, respectively, δ_L and δ_G upstream of the injector face. The correlating equation was retained in the rectangular coordinate form as illustrated, with the element geometry, in Fig. 14.

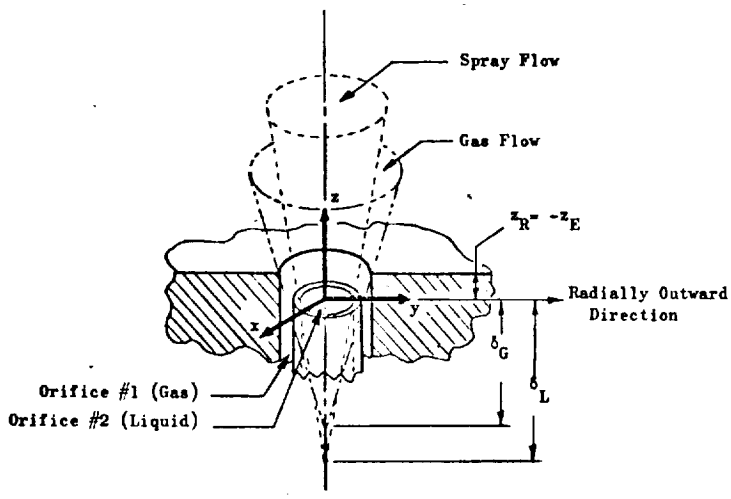

Type 6: Coaxial Jet Element

Note: D_2 = Central Tube I.D.

A_1 = Annular Passage Area

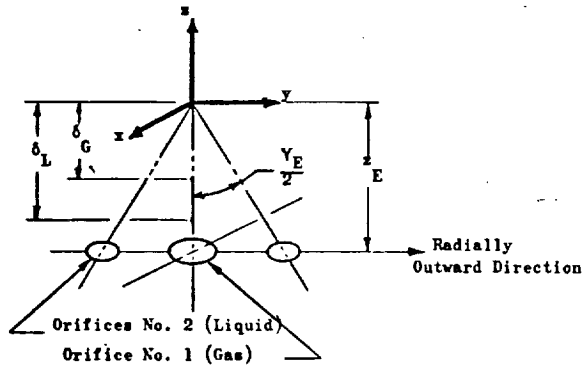

Type 10: Triplet (Note Reversal of Orifice Numbers from Liquid/Liquid Triplet)

Figure 14. Gas/Liquid Injection Elements Included in LISP Subprogram Block

An expression was developed for calculating partial gasification of the liquid propellant, both within the "cup" formed by recessing the discharge end of the liquid tube and in the combustor between the injector and the LISP collection plane. For one injector analyzed in Ref. 18, over 50 percent of the liquid jet was calculated as being vaporized within an inch of its discharge from the tube. Disposition of the vapors formed was found to be crucial to achieving an adequate LISP analysis.

As first programmed, it was assumed that the vaporized liquid vapors mixed uniformly with the gaseous injectant stream, and that the resultant, uniform mixture ratio mixed gas stream retained the cold-flow gas velocity profile. Allowing the mixed gases to burn to local equilibrium and scaling the velocity profile to preserve continuity, however, resulted in a physically unacceptable solution having supersonic gas jets downstream of the elements.

Consequently, for calculation of the combustion gas flow field, the gaseous mass flux distribution was modified by the following assumptions:

1. The gaseous propellant and the vapors from the evaporated liquid propellant from a single element are assumed to mix intimately and react chemically equilibrium at the local resultant mixture ratio with corresponding gas molecular weight and temperature.
2. Momentum of the jet is assumed to be conserved, i.e., the jet expands with combustion such that the momentum of the resultant hot gas and of the unevaporated liquid are equal to the initial momentum of the injected propellants.
3. The mass flux distribution of the hot combustion gas from a single element is assumed to be described by a Gaussian radial profile.

The distribution of the unevaporated liquid is assumed to be described by the corresponding cold-flow mass flux distribution.

Single element cold-flow data for gas/liquid triplet elements were obtained under Contract NASw-2106 (Ref. 39). Two liquid streams impinged on a central gas jet, Fig. 14. Gaseous injection velocity was varied as was the liquid/gas weight-flowrate (mixture) ratio.

These data were correlated to a Cartesian-coordinate version of Eq. 3, transformed to permit use of δ_G and δ_L pseudo-impingement points, as with the gas/liquid coaxial elements. The derived correlation coefficients are given in Ref. 19.

The calculation of spray vaporization for gas/liquid triplets was retained the same as for any liquid/liquid elements. Vapors produced were assumed to be mixed uniformly with the gaseous injectant. In a manner similar to the treatment of the coaxial element's gas jet, the general shape of the cold-flow gas velocity profile was preserved while allowing it to spread to conserve gaseous weight flowrate and momentum.

The gas/liquid coaxial and triplet element were coded in LISP as Types 6 and 10, respectively. Additionally, a uniform velocity and mixture ratio gas stream over the entire chamber cross section can be provided with either of these types by a Type 9 element specification.

The analytical models of gas/liquid elements produce nonuniform combustion gas flow fields for single elements in a manner that conserves weight flowrate and momentum within a single element's flow. When multiple element flows are combined, however, momentum will be conserved only if the weight flux profiles do not overlap significantly. If they do overlap appreciably, linear superposition of gaseous weight fluxes is not a physically sound assumption. A symptom that might indicate a problem in this regard is the appearance of high axial gas velocities between elements.

Spray Combustion Model: STC Modification

Stream Tube Initialization. If one propellant is completely gasified, the option (2) method given on page 26 for initializing stream tube flows from LISP mesh point data cannot be used because the spray mixture ratio is either zero or infinite. The method was changed, therefore, and was made somewhat more general in the process. LISP's calculated gaseous weight fluxes at the mesh points are re-formed, rather than being averaged out to a uniform bulk gas flux as is done if bipropellant sprays are present. There is an option to prescribe a uniform gas flux, however. (As noted in describing LISP, the gas mixture ratio is currently considered by LISP to be uniform, whether or not the weight flux is uniform. The stream tube initialization method can treat nonuniform gas mixture ratios, as well, if LISP were to supply such data.) With the gas fluxes determined, either of the methods described earlier for combining mesh point flow into stream tubes may be selected.

Cases involving bipropellant sprays are handled directly by the earlier methods. One major difference is that the user's prescribed numbers of fuel and oxidizer spray size groups per stream tube are no longer overridden and he may not prescribe the distribution of spray weight among the size groups.

STC/TDK Interface. Were the stream tube properties in the neighborhood of the nozzle throat computed by STC transferred to TDK and used for finding local equilibrium properties, discrepancies like those described on page 54 would be encountered. Rather than modifying STC further to eliminate that source of error in DER's performance prediction, the TDK used in the earlier versions of DER was removed from the (December 1971) version. This made it possible to interface STC with an improved version of TDK (Ref. 24) which is capable of performing kinetic expansion analyses in subsonic and transonic flow regimes as well as in the supersonic nozzle flow. STC's frozen expansion from local stagnation equilibrium was retained under the assumption that, although it yields erroneous (i.e., nonequilibrium) temperatures, densities, etc. in the transonic flow regime, the errors it causes in vaporization efficiency may be inconsequential.

A subroutine was added which prints and punches, in NAMELIST format, the throat plane data needed from STC to continue the multiple stream tube analysis via the improved TDK computer program. Throat plane data punched out are illustrated in Table 5. Those in NAMELIST format (and the TDK parameters to which they correspond) are: the number of stream tubes (NZØNES), a stream-tube-area-weighted mean stagnation pressure [P(1)],

$$\overline{P_o^*} = \frac{\sum_{i=1}^{n_t} P_o^*{}_i A_i}{\sum_{i=1}^{n_t} A_i} \tag{55}$$

and, for each stream tube, the gasified propellant mixture ratio (ØFSKED) and mass fraction of the total gasified propellant flow within that stream tube (XM). Also, additional data are computed and printed out (Table 5) which will probably be used in a future revision of TDK. These include: each stream tube's cross-sectioned area, static pressure, and stream gas velocity at the point in the nozzle where the TRANS pressure distribution is first invoked (z = ZPVSR) and, at the nozzle throat plane, each stream tube's total flow mass fraction of the total injected flow, overall mixture ratio, stagnation pressure, mean evaporation efficiency, and mean fuel and oxidizer spray velocities.

It is anticipated that these stream tube data may be used to initiate TDK nozzle expansion analysis at the throat plane or, if kinetic effects are believed to be important in the subsonic flow, at some plane upstream of the nozzle throat. Thus, it is now possible to overlap the spray gasification analysis of STC with the nonequilibrium combustion analysis of TDK, but in an uncoupled manner. The location of the TDK initial plane is designated by the program user, by specifying the contraction ratio (ECRAT) for that start plane and also the subsonic area ratio for that plane [SUBAR(1)], equal to the contraction ratio . This nonphysical stream tube data transfer is illustrated in Fig. 15. Other data needed for initializing TDK are*: reactant cards (pages 6-9 and 10), reactions cards (pages 6-27 to 31), nozzle design parameters (pages 6-32 to 34), integration and print controls (pages 6-35 to 37) and TDK controls and nozzle divergence geometry (pages 6-42 to 46).

*Page numbers in parentheses refer to the Program User's Manual Section of Ref. 24.

TABLE 5. EXAMPLE OF THROAT PLANE DATA IN NAMELIST FORMAT FOR TDK INPUT AND ADDITIONAL COMPUTED DATA

```
          PUNCHED-CARD OUTPUT FOR REVISED  T D K (12/74)
ITLE   TDK ANALYSIS OF MULTI-STREAM-TUBE GASES FROM STC
ITLE            EXAMPLE CASE FOR  D E R  PROGRAM USERS GUIDE.
ITLE                    * * * *  * * * *
ITLEA PULSE MODE ATTITUDE CONTROL ENGINE,  N2O4/A-50(N2H4-UDMH(50-50) PROPELLANTS
ITLE          WITH PC=130-PSIA,  MR=1.65,  L*=11.8,  CONTR. RATIO=5
ROBLEM ODE,ODK,TDK, NZONES= 11,
EACTANTS
* * REPLACE THIS CARD WITH ALL APPROPRIATE REACTANT CARDS * *

AMELISTS
$ODE
NP = 1,  P=   134.43, RKT=.TRUE., PSIA=.TRUE., FROZ=.FALSE.,
NOMZPR=4TRUE., NSUP=0, NSUB=1, NOCP=6, PCP= 1.01,1.05,1.1,1.5,2.,4.,
* * REPLACE THIS CARD WITH ONE SPECIFYING  EQRAT & SUBAREA  * *
  OFSKEQ=   1.61067,    1.91926,    2.25516,    2.63570,    4.77404,
  1.14438,    1.19495,    1.30697,    1.57329,    2.35557,
  0.58945,
$END
EACTIONS
* * REPLACE THIS CARD WITH A COMPLETE, APPROPRIATE SET OF REACTION CARDS * *
AST CARD
$ODK
* * REPLACE THIS CARD WITH ONE OR MORE SPECIFYING NOZZLE DESIGN PARAMETERS * *
$END
$TRANS
  XM=   0.14015,    0.09545,    0.10803,    0.11611,    0.11045,
  0.05763,    0.05670,    0.05207,    0.05758,    0.04722,
  0.15851,
$END
$TDK
* * REPLACE THIS CARD WITH ONE SPECIFYING APPROPRIATE  T D K  CONTROLS * *
$END
```

ADDITIONAL COMPUTED DATA

SUBSONIC FLOW AT Z=ZPVSR IN NOZZLE CONVERGENCE

J	ASUBS(J)	VSUBS(J)	PSUBS(J)
1	4.467668E-02	1.434218 03	1.259358 02
2	3.035538-02	1.409188 03	1.259858 02
3	3.357538-02	1.375328 03	1.259858 02
4	3.592528-02	1.344248 03	1.259858 02
5	3.033848-02	1.229338 03	1.259858 02
6	1.974668-02	1.432768 03	1.259858 02
7	1.997108-02	1.437658 03	1.259858 02
8	1.620018-02	1.443468 03	1.259858 02
9	2.013578-02	1.437418 03	1.259858 02
10	1.574638-02	1.371178 03	1.259858 02
11	5.596808-02	1.416858 03	1.259858 02

NOZZLE THROAT PLANE

J	XNI(J)	DFI(J)	PNS(J)	ETAVAP(J)	VBARF(J)	VBARD(J)
1	1.408728-01	1.420778 00	1.343918 02	9.331048-01	8.052468 02	8.770718 02
2	9.528828-02	1.697408 00	1.344668 02	9.445418-01	8.115038 02	8.846998 02
3	1.073668-01	1.996428 00	1.344908 02	9.488358-01	8.144548 02	8.867668 02
4	1.145828-01	2.353438 00	1.347688 02	9.555318-01	8.220518 02	8.934518 02
5	1.067118-01	4.338648 00	1.338458 02	9.758658-01	8.212078 02	8.685658 02
6	5.882288-02	1.009228 00	1.340448 02	9.277048-01	8.532498 02	9.207898 02
7	5.752548-02	1.055158 00	1.340368 02	9.294648-01	8.597478 02	9.296838 02
8	5.755038-02	1.155598 00	1.340768 02	9.338058-01	8.634438 02	9.389478 02
9	5.758958-02	1.397048 00	1.342548 02	9.414038-01	8.671298 02	9.472488 02
10	4.665278-02	2.104558 00	1.345298 02	9.543558-01	8.634638 02	9.433218 02
11	1.620098-01	6.735308-01	1.337878 02	9.225698-01	8.643268 02	9.522878 02

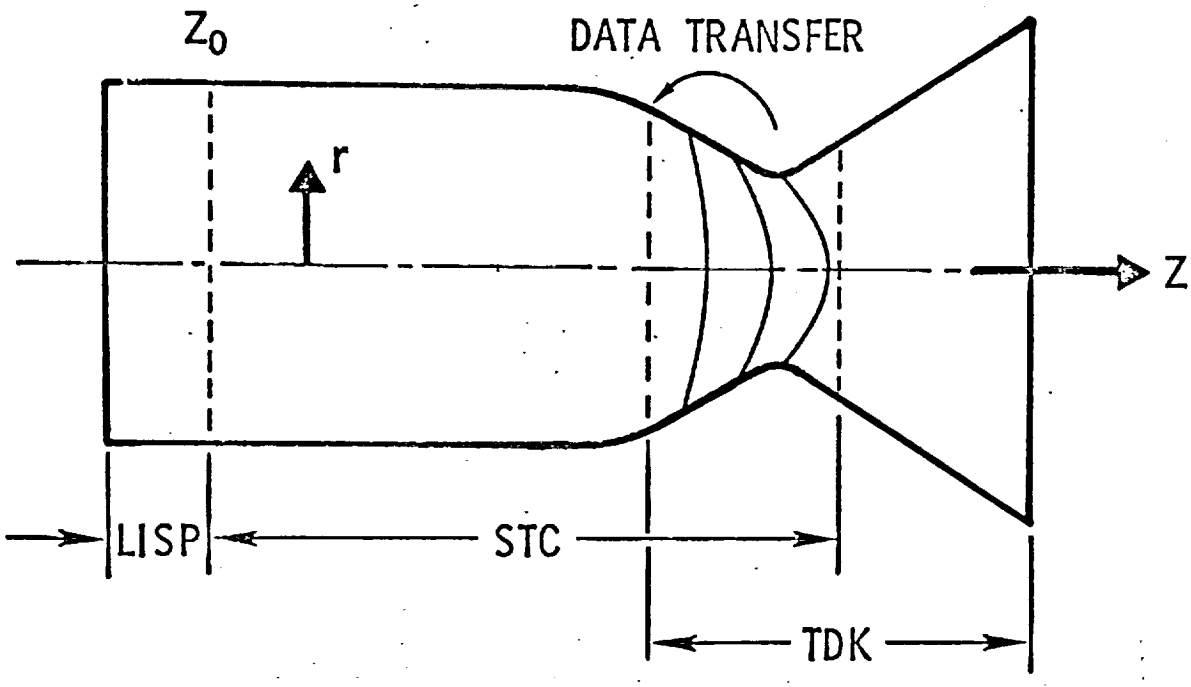

Figure 15. Distributed Energy Release
Revised STC/TDK Interface

No modifications have been made to the improved TDK program to make it compatible with DER. TDK analyzes only the gasified propellant flow. No account is taken of either the propellant mass loss represented by residual sprays passing through the throat nor of continued evaporation and acceleration that such sprays might undergo in the supersonic nozzle expansion section. Neither is their momentum added to the TDK initial plane momentum. Until such time as TDK is modified to utilize additional input data from STC, it appears that only the following simple corrections to the TDK computed performance data can be made:

$$I_{SP} = \left(I_{SP}\right)_{TDK}\left(\eta_{vap}\right)_{STC} \tag{56}$$

$$C_F = \left(C_F\right)_{TDK}\left(\overline{\eta}_{vap}/\,\overline{\eta}_{c*}\right)_{STC} \tag{57}$$

The two efficiencies, $\overline{\eta}_{vap}$ and $\overline{\eta}_{c*}$ are printed out at the throat plane during multiple stream tube STC analysis.

Evaluation of Model

The capabilities of the gas/liquid LISP subprogram block were partially evaluated in Ref. 18 for coaxial LOX/GH_2 element. What appeared, from inspection of LISP printouts, to be acceptable weight flux profiles often had such steep transverse gradients in axial gas velocity and/or in spray concentration that the numerical analysis method in 3D-CØMBUST broke down. In those cases, the analyses were completed by reverting to a gross uniform weight flux and mixture ratio gas stream.

Similarly, partial evaluation was obtained by performing DER analyses of a single element GH_2/LOX triplet at two mixture ratios and with varied combustion chamber diameters and with several methods of initializing stream tubes from LISP mesh point data. A number of conditions were encountered wherein steep radial gradients in axial gas velocity across the STC initial plane could not be accepted by the STC multiple stream tube combustion analysis. Again, selection of the uniform gas option allowed this problem to be sidestepped.

Several cases were run with N_2O_4/N_2H_4-UDMH(50-50) propellants, demonstrating that the liquid/liquid systems could still be analyzed by this version of DER. One of these cases was used to demonstrate that the STC punched-card data are acceptable to the improved TDK program. Additional reactants, reactions, nozzle design, and program control data not punched by STC were added, and TDK was initialized at the beginning of nozzle convergence (rather than at the throat). While this kind of nonphysical data transfer was shown to be feasible, it was quite expensive: the ODK subsonic analysis cost about 1 minute of CPU time per stream tube on the IBM System 360, Mod 50/65 computer.

COMPUTER PROGRAM OPERATION

All versions of the DER computer program were developed for operation on Rocketdyne's IBM System 360, Mod 50/65 computer which is designed to run programs written in Fortran H. So that the programs would be compatible with other computers, however, they were written in Fortran IV (which is a subset of Fortran H). There are, of course, some subprograms which may not be operable on other than

the Rocketdyne computer; for most other computers, these are probably restricted to the data-plotting functions and can be replaced by dummy subroutines without detriment to the rest of the program functions. Also, some trigonometric functions called for in DER may not be in a computer's library and would need to be defined.

To run the program on any computer, a user must supply program control cards that are compatible with his compiler, link editor, etc. The program makes extensive use of overlay to reduce computer storage requirements. Approximately 50,000 words are needed for each version of DER.

Operation of the DER computer program also depends upon a user-supplied data deck, through which he specifies details for the particular injector, combustor, and propellants he desires to analyze. Details concerning the assemblage of a data deck and a complete sample calculation are given in program documentation supplied to JPL for each version of DER. A brief summarization of the calculation procedure is given in the following paragraphs.

Calculation Procedure

Initially, the calculation procedure for using any of the versions of the DER computer program involves expenditure of a substantial effort to assemble a data deck. There are separate sections of the data deck for each of the major program blocks except TRANS; they are assembled in the order in which the program calculations proceed (Fig. 2).

DER main control program input consists only of a set of comment cards describing the case and a set of four flow control integers, whose values determine whether LISP, STC, TRANS, and TDK program blocks are utilized.

The LISP computer program block may require a fairly large input data deck, depending upon the complexity of the injector design and upon whether the injection element types used are represented in the LISP library of distribution correlations. A user must study his injector design to determine what, if any, pie-shaped sector

of the injector/combustor is truly representative of the entire combustor. An appropriate mesh size is denoted by specifying Δr and $\Delta\theta$. He must then decide how many injection elements supply spray to that sector, whether or not it is desirable to analyze only elements that lie within the sector and, if so, what kind of spray flux symmetry exists at lines of symmetry bounding the sector. In defining elements to be analyzed, he must make certain that the sector receives only its proportionate share of the total injected flows. Each injection element's type, location, orientation, scale (hole diameters), discharge coefficients, and propellant species must be given. Additional input of mean drop sizes and mass distribution coefficients are required if an element type is not represented in the LISP library or if, for any reason, the user wishes to override the library functions.

The LISP collection-plane is normally the STC initialization plane. However, in the December 1971 version, it is possible to specify STC initialization upstream of the LISP collection plane. The combining of LISP mesh point flows into stream tube flows is controlled by specifying the number of geometric zones to be considered and the number of stream tubes in each zone. The user exercises no further control over this process.

The number of spray droplet size groups in each stream tube and their division between fuel and oxidizer are input variables. In the September 1970 and March 1971 versions, however, unless only one size group for each propellant is specified, STC will override the input data and select a total of 12 size groups, 6 for each propellant, with the droplet sizes distributed about the $\overline{D}$'s from LISP as if the elements were like doublets. The December 1971 version permits nearly complete freedom in selecting the numbers of propellant droplet size groups and in distributing the sizes around the $\overline{D}$'s. The only restrictions are that there must be at least one size group for each propellant, even if it is completely gasified, and the sum of the fuel and oxidizer size groups cannot exceed 12.

STC computer program block input data are concerned principally with the combustor geometry, combustion gas properties, propellant properties and thermodynamic properties used for calculating spray evaporation coefficients. It is important

that a reasonable effort be devoted to obtaining best available values or estimates.

The STC-marching interval, Δz, is specified implicitly by stating the number of Δz's between the STC initial-plane and the nozzle throat. Too small a value of Δz will result in excessive computer times and too large a value will degrade the accuracy of the solution. Values of $0.033 \leq \Delta z \leq 0.10$-inch have been used in DER checkout analyses. Other user options that may influence both accuracy and computer time are the number of corrector cycles made in each Δz step, and the tolerances placed on convergence upon the throat boundary condition. Too tight a tolerance may require an excessive number of iterations through the STC analysis, resulting in excessive execution times. Input variables specify the maximum number of iterations allowed for both the single and multiple stream tube analyses.

The only user option concerning the TRANS computer program block is whether or not to use it. It is possible to specify that the stream tubes not be analyzed by STC as if they were axisymmetric. In that case, there is no reason to perform the TRANS analyses, STC computations are stopped at the nozzle throat plane (without testing on satisfaction of the nozzle boundary condition or iterating), and TDK input data are not generated. Otherwise, there are no user options concerning calculation, printing and punching of data to be used for initializing TDK.

The TDK portion of the data deck is quite small compared to those portions for LISP and STC, consisting principally of some propellant thermochemical data, nozzle throat, and divergent section geometric data. The user can input data to override a number of default options, such as numbers of iterations, integration stepsize, convergence tolerances, etc., as detailed in Ref. 14. Some of these may influence the performance predictions, but they have not been explored with respect to DER program usage.

Available Adjustments

A summarization is given here of user-adjustable parameters which may influence the performance computed by DER. These are listed separately for the LISP and STC subprogram blocks.

LISP. Choices, made in setting up the LISP analysis, for a number of geometric parameters may conceivably influence the performance prediction. The principal ones are the numbers of radial and circumferential mesh lines used to define the chamber sector to be analyzed, the numbers of mesh lines defined outside of the sector (for folding-in along lines of symmetry or accumulation on solid surfaces) and the axial location of the collection plane, z_0. The weight fluxes computed at a mesh point are multiplied by the chamber cross-sectional area associated with that mesh point to obtain mesh point flowrates; definition of too coarse a grid will not satisfy propellant continuity and will degrade the validity of the entire analysis. Providing two or more mesh lines outside the sector is particularly appropriate when spray impingement on walls or baffles is likely to occur. Such provision is also the manner in which reflecting-or repeating-image folding is invoked along lines of symmetry. The collection plane should be far enough downstream to account for substantial spray spreading and wall impingement. Because LISP does not account for interelement spray interactions, however, spray mixing and impingement effects can be over-predicted if z_0 is too for downstream.

The selection of a chamber sector for analysis should have little influence on performance provided that it is truly bounded by lines of symmetry. If folding by repeating or reflecting symmetry is not invoked, specification of injection elements outside of the sector may influence perfornance. In general, defining more elements should improve validity.

Probably the most important adjustable parameters in LISP are the mass median droplet diameters for the propellant sprays. These usually bear a direct relationship to evaporation efficiencies and, through them, to specific impulse and c* efficiencies. It has been pointed out that, even though LISP will provide calculated $\overline{D}$'s for some element types, the user should satisfy himself that the best available representations of mean droplet sizes for his designs and conditions are used.

Values used for the propellant evaporation coefficients (k') are also important. With liquid/liquid propellant combinations, for which LISP forms a bulk uniform gas flux, LISP gasification is synonymous with forced mixing; overestimated

gasification may result in overestimated mixing and performance efficiencies. With gas/liquid combinations, high percentages evaporated within LISP are likely, and may lead to erroneously high mixing efficiencies. These problems can be partially offset, with the December 1971 version of DER, by intentionally using low values of k' in LISP and moving the STC start plane substantially upstream of the LISP collection plane.

STC. Primarily, the adjustable parameters within STC which are most likely to influence performance predictions are those concerned with stream tube initialization. The minimum percentage of total flow assigned to a wall boundary layer stream tube, the number of annular zones of mesh points and the number of stream tubes per zone all affect the fidelity with which the mixing efficiency represented by the LISP mesh point flows is reproduced in the stream tube flow.

The number of spray droplet size groups, their distributions of diameters about $\overline{D}$ and their spray mass fractions are adjustable parameters. It would seem that using more size groups would yield smoother and more accurate spray burning profiles. If only one size group is initialized for either propellant, however, the computational method is altered in an attempt to preserve burning rate accuracy. Then, rather than retaining a constant number flowrate of size group droplets whose diameters are reduced by spray evaporation, the size group diameter is held constant and evaporation is assumed to deplete the number flowrate of droplets. This reflects the observation that mean droplet diameter of a distributed spray tends to remain constant as it is burned (Ref. 40).

Detailed attention devoted to assembling the input propellant and combustion gas properties tables can affect the performance prediction. In particular, the table of equilibrium combustion gas properties should span the range of gas mixture ratios likely to be computed in any stream tube, and should include enough mixture ratio points to ensure accurate interpolation on the properties.

If the chamber length marching interval, Δz, is small enough, it should not affect performance prediction accuracy. Values used in STC development and evaluation runs ranged between 0.033 inch and 0.10 inch and were satisfactory.

Finally, the single and multiple stream tube analysis convergence tolerances may exercise a slight effect on vaporization and c* efficiencies, but their main use is to ensure that satisfactory results have been computed before proceeding to the next, and perhaps more costly, part of the analysis.

LIQUID OXYGEN SPRAY VAPORIZATION EFFICIENCY CHARTS

The JANNAF Performance Standardization Working Group was assigned, during 1970, the responsibility of ensuring that the JANNAF performance analysis methodology was applicable to space shuttle propulsion systems and designs. For calculation of combustion energy release losses, the committee had planned to use this contract's extension of the Distributed Energy Release (DER) computer program to gas-liquid propellant systems and to burning at highly supercritical pressures. The program schedule, however, could not support such usage. Accordingly, a simplified method was developed which involved the use of simplified LOX spray vaporization efficiency charts (Ref. 41). These were derived from runs of the one-dimensional LOX/GH_2 combustion computer program of Ref. 37, which included the droplet heating and diffusion model used in the March 1971 version of DER. Details concerning the development of these charts are given in Appendix I.

Each chart shows vaporization efficiency vs initial spray size group droplet diameter for several chamber lengths and fixed values of chamber pressure and chamber contraction ratio. Assuming that the spray is initially distributed into N_D size groups with spray mass fractions $X(D_i)$, overall vaporization efficiencies were calculated as

$$\overline{\eta}_{vap} = \sum_{i=1}^{N_D} \eta_{vap}(D_i)\ X(D_i) \qquad (58)$$

with $\eta_{vap}(D_i)$ values read from the appropriate chart. The method was actually applied to the flow in each of several stream tubes representative of striated flow within an engine. Following its utilization by several agencies and contractors, this simplified method was evaluated as having good utility and validity (Ref. 42).

CATALOG OF INJECTOR SPRAY CORRELATIONS

A catalog of injector spray correlations for use with the LISP computer subprogram block was assembled and submitted as a separate report (Ref. 19). This report provides information concerning specific numerical values of liquid spray mass distribution and droplet size correlations for use in the LISP subprogram block of the DER computer program. A technical description of LISP is followed by a discussion of the approach used in deriving empirical mass flux distribution correlation coefficients from injection element cold-flow test data. A detailed numerical example illustrates the correlation techniques. The remainder of the report is devoted to descriptions and brief discussions of the correlations that are programmed into (or are available for use in) the December 1971 version of the DER computer program. These data are catalogued by injection element type. To the extent possible, each section contains: (1) elemental mass flux correlation coefficients; (2) sources of elemental spray data, fluids used, and limitations of the data as to element sizes and flowrate ranges tested; (3) information on droplet size distributions and mean diameter correlations for propellant sprays; and (4) brief summaries of experience in using these correlations for predicting performance, including empirical adjustments found necessary to obtain agreement between experimental and analytical performance predictions. The primary purpose of this catalog is to systematize what is known at this time in a form which can readily incorporate additional data as they are obtained.

STATUS OF THE DER COMPUTER PROGRAM

RELATIONSHIPS TO OTHER PROGRAMS

The various subprogram blocks that comprise the DER computer program all have their counterparts in other computer programs. The other programs are summarized in Tables 6 and 7; their relationships to DER are discussed briefly below.

LISP

The LISP subprogram block in the December 1971 version of DER is, at this writing, the most recent version of LISP. It differs from the LISP of the Injector Chamber Compatability system of computer programs (Ref. 18) in that it has the gas/liquid triplet element capability, it has the polar coordinate contour plotting subroutines, and it generates a scratch data record for STC usage rather than puching 3D-CØMBUST input data. It differs from the LISP of the Pulse Mode Performance Model only in that it has the gas/liquid analysis capability and a more up-to-date library of correlation coefficients.

STC

The STC subprogram of DER, while derived from the Thrust Chamber Compatability program STRMTB, is quite different from STRMTB. It does not generate and punch data for Boundary Layer Heat Transfer (BLEAT) program input. STC is considerably more subroutinized, has an improved gas dynamic solution method and, through an axisymmetric flow option, analyses through the nozzle throat, generating data for initializing TDK analyses.

Similarly, the Pulse Mode Performance Model's PMSTC subprogram (Ref. 25) has a number of significant extensions beyond even the most recent STC. PMSTC solves for local static equilibrium combustion gas properties by means of double interpolations on a bounded mixture ratio function and Mach number. By bounding the mixture ratio function between zero and unity, extrapolation problems were avoided.

TABLE 6. COMPUTER PROGRAMS WHICH HAVE SUBPROGRAMS RELATED TO DER SUBPROGRAM BLOCKS

Name	Ref.	Description
ICC	11, 18	A system of computer programs for analyzing injector design effects on thrust chamber heating and erosion (Injector Chamber Compatibility). Run sequentially, individual programs are: LISP (Liquid Injector Spray Pattern): Combines propellant flows from individual elements of an injector to define spray fluxes and mass median drop diameters in a "collection plane," as well as gas fluxes resulting from partial gasification. Program requires empirical correlation coefficients for element types. A gas/liquid version exists for a few element types but is not accurate enough for general use. 3D-COMBUST (Three-Dimensional Combustion): Initial combustion downstream of the LISP collection-plane is analyzed as an evaporation-controlled process with continued dispersion of sprays and an approximate solution for transverse flow of combustion gases. This program runs rather slowly so as soon as transverse flow subsides, it is replaced by a stream-tube combustion analysis. STRMTB (Stream-Tube Combustion): At a given axial plane, the 3D-COMBUST flows are cast into stream-tubes for a more rapid analysis of the spray combustion up to the throat plane. The stream-tube solutions are loosely coupled but no transfer among them of mass, momentum or energy is allowed. BLEAT (Boundary Layer Heat Transfer): This program accepts combustion gas properties along the wall as calculated by 3D-COMBUST and STRMTB and calculates heat transfer rates to the combustor by a modified Elliot-Silver-Bartz method. Enhanced heating due to radial components of gas velocity and cooling due to spray impingement on the wall are accounted for. 2D-ABLATE: Two-dimensional wall response model accepts surface heat transfer rate data from BLEAT and analyzes conduction within the wall and predicts whether or not wall erosion will occur and its severity. 3D-DEAP: This alternate wall response model analyzes the three-dimensional wall heating under imposed surface heat fluxes. It is more versatile than 2D-ABLATE in many ways but cannot predict erosion. IHTM (Injector Heat Transfer Model): A simplified model of the gaseous recirculating flow near the injector driven by spray drag aspiration effects, analyzes local surface convective heat transfer rates.

TABLE 6. (Concluded)

Name	Ref.	Description
CSS	37	An axisymmetric model of flow and combustion for coaxial jet injection of gaseous hydrogen and liquid oxygen, this model has been used in analyzing the Space Shuttle engine performance. Included in the analysis are recessed-post, cup combustion, distributed atomization (stripping by surface shear) and an axisymmetric 2-zone combustion field. A droplet heating and diffusion spray combustion model is used. The program is fully operational at Rocketdyne but has not been documented with a user's guide for external applications.
PMPM	25	The Pulse Mode Performance Model consists of three major subprogram blocks: PMDER analyzes steady-state engine performance; PULSE sets up parametric tables of performance parameters for each pulse in sequences of short-duration "standard" pulses; DCYCLE synthesizes, from steady-state and standard pulse transient performance data, the performance prediction for each pulse in a specified duty cycle. The PMDER program is the main one of interest. PMDER represents a substantial rework and adaptation of the DER computer program for pulse mode analysis. Several significant improvements have been provided. Combustion products are derived from local equilibrium, expressed as functions of a local mixture ratio function (bounded between 0 and 1) and local Mach number; this removes an earlier discontinuity in properties between DER and TDK. An engine balance analysis has been added which both makes the program more versatile and permits coupling LISP and PMSTC solutions. An option provides for bypassing TDK while calculating all performance parameters if a nozzle vacuum thrust coefficient efficiency is known. The evaporation coefficient (k') spray burning concept is used. This new model is operational and a user's guide is being prepared.

TABLE 7. COMPUTER PROGRAMS COMPRISING THE JANNAF PERFORMANCE EVALUATION METHODOLOGY

Name	Ref.	Description
CPIA Pub. #178	1	Manual presents basic rocket thrust chamber model, including the primary loss processes and describes the JANNAF methodology and computer programs available in 1968. Combustion process losses are approximated by an empirical reduction of propellant enthalpy.
Addendum No. 1 to CPIA Pub. #178	41	Interim updating of performance calculation methodology for application specifically to the high-pressure oxygen/hydrogen Space Shuttle Main Engine designs. (January 1971)
ODE	43	One-dimensional equilibrium reference program calculates combustion product properties at selected points in isenthalpic gas flow. This program is completely functional.
TDE	44	Two-dimensional equilibrium reference program calculates divergence efficiency using equilibrium gas flow and method of characteristics. This program has not been kept up to date.
ODK	45	One-dimensional kinetic reference program calculates expanding isenthalpic streamtube gas flow with kinetically controlled reaction rates. Begins from an ODE solution at some specified subsonic point in the flow. Program is completely functional but runs slowly for near-equilibrium cases.
TDK	14, 15	Two-dimensional kinetic reference program utilizes ODE, ODK, and a transonic flow solution to calculate supersonic start-line conditions for a two-dimensional method-of-characteristics solution of the isenthalpic (stream-wise) kinetically limited supersonic expansion. TDK also has the option to calculate a divergence efficiency using perfect gas relationships. Program has had problems with near-equilibrium systems like O_2/H_2 and is currently being revised.
TBL	46	Turbulent boundary layer program calculates the lengthwise heat losses from the combustion gas stream (defined by TDK) to the combustor/nozzle walls. Also calculates a lengthwise boundary layer displacement thickness which may be used to modify the wall contour in a subsequent rerun of TDK. This program is operational but the heat transfer calculations required for engine system analysis have not been standardized and may be erroneous.
MABL	47	Mass addition boundary layer program calculates boundary layer conditions for reacting flow with or without mass addition using differential approach. Program is slow and sensitive to inputs. Matching of wall properties to TDK is also a potential source of error.

Execution times were reduced by adopting a more efficient interpolation method. Incorporation of an engine balance analysis provided a much more versatile solution scheme and more realistic satisfaction of the throat boundary condition, as well as permitting LISP to be coupled into the adjustments made for that purpose. Finally, PMSTC computes and prints a complete performance summary, whereas STC is limited to vaporization and c* efficiencies.

TRANS

The TRANS subprogram in DER is unlike any other known computer program for analyzing transonic flow, in that it has been modified to compute isobars for substantially subsonic flows. It has apparently been made obsolete by the multistream tube transonic analysis in the improved TDK (Ref. 15), but it also appears to be quite adequate for DER's usage and need not be changed.

TDK

The revised, long-form-option version of TDK used by DER is not so versatile and lacks many of the features of the improved version (Ref. 15). For many nozzles and propellant systems, however, its restriction to supersonic flow may be perfectly appropriate so that a better argument for supplanting it might require more efficient, less costly computation.

RELATIONSHIP TO JANNAF PERFORMANCE ANALYSIS METHODOLOGY

The JANNAF Performance Evaluation Methodology, Table 7, needed an analytical method for accounting for the "distributed energy release" performance loss mechanisms associated with propellant spray combustion. The DER computer program was designed to fill that need by performing detailed calculations concerning the progress of the combustion processes, linking them directly to known injector design parameters and propellant supply properties.

DER presumably will be formally adopted by the JANNAF committee at some future date. Adoption could be hastened by obtaining more information on model validity (verification) and by demonstrating general applicability to a wide variety of problems, operability on several different computers and economical operation. Status with respect to each of these categories and additional work that might be required are summarized below.

Verification

DER model validity has been only partially demonstrated by comparison with c* and specific impulse efficiency data from a FLOX/CH_4-C_2H_6 engine with like-doublet pair injection. Indications of validity have been obtained indirectly with other propellants by combining one-dimensional combustion analysis with cold-flow mixing data. Much remains to be done here. Critical comparisons of predictions with test data for other injector and combustor designs and other propellants need to be a continuing effort to establish prediction accuracy and ranges of model validity, as well as to denote areas where the model is deficient.

One aspect that bears strongly on verification analyses is the sensitivity of performance predictions to input spray droplet sizes. The expressions used by LISP are, in general, derived from cold-flow experiments using propellant simulants. There are not well-defined methods for adjusting such data for the effects of going from simulants to propellants or for going from atmospheric tests to rocket combustor environments. It appears that this aspect will ultimately control the validity of a priori predictions.

Generality of Application

Application of DER depends on the model formulation fitting the combustor design and upon having dropsize and mass distribution correlations for the injector design. The formulation is restricted to cylindrical chamber designs and axisymmetric stream tubes; extension to annular and rectangular designs might be desirable. Distribution correlations have been obtained for liquid/liquid like and unlike doublets, triplets, and four-on-one elements, and for gas/liquid triplets and

coaxial jets. Some of these correlations are for rather restricted ranges of design variables. An obvious need is for continued extension to wider ranges of element types and design variables. Also, a second-generation gas/liquid LISP program will be needed.

Operability

Run only on Rocketdyne's IBM System 360 and JPL's Univac 1108, the DER program's operability has not been adequately determined. To facilitate and encourage use by other agencies and contractors, some work may need to be done toward simplifying input data formats, which differ considerably from the other programs in the JANNAF methodology. Additionally, DER needs to be provided with logic to effect appropriate interface with the TBL and MABL boundary-layer analysis programs.

Operational Costs

Computer program operating costs vary considerably among computers. The k' version of DER is relatively economical. The LISP/STC portions cost perhaps a fraction of the TDK portion, depending of course on the number of stream tubes analyzed, chamber length, and nozzle expansion ratio.

The droplet diffusion version of STC, on the other hand, costs as much or more than the TDK part. Significant economies might be effected in future versions of DER by utilizing more efficient interpolation and iteration techniques and by investigating some other potential economies that have not been explored during program development.

CONCLUSIONS AND RECOMMENDATIONS

Development of the DER computer program has provided several significant advances in analysis of liquid rocket propellant combustion and performance:

1. The effects of injector design variables on spray combustion and propellant mixing efficiencies and, therefore, on performance are accounted for in a manner that can be incorporated directly into the JANNAF performance analysis methodology.

2. The multi-stream tube approach to modelling propellant spray combustion processes has been perfected. Both the simplified evaporation coefficient method and a more rigorous droplet heating and diffusion model for calculating spray droplet burning rates have been included.

3. Transonic flow effects on spray combustion in rocket nozzle convergent sections have been taken into account for the first time. The method used permits accurate modelling of the nozzle throat boundary condition on the combustor.

The resultant DER computer program is capable of analyzing accurately the effects of distributed spray combustion energy release on liquid rocket performance. A number of precautionary notes should be listed, however, concerning its application and areas of possible improvement:

1. A substantial number of available input data adjustments may influence the performance prediction accuracy. The user must select input parameters carefully. Particularly influential parameters are those describing the propellant atomization (median droplet diameters and diameter distributions). Although there are formulae in LISP to calculate mass median diameters produced by several injection element types, a user may be well advised to determine more accurate values for his cases.

2. LISP spray distribution correlation coefficients cover somewhat limited ranges of injection element types and design conditions. A user may need to derive and supply his own coefficients in order to perform the full DER analysis.

3. The gas/liquid version of LISP has only limited applicability. It is restricted to coaxial and triplet elements spaced not too closely together. Further, its calculated transverse mass flux gradients may be so steep that the subsequent combustion analysis encounters numerical problems.

4. In the first two (September 1970 and March 1971) versions of DER, a discontinuity in combustion gas properties at the STC/TDK interface prevents accurate analysis of the supersonic nozzle expansion by the modified TDK program section of DER. Rather than using the modified TDK included in these versions, it is recommended that STΔ-computed data be used to assemble a data deck for subsequent, separate TDK analyses.

5. The validity of DER's performance predictions should continue to be evaluated by comparison with available experimental engine and thrust chamber performance data. This is the most direct and reliable way of discerning aspects that may need to be improved in future work.

Notwithstanding these several precautionary notes and areas where additional work could benefit performance prediction accuracy or computer program operability, it is recommended that the DER computer program be incorporated into the JANNAF liquid rocket performance evaluation methodology.

REFERENCES

1. Pieper, J. L.: ICRPG Liquid Propellant Thrust Chamber Performance Evaluation Manual, CPIA Publication No. 178, Chemical Propulsion Information Agency, Silver Spring, Md., September 1968.

2. Powell, W. B., Current Status of the ICRPG Liquid Propellant Thrust Chamber Performance Evaluation Methodology, AIAA Paper No. 69-468, June 1969.

3. Priem, R. J. and M. F. Heidmann, Propellant Vaporization as a Design Criterion for Rocket Engine Combustion Chambers, NASA TR-67, 1960.

4. Lambiris, S., L. P. Combs, and R. S. Levine: "Stable Combustion Processes in Liquid Propellant Rocket Engines," Combustion and Propulsion Fifth AGARD Colloquium: High Temperature Phenomena, The MacMillan Co., New York, N.Y., 1962, 569-636.

5. Breen, B. P., et al.: Injection and Combustion of Hypergolic Propellants, AFRPL-TR-69-48, Dynamic Science, a division of Marshall Industries, Irvine, California, April 1969.

6. Breen, B. P. and M. R. Beltran: Steady-State Droplet Combustion With Decomposition: Hydrazine/NTO, AICHE 61st National Meeting, Houston, Texas, February 1967.

7. Campbell, D. T. and W. D. Chadwick: Combustion Instability Analysis at High Chamber Pressures, AFRPL-TR-67-222, Rocketdyne, a Division of North American Rockwell Corporation, Canoga Park, California, August 1967.

8. Godsave, G. A. E.: Fourth Symposium (International) on Combustion, Baltimore, Maryland, Williams and Wilkens Co., (818-830) 1953.

9. Nurick, W. H. and S. D. Clapp: J. of Spacecraft and Rockets, Vol. 6, No. 11, November 1969, 1312.

10. Kors, D. L., L. B. Bassham, and R. E. Walker: A Liquid Rocket Performance Model Based on Vaporization Interactions, AIAA Paper No. 69-470, June 1969.

11. Hines, W. S., L. P. Combs, W. M. Ford, and R. VanWyk: Development of Injector Chamber Compatibility Analysis, Final Report, AFRPL-TR-70-12, Rocketdyne, a Division of North American Rockwell Corporation, Canoga Park, California, March 1970.

12. Sutton, R. D., W. S. Hines, and L. P. Combs: "Development and Application of a Comprehensive Analysis of Liquid Rocket Combustion", AIAA Journal, Vol. 10, No. 2, February 1972.

13. Combs, L. P., W. D. Chadwick, and D. T. Campbell: Liquid Rocket Performance Computer Model With Distributed Energy Release, Interim Final Report, NASA-CR-111000, (R-8298), Rocketdyne, a Division of North American Rockwell Corporation, Canoga Park, California, September 1970.

14. Kliegel, J. R., et al.: ICRPG Two-Dimensional Kinetic Reference Program, Dynamic Science, a Division of Marshall Industries, Irvine, California, July 1968.

15. Frey, H. M. and G. R. Nickerson: TDK, Two-Dimensional Kinetic Reference Program, Improved Version, Dynamic Science, a Division of Marshall Industries, Irvine, California, December 1970.

16. Hines, W. S., et al., "Analytical Description of Injected Propellant Spray Mass Distributions", Sixth ICRPG Combustion Conference, CPIA Publication No. 192, December 1969.

17. Rupe, J. H. and G. H. Jaivin: The Effects of Injection Mass Flux Distributions and Resonant Combustion on Local Heat Transfer in a Liquid Propellant Rocket Engine, Progress Report 32-648, Jet Propulsion Laboratory, Pasadena, California, October 1964.

18. Hines, W. S., M. D. Schuman, W. M. Ford, and K. W. Fertig: Extension of a Thrust Chamber Compatibility Model, Final Report, AFRPL-TR-72-19, (R-8745), Rocketdyne, a Division of North American Rockwell Corporation, Canoga Park, California, March 1972.

19. Combs, L. P.,: Catalog of Injector Spray Correlations, Rocketdyne, a Division of North American Rockwell Corporation, Canoga Park, California, June 1972.

20. Dickerson, R. A., K. Tate, and N. Barsic: Correlation of Spray Injector Parameters With Rocket Engine Performance, Final Report, AFRPL-TR-68-147, Rocketdyne, a Division of North American Rockwell Corporation, Canoga Park, California, June 1968.

21. Falk, A. Y., S. D. Clapp, and C. K. Nagai: Space Storable Propellant Performance Study, Final Report, NASA CR-72487, Rocketdyne, a Division of North American Rockwell Corporation, Canoga Park, California, November 1968.

22. Nickerson, G. R., Instructions for Replacing the Transonic Analysis of the TDK Computer Program, Dynamic Science Letter Report, April 1970.

23. Kliegel, J. R. and J. N. Levine: "Transonic Flow in Small Throat Radius of Curvature Nozzles," AIAA Journal, Vol. 7, No. 7, July 1969.

24. Ingebo, R. D.: Drop Size Distributions for Impinging-Jet Breakup in Airstreams Simulating the Velocity Conditions in Rocket Combustors, NACA TN4222, March 1958.

25. Chadwick, W. D. and L. P. Combs: Pulse Mode Performance Model, Final Report, Contract F04611-70-C-0074, AFRPL-TR-72-16 (R-8864), Rocketdyne, a Division of North American Rockwell Corporation, Canoga Park, California, to be published in late 1972.

26. Penner, S. S.: Chemistry Problems in Jet Propulsion, Pergamon Press, 1957.

27. Williams, F. A.: Combustion Theory, Addison-Wesley, Chapter 11, 1965.

28. Dickerson, R. A.: Comprehensive Single Droplet Combustion Model, EE-70-12-7, Rocketdyne Internal Memo, Rocketdyne, a Division of North American Rockwell Corporation, Canoga Park, California, March 1970.

29. El Wakil, M. M.: Experimental and Calculated Temperature and Mass Histories of Vaporizing Fuel Droplets, NACA TN 3480, January 1956.

30. Agosta, V. D.: "Nonlinear Combustion Instability: Longitudinal Mode," 6th ICRPG Combustion Conference, CPIA Publication No. 192, December 1969.

31. Ranz, W. E., and W. R. Marshall, Jr.: Chemical Engineering Progress, 48, 141-146, and 173-180, 1952.

32. Savery, C. W.: Experimental Studies of the Vaporization of Droplets in Heated Air at High Pressures, NASA CR-72574, Department of Mechanical Engineering, University of Wisconsin, Madison, Wisconsin, August 1969.

33. Chueh, P. L., and J. M. Prausnitz: "Calculation of High Pressure Vapor-Liquid Equilibria," Industrial and Engineering Chemistry, Vol. 60, 1968, pp. 34-52.

34. Reid, R. C., and T. K. Sherwood: The Properties of Gases and Liquids, 2nd Edition, McGraw-Hill, New York, 1966.

35. Spalding, D. B.: "Theory of Particle Combustion at High Pressures," ARS Journal, Vol. 29, No. 11, November 1959.

36. Faeth, G. M., et al.: "Supercritical Bipropellant Droplet Combustion," Twelfth Symposium (International) on Combustion, The Combustion Institute, Pittsburgh, Pa., 9-17, 1969.

37. Sutton, R. D., and M. D. Schuman: "Liquid Combustion Analysis for Coaxial Jet Injection of Gas/Liquid Propellants," 7th JANNAF Combustion Meeting, CPIA Publication No. 204, Vol. 1, 511-530, February 1971.

38. Unpublished data obtained by Rocketdyne under Contract NAS3-11199. Also, see Burick, R. J.: "Atomization and Mixing Characteristics of Gas/Liquid Coaxial Injector Elements," AIAA Paper No. 71-672, June 1971.

39. Unpublished data obtained by Rocketdyne under Contract NASw-2106. Also, see Nurick, W. H.: Experimental Investigation of Combustor Effects on Rocket Thrust Chamber Performance, Interim Report R-8903, Rocketdyne, a Division of North American Rockwell, Canoga Park, California, June 1972.

40. Ingebo, R. D.: "Heat Transfer and Drag Coefficients for Ethanol Droplets in a Rocket Chamber Burning Ethanol and Liquid Oxygen," Eighth Symposium (International) on Combustion, Williams and Wilkens, Baltimore, (1104-1112), 1962.

41. "JANNAF Interim Performance Calculation Methodology for Use in the SSME Proposal Response," Addendum No. 1 to CPIA Publication No. 178, Manual and Procedures Revision Subcommittee, February 1971.

42. Private communication, Tyson, T., Dynamic Science, a Division of Marshall Industries, Minutes of the 10 May 1971 Meeting of the JANNAF Manual and Procedures Revision Subcommittee.

43. ICRPG One-Dimensional Equilibrium Reference Program - Preliminary Description of ODE, a Computer Program for the Calculation of Chemical Equilibrium Compositions with Applications, ICRPG Performance Standardization Working Group, July 1968.

44. Aceto, L., and Zupnik, T. F., Two-Dimensional Equilibrium Nozzle Analysis Computer Program-TDE, prepared for the ICRPG Performance Standardization Working Group, July 1968.

45. Frey, H. M., G. R. Nickerson and T. J. Tyson: ODK, One Dimensional Kinetic Reference Program, Improved Version, Dynamics Science, a division of Marshall Industries, Irvine, California, September 1970.

46. Weingold, H.D.: TBL, ICRPG Turbulent Boundary Layer Nozzle Analysis Computer Program, Pratt and Whitney Aircraft, division of United Aircraft Corporation, East Hartford, Connecticut, July 1968.

47. Levine, J. N.: Transpiration and Film Cooling Boundary Layer Computer Program, SN-230, Dynamic Science, a division of Marshal Industries, Irvine, California, June 1971.

APPENDIX I

REPORTS, DOCUMENTS AND PRESENTATIONS RESULTING FROM CONTRACT NAS7-746

As a result of work performed under Contract NAS7-746, "The Effects of Distributed Energy Release on Liquid Rocket Performance," the following reports, documents and presentations have been produced. They are listed in chronological order. The scope of each and whether it is of current interest are indicated.

1. NASA CR-111000, Liquid Rocket Performance Computer Model with Distributed Energy Release, Interim Final Report, September 1970. Described the development and evaluation of the September 1970 version of DER. In large measure, it is incorporated into this final report, which supercedes it.

2. "Liquid Rocket Performance Computer Program with Distributed Energy Release, DER Computer Program Documentation and User's Guide," September 1970. An unnumbered report describing the September 1970 version of DER including instructions for inputting data and running it and an example case. Superseded by Item 7, below.

3. "Liquid Rocket Performance Analysis with Distributed Energy Release," 7th JANNAF Combustion Meeting, CPIA Publication No. 204, Vol. 1, pages 493-510, February 1971. A summarization of the first year's effort, presented in October 1970.

4. "Vaporization Efficiency Charts for SSME Combustor Designs;" an unnumbered memorandum to the Liquid Rocket Performance Committee of JANNAF Performance Standardization Working Group, December 1970. The charts presented (see Appendix II) were incorporated in "JANNAF Interim Performance Calculation Methodology for Use in the SSME Proposal Response," Addendum to CPIA Publication No. 178, February 1971.

5. "Liquid Rocket Performance Computer Model with Distributed Energy Release, Documentation for Interim Delivery of the Revised Computer Program with Droplet Heating." This is an unnumbered report describing the March 1971 version of DER. Only those parts concerned with the STC subprogram block differ from Item 2, above. An STC example calculation is given for gaseous hydrogen/liquid oxygen at supercritical conditions for the oxygen spray. This report is still in use.

6. "Extension and Status of the Distributed Energy Release (DER) Computer Program," 8th JANNAF Combustion Meeting, CPIA Publication No. 220, Vol.1, pages 659-669, November 1971. A summarization of the work under Contract NAS7-746 and the status of the DER program with respect to its implementation in the JANNAF performance methodology.

7. "Liquid Rocket Combustion Computer Program with Distributed Energy Release, DER Computer Program Documentation and User's Guide," December 1971. This unnumbered report provides updated descriptions and input instructions for using the December 1971 version of DER. It supersedes Item 2, above.

8. "Catalog of Injector Spray Correlations," June 1972. This report describes the methods in deriving LISP correlation coefficients from cold-flow spray distribution data, including a complete example calculation, and catalogs the coefficient values actually programmed into (or available as input data) the December 1971 version of DER. The format is amenable to periodic updating.

APPENDIX II

LIQUID OXYGEN SPRAY VAPORIZATION EFFICIENCY CHARTS

A series of charts for calculating liquid oxygen spray vaporization efficiency in high pressure LOX/GH_2 propulsion systems was derived from runs of a one-dimensional combustion computer program* which was based on the droplet heating and diffusion model described in pages 60 to 65 . The approach taken was to make a large number of model runs, with variations in design and operating conditions, and cross-plot individual droplet size group vaporization efficiencies versus size group initial droplet diameters.

DESIGN CONDITIONS FOR CHART CALCULATION

Nominal engine design conditions were determined by telephone consultations with NASA and contractor representatives. Design parameters selected were:

Chamber lengths, injector-to-throat, inches	6, 10, and 14
Chamber contraction ratio, ε	2 and 3
Nozzle convergence angle, degrees	30
Nozzle throat radius ratio	0.75
Radius ratio at start of convergence	1.0
Chamber pressures, psia	1500 and 3000
Total injection mixture ratio, o/f	6.0
Hot gas injection mixture ratio	1.0
Liquid oxygen injection temperature, R	220
Liquid oxygen injection velocity, ft/sec	
(at 3000 psia)	100
(at 1500 psia)	50
Liquid oxygen spray, distribution	Log-normal
atomization	5 values of $\overline{D}$

(For the 6-inch long, 3.0 contraction ratio chamber, a 38 degree conical convergence beginning at the injector face was required.)

*Sutton, R. D. and M. D. Schuman: "Liquid Combustion Analysis for Coaxial Jet Injection of Gas/Liquid Propellants," 7th JANNAF Combustion Meeting, CPIA Publication No. 204, Vol. 1, 511-530, February 1971.

The log-normal droplet distribution used by Priem and Heidmann* is given by:

$$\frac{d\mathcal{R}}{dD} = \frac{c_1}{D} \exp \left\{ - \frac{1}{2} \left[\frac{\ln(D/\overline{D})}{\ln\sigma} \right]^2 \right\} \qquad \text{(II-1)}$$

The volume fraction of spray in a given droplet size range is controlled by the two parameters $\overline{D}$, which controls the coarseness of the spray, and σ, which controls the relative spread in droplet sizes in a spray of given $\overline{D}$. In investigations conducted by Priem and Heidman* and in other investigations, some preference was indicated for σ=2.3 to represent rocket injector sprays, therefore, this value was used for the nominal condition cases.

The spray distribution was approximated by nine discreet droplet size groups. Because the largest droplets are those which may degrade performance, the size group diameters were selected to give a finer division of mass flux among the large droplets than among the small ones:

Size Group No.	1	2	3	4	5	6	7	8	9
Diameter Ratio, $D/\overline{D}$	0.37	0.65	1.00	1.40	1.73	2.6	2.60	3.2	4.7
Volume Fraction	0.20	0.20	0.20	0.10	0.10	0.05	0.05	0.05	0.05

Some preliminary computer runs were made to determine approximately the range of $\overline{D}$'s which would result in vaporization efficiencies above 90 percent. A maximum $\overline{D}$ of 120 microns was indicated; most of the curves were generated with $\overline{D}$'s of 20 or 30, 40, 60, 80, and 120 microns.

In addition to the systematic variations of chamber length, chamber contraction ratio, and chamber pressure, a few auxiliary calculations were made to indicate the effects of anticipated variations of both liquid oxygen injection velocity and temperature, of hot-gas injection mixture ratio and of the σ parameter in the log normal distribution. These auxiliary cases were run with a 10-inch long, 3.0 contraction ratio chamber at 3000 psia.

*Priem, R. J. and M. F. Heidmann, Propellant Vaporization as a Design Criterion for Rocket Engine Combustion Chambers, NASA TR-67, 1960.

CALCULATED RESULTS

The composite results from approximately 60 computer runs representing the listed nominal conditions were given in a set of four vaporization efficiency charts, each of which consisted of a family of three chamber length curves showing vaporization efficiency at the nozzle throat plane versus droplet size group initial diameter for a particular combination of chamber pressure and chamber contraction ratio. The four charts are shown in Fig. II-1 through II-4.

Some scatter of the individual droplet size group data points about the curves drawn resulted from having started with different values of $\overline{D}$, σ, mixture ratio, etc. In general, deviations from the curves were well within ±2 percent.

The method of using these charts was described on page 85.

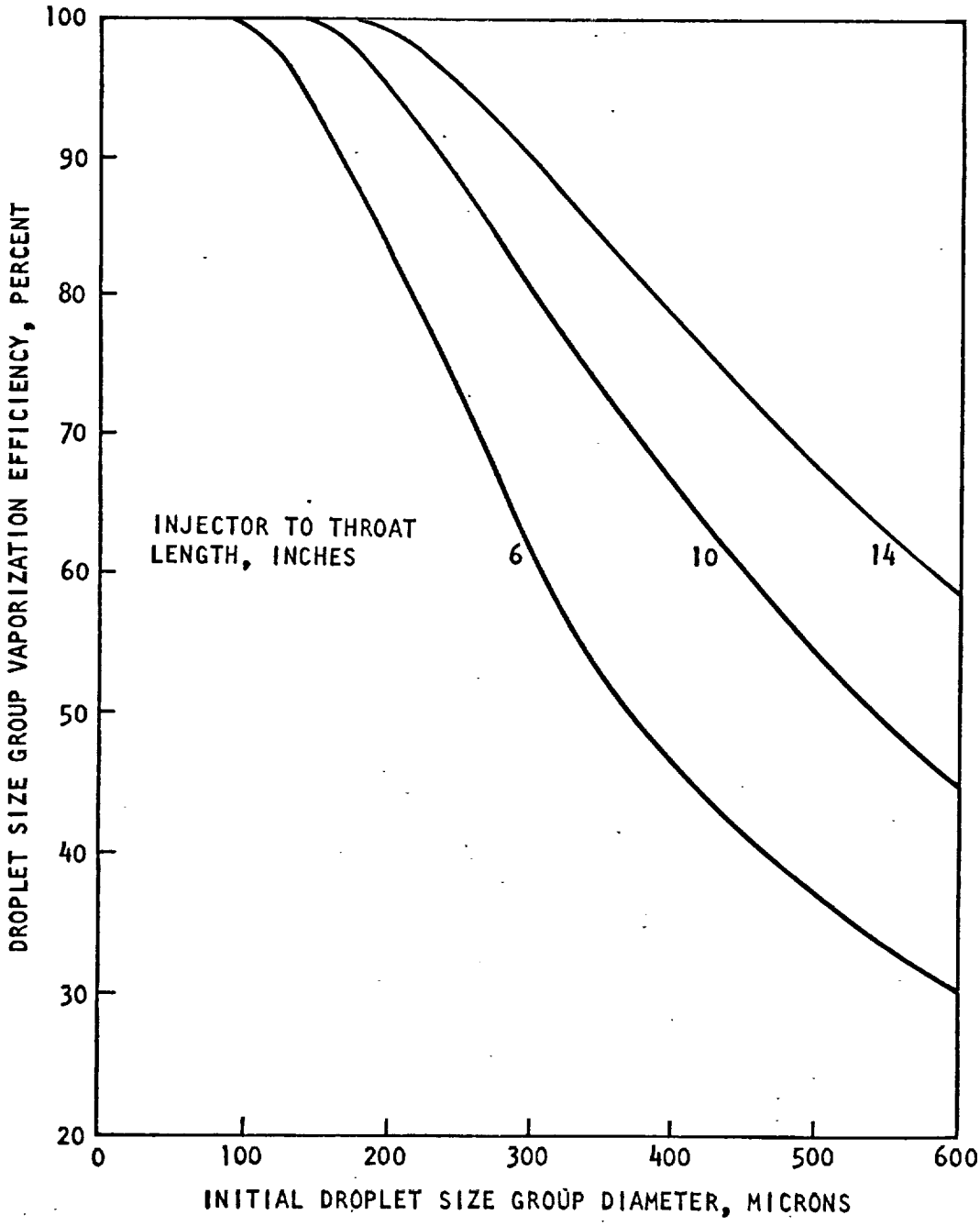

Figure II-1. Droplet Size Group Vaporization Efficiency
(3.0 Contraction Ratio, 3000 psia Chamber Pressure)

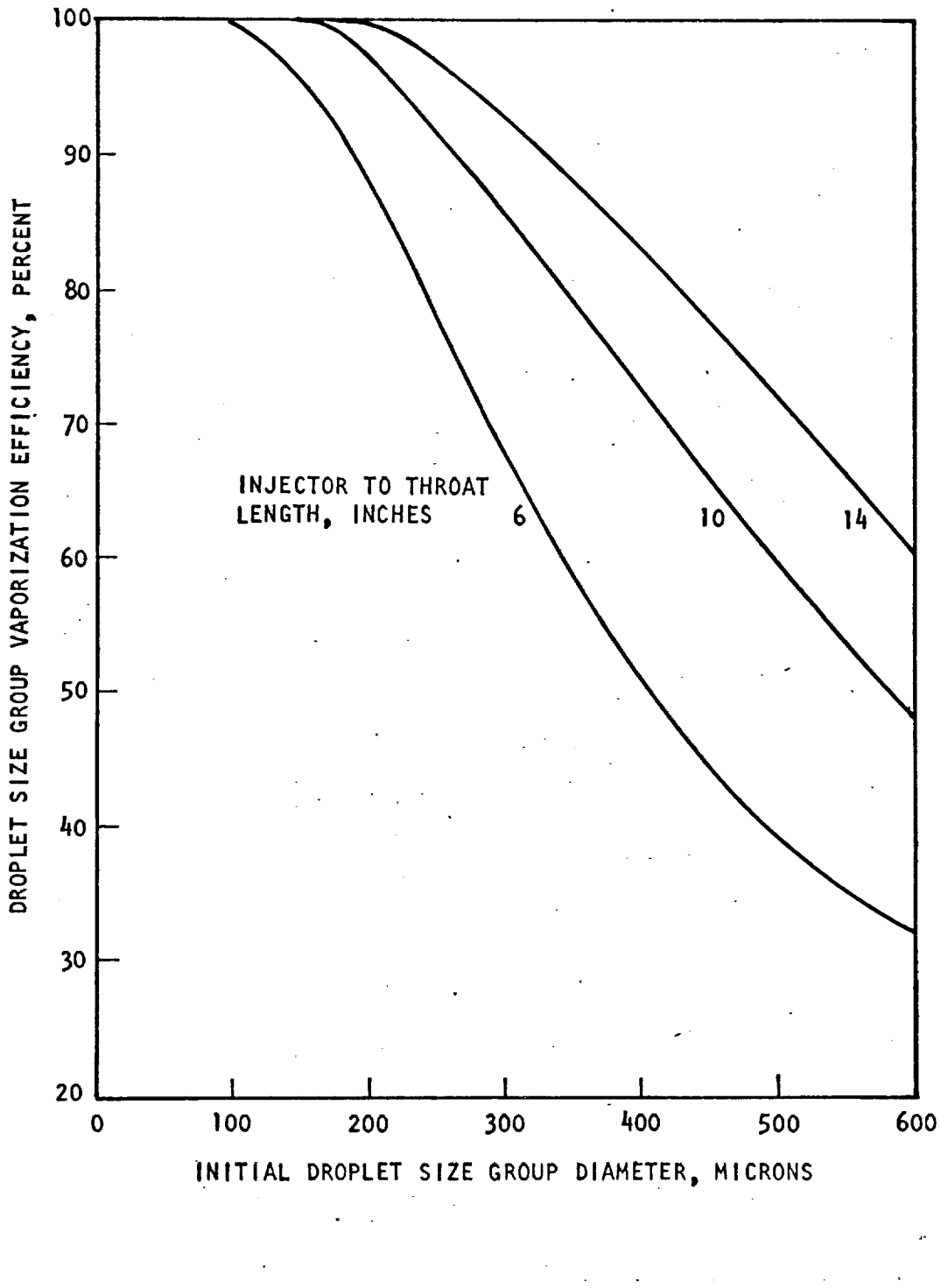

Figure II-2. Droplet Size Group Vaporization Efficiency (3.0 Contraction Ratio, 1500 psia Chamber Pressure)

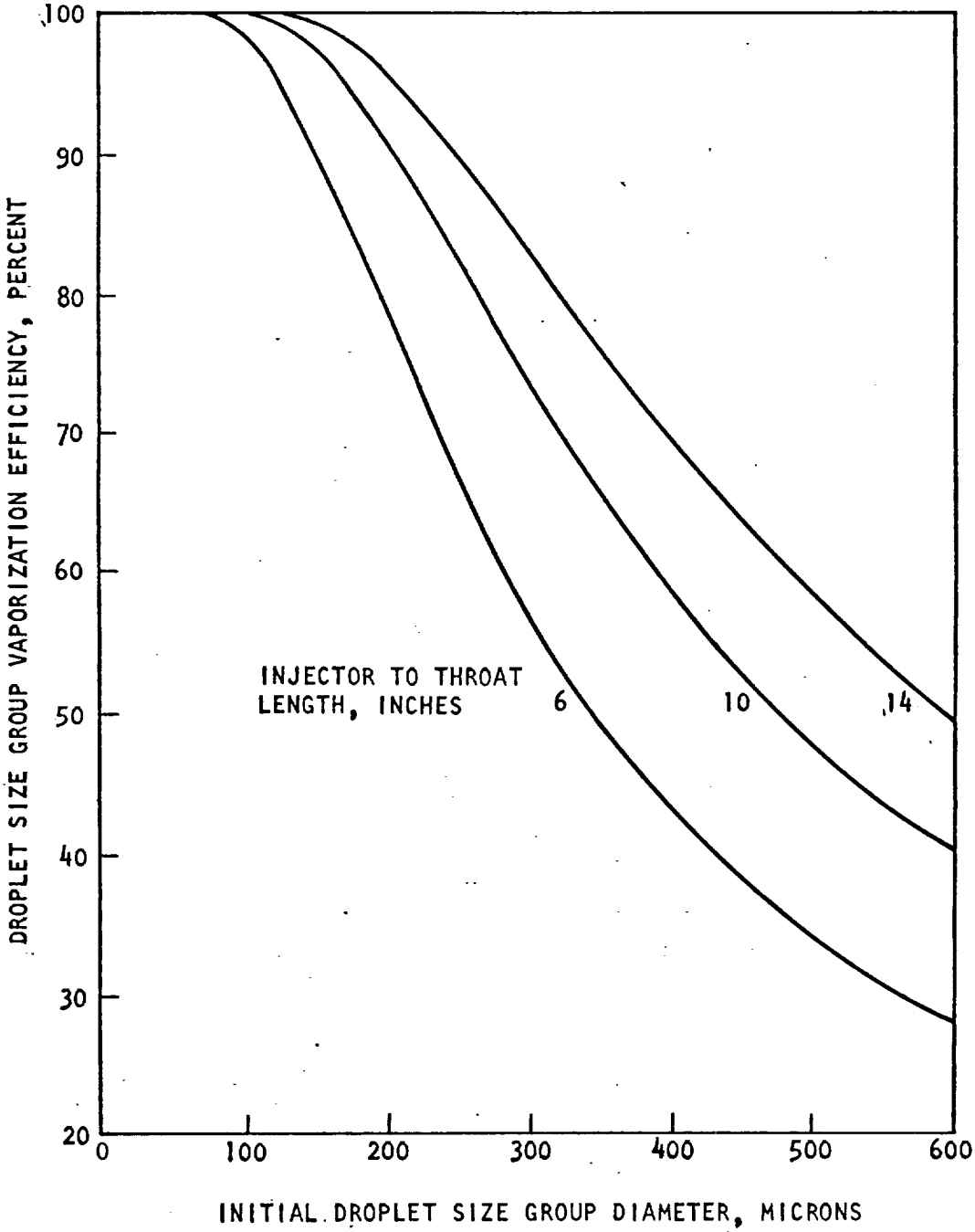

Figure II-3. Droplet Size Group Vaporization Efficiency (2.0 Contraction Ratio, 3000 psia Chamber Pressure)

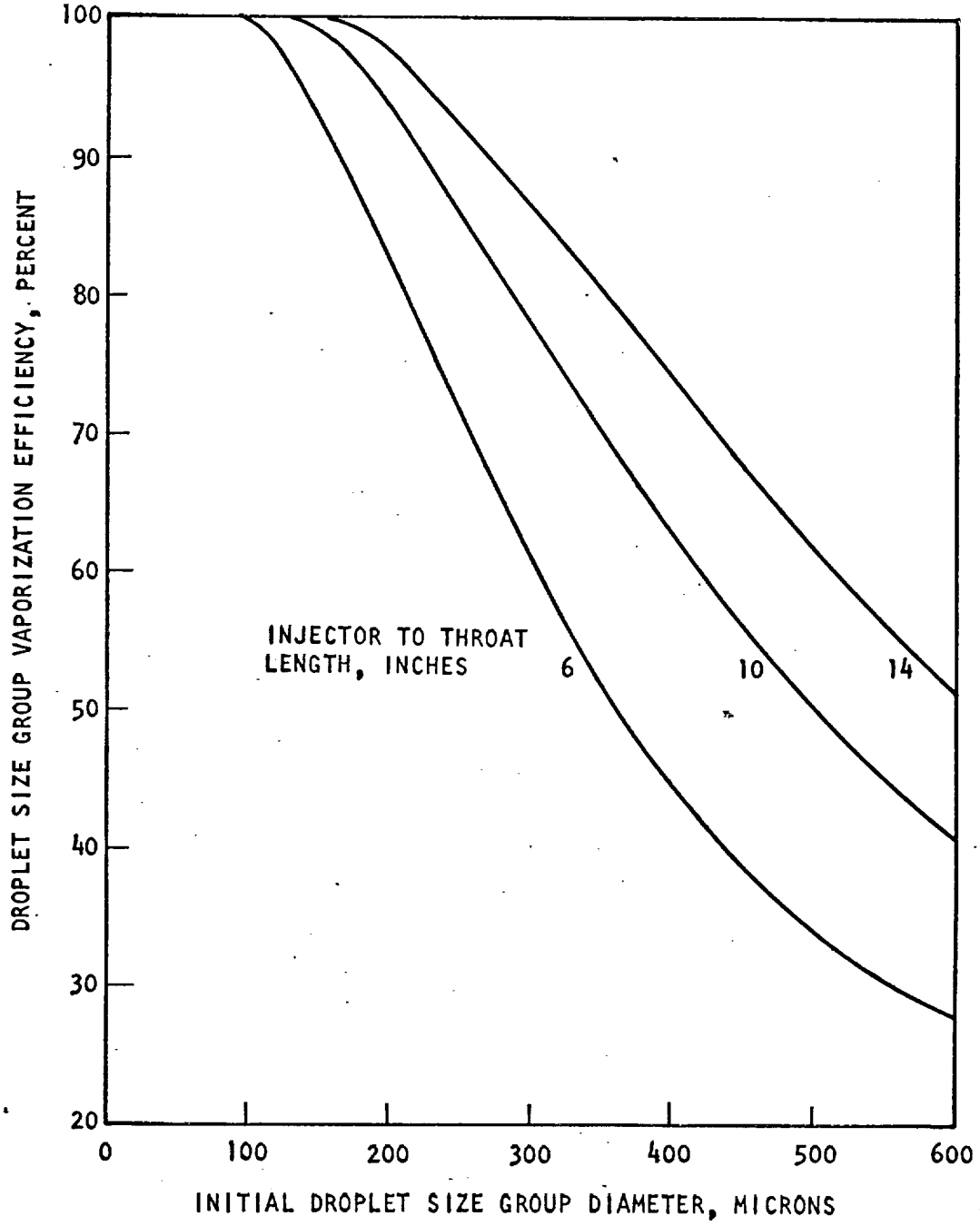

Figure II-4. Droplet Size Group Vaporization Efficiency (2.0 Contraction Ratio, 1500 psia Chamber Pressure)

UNCLASSIFIED
Security Classification

DOCUMENT CONTROL DATA - R & D

(Security classification of title, body of abstract and indexing annotation must be entered when the overall report is classified)

1. ORIGINATING ACTIVITY *(Corporate author)*

ROCKETDYNE
a division of North American Rockwell Corporation
6633 Canoga Avenue, Canoga Park, California 91304

2a. REPORT SECURITY CLASSIFICATION

Unclassified

2b. GROUP

3. REPORT TITLE

LIQUID ROCKET PERFORMANCE COMPUTER MODEL WITH DISTRIBUTED ENERGY RELEASE

4. DESCRIPTIVE NOTES *(Type of report and inclusive dates)*

Final Report, August 1969 to 15 January 1972

5. AUTHOR(S) *(First name, middle initial, last name)*

L. P. Combs

6. REPORT DATE	7a. TOTAL NO. OF PAGES	7b. NO. OF REFS
10 June 1972	130	47

8a. CONTRACT OR GRANT NO.	9a. ORIGINATOR'S REPORT NUMBER(S)
NAS7-746	R-8888
b. PROJECT NO.	
c.	9b. OTHER REPORT NO(S) *(Any other numbers that may be assigned this report)*
d.	NASA CR-

10. DISTRIBUTION STATEMENT

11. SUPPLEMENTARY NOTES	12. SPONSORING MILITARY ACTIVITY

13. ABSTRACT

Development of a computer program for analyzing the effects of bipropellant spray combustion processes on liquid rocket performance is described and discussed. The Distributed Energy Release (DER) computer program was designed to become part of the JANNAF Liquid Rocket Performance Evaluation Methodology and to account, therein, for performance losses associated with the propellant combustion processes, e.g., incomplete spray gasification, imperfect mixing between sprays and their reacting vapors, residual mixture ratio striations in the flow, and two-phase flow effects. It does not account for losses associated with chemical kinetic deviations from equilibrium nor with the chamber wall boundary layer; those losses are analyzed by other computer programs in the JANNAF methodology. The DER computer program initializes the combustion field at the injection end of a conventional liquid rocket engine, based on injector and chamber design detail, and on propellant and combustion gas properties, and analyzes bipropellant combustion. The JANNAF reference computer program, TDK, is used for analyzing the supersonic flow in the nozzle expansion section. Depending upon the version of DER, the TDK analysis may either be included in the DER computations or done subsequently by a separate TDK run. Accurate predictions are possible, but depend upon proper selection of available adjustments in the input data. The propellant atomization (mass median drop diameter and distribution of diameters) and the location of the combustion initialization plane are probably the most important adjustments for many engines.

DD FORM 1 NOV 65 1473

UNCLASSIFIED
Security Classification

14 KEY WORDS	LINK A		LINK B		LINK C	
	ROLE	WT	ROLE	WT	ROLE	WT